Scholars' Mine

Doctoral Dissertations     Student Theses and Dissertations

Fall 2017

# The maculoprotective effect of a thiol antioxidant in retinal degeneration models

Hsiu-Jen Wang

THE MACULOPROTECTIVE EFFECT OF A THIOL ANTIOXIDANT IN RETINAL
DEGENERATION MODELS

by

HSIU-JEN WANG

A DISSERTATION

Presented to the Faculty of the Graduate School of the

MISSOURI UNIVERSITY OF SCIENCE AND TECHNOLOGY

In Partial Fulfillment of the Requirements for the Degree

DOCTOR OF PHILOSOPHY

in

CHEMISTRY

2017

Approved by

Nuran Ercal, Advisor
Robert S. Aronstam, Co-Advisor
Shubhender Kapila
Jeffrey G. Winiarz
Klaus Woelk

**PUBLICATION DISSERTATION OPTION**

This dissertation includes two articles that have been published or submitted elsewhere, in addition to an original introduction and conclusion. This dissertation is formatted in the style used by Missouri University of Science and Technology;

Paper I, pages 62-84 have been published in *Free Radicals and Antioxidants* Journal.

Paper II, pages 85-112 have been submitted to *Free Radical Research* Journal.

**ABSTRACT**

Age-related macular degeneration (AMD) is a leading cause of irreversible blindness among adults, age 60 and older, in developed countries. While oxidative stress is implicated in the pathogenesis of AMD, clinical studies have shown that dietary antioxidants can delay progression of AMD. Currently, there is no FDA-approved treatment for AMD. Therefore, we hypothesized that N-acetylcysteine amide (NACA), a thiol antioxidant, would protect retinal pigment epithelium and impede the progression of retinal degeneration. The goal of this work was to evaluate the efficacy of NACA in preventing retinal pigment epithelial cell and photoreceptor death in AMD models. To achieve this, we used the oxidants *tert*-butyl hydroperoxide (TBHP) and sodium iodate (NaIO$_3$) in a cell model and an animal model to evaluate the effects of NACA. Our data suggest that pretreatment with NACA reduces the sub-lethal (but not lethal) effects of TBHP in primary cultures of human retinal pigment epithelial cells. NACA significantly improves cell survival when administered prior to and during the occurrence of oxidative damage similar to that observed in the development of dry AMD. In the chemically-induced retinal degeneration animal model, NACA eye drops partially prevented reduction in visual function, as determined from electroretinograms (ERG) recorded 36 hours after NaIO$_3$ injection. Other toxic effects were observed at a later time point after NaIO$_3$ injection: increased lipid peroxidation (as measured by formation of 4-hydroxynonenal, 4-HNE), elevated cysteine levels, and death of photoreceptors resulting in outer nuclear layer thinning. NACA eye drops reversed these toxic effects. In conclusion, this potent antioxidant should continue to be investigated as a treatment for AMD.

# ACKNOWLEDGEMENTS

# TABLE OF CONTENTS

# LIST OF ILLUSTRATIONS

# LIST OF TABLES

## LIST OF ABBREVIATIONS

| Symbol | Description |
| --- | --- |
| 4-HNE | 4-hydroxynonenal |
| 6PG | 6-phosphogluconate |
| 7-AAD | 7-aminoactinomycin-D |
| AGEs | advanced glycation end products |
| AMD | age-related macular degeneration |
| annexin V-FITC | annexin V -Fluorescein isothiocyanate |
| AR | aldose reductase |
| AREDS | Age-Related Eye Disease Studies |
| CAT | catalase |
| CEP | carboxyethylpyrrole |
| CM-$H_2$DCFDA | 5-(and-6)-chloromethyl-2′,7′-dichlorodihydrofluorescein diacetate, acetyl ester |
| DAG | diacylglycerol |
| DM | diabetes mellitus |
| DR | diabetic retinopathy |
| EDTA | ethylenediaminetetraacetic acid |
| eNOS | endothelial nitric oxide synthase |
| ERG | electroretinogram |
| FDA | US Food and Drug Administration |
| G6P | glucose-6-phosphate |

| Symbol | Description |
|--------|-------------|
| G6PD | glucose-6-phosphate dehydrogenase |
| GADPH | glyceraldehyde 3-phosphate dehydrogenase |
| GCL | γ-glutamylcysteine ligase |
| GCL | ganglion cell layer |
| GCS | glutamylcysteine synthetase |
| GGT | γ-glutamyltransferase |
| GPx | glutathione peroxidase |
| GR | GSH reductase |
| GS | glutathione synthetase |
| GSH | glutathione |
| GSSG | glutathione disulfide |
| H&E | Hematoxylin and Eosin |
| $H_2O_2$ | hydrogen peroxide |
| $HO^{\bullet}$ | hydroxyl radical |
| HRPEpiC | human retinal pigment epithelial cells |
| INL | inner nuclear layer |
| IP | intraperitoneal |
| IPL | inner plexiform layer |
| MDA | malondialdehyde |
| MGO | methylglyoxal |
| NAC | N-acetylcysteine |
| NACA | N-acetylcysteine amide |

| Symbol | Description |
|--------|-------------|
| NADPH | nicotinamide adenine dinucleotide phosphate |
| NaIO$_3$ | sodium iodate |
| NO$^\cdot$ | nitric oxide |
| Nox | NADPH oxidases |
| NPDR | non-proliferative diabetic retinopathy |
| NPM | N-(1-pyrenyl) maleimide |
| O$_2^{\cdot-}$ | superoxide |
| ONL | outer nuclear layer |
| OPL | outer plexiform layer |
| PARP | poly-ADP-ribose polymerase |
| PBS | Phosphate buffered saline |
| PDR | proliferative diabetic retinopathy |
| PDT | photodynamic therapy |
| PEX | pseudoexofoliation syndrome |
| PKC | protein kinase C |
| POS | photoreceptor outer segments |
| p-PTEN | phospho-PTEN |
| PRX | peroxiredoxin |
| PTEN | phosphatase and tensin homolog deleted on chromosome ten |
| PUFA | polyunsaturated fatty acid |
| ROO$^\cdot$ | peroxyl radicals |

| Symbol | Description |
|---|---|
| ROS | Reactive Oxygen Species |
| RP | retinitis pigmentosa |
| RPE | retinal pigment epithelium |
| SDH | sorbitol dehydrogenase |
| SOD | superoxide dismutase |
| TBHP | tert-butyl hydroperoxide |
| TEER | transepithelial electrical resistance |
| TM | trabecular meshwork |
| TRX | thioredoxin |
| UDPGlcNAc | uridine diphosphate-N-acetylglucosamine |
| VEGF | vascular endothelial growth factor |

## 1. INTRODUCTION

### 1.1. OXIDATIVE STRESS

Oxidative stress results from an imbalance between reactive species and antioxidant defense processes, that lead to a highly oxidizing environment that is harmful to cells [1]. The term "reactive species" includes both free radicals that contain one or more unpaired electrons, and non-radicals with strong oxidizing potential. It encompasses reactive oxygen, nitrogen, halogen, and sulfur species. Figure 1.1 shows the major reactive species relevant to physiological processes [2]. This section will focus on the definition of reactive oxygen species (ROS), sources of ROS, redox balance, and oxidative stress and its by-products.



Figure 1.1 Reactive oxygen species and reactive nitrogen species (adapted from slide player [2]).

**1.1.1. The Definition of ROS.** Reactive species, including ROS, play an important role in a cell's life and death [3-5]. The National Cancer Institute defines ROS as "a type of unstable molecule that contains oxygen and easily reacts with other molecules in a cell." These molecules can damage lipids, nucleic acids, and proteins, which can result in cell death. The terms "ROS," "oxygen-derived species," and "pro-oxidant species" are generally interchangeable in biological scientific literature [6]. ROS can be classified as radicals or non-radicals. Radicals are chemical species with an unpaired electron, such as superoxide ($O_2^{\bullet-}$), hydroxyl radical ($HO^{\bullet}$) and peroxyl radicals (formed from non-radical lipid peroxides and peroxides of proteins and nucleic acids). Hydrogen peroxide ($H_2O_2$) is a non-radical, but it forms the most reactive free radical, hydroxyl radical ($HO^{\bullet}$), through the Fenton reaction. Figure 1.2 shows the Lewis structures of molecular oxygen, superoxide, hydrogen peroxide, and hydroxyl radical [7]. Their energy- and electron-transfer reactions are shown in Figure 1.3 [8].
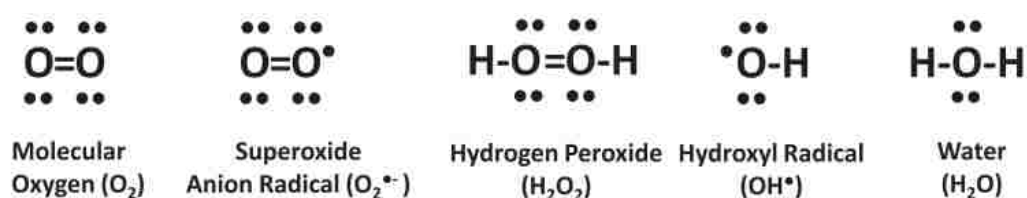


Figure 1.2 The Lewis structures for molecular oxygen and its singlet electron derivatives superoxide, hydrogen peroxide, and hydroxyl radical (adapted from Mailloux, R.J. [7]).

**1.1.2. Sources of ROS.** ROS can be generated endogenously or exogenously [6, 9]. Endogenous sources of ROS include leakage of electrons to $O_2$ in the mitochondrial

respiratory chain (Figure 1.4) [10], direct or indirect generation by numerous enzymes, and the Fenton reaction (Figure 1.5) [11]. In addition, certain diseased states may increase endogenous ROS production as a result of dysfunctional regulation of the immune response. High-energy electromagnetic radiation (UV, X-ray, and γ radiation), certain foods, medicines (acetaminophen, doxorubicin, and nitrofurantoin), and illicit drugs (methamphetamine and heroin), cigarette smoke, pollutants, and xenobiotics are common exogenous sources of ROS [12-16].
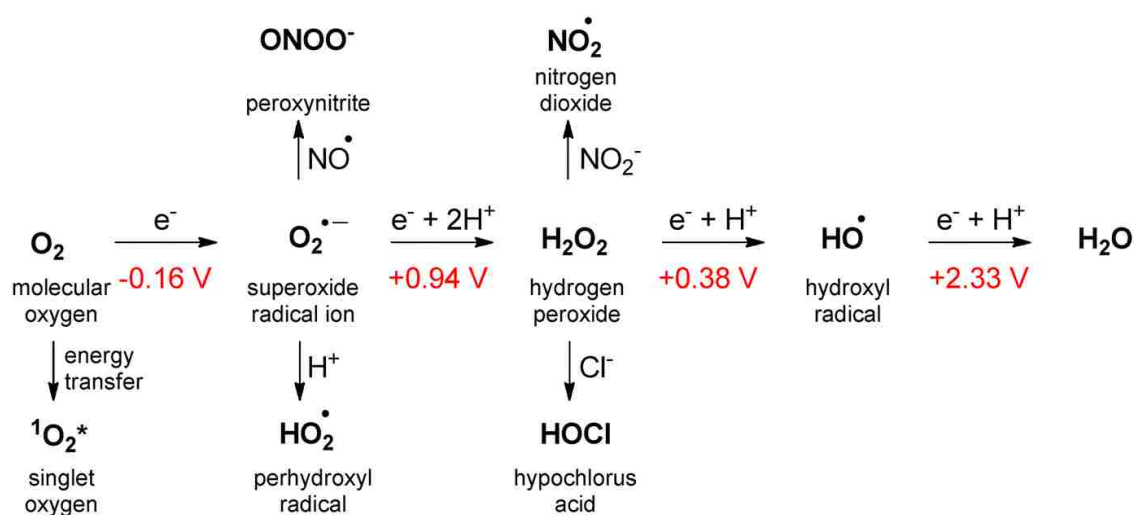


Figure 1.3 Formation of ROS through energy- and electron-transfer reactions (adapted from Katerina K. & Cosa G. [8]).

**1.1.3. Redox Balance and Oxidative Stress.** ROS can play either beneficial or deleterious roles in the body. Certain ROS and their derivatives are involved in important physiological functions, such as regulation of vascular tone, control of erythropoietin production, and hypoxia-inducible functions, smooth muscle relaxation, signal

transduction, and maintenance of redox homeostasis [3]. However, mitochondria-derived ROS can serve as a meditator of cell death in eukaryotes [17]. ROS scavengers (also known as antioxidants) can remove extra ROS and stabilize the redox balance in cells. Figure 1.6 shows the mechanism of redox homeostasis [3]. With an overwhelming production of ROS, the redox balance can be shifted toward a more oxidative status, in which the overproduction of ROS is associated with numerous disorders, such as Alzheimer's disease, cardiovascular disease, atherosclerosis, cataract, and retinal degeneration [4, 9, 18]. A summary of oxidative stress-induced diseases in humans is shown in Figure 1.7 [4]. More details about oxidative stress by-products and the role of oxidative damage will be discussed in the following sections.



Figure 1.4 The ROS generation in the mitochondria (adapted from Sabharwal, S. and Schumacker, P. [10]).

Figure 1.5 Sources and generation of different reactive oxygen species (adapted from Ajuwon, O.R. *et al.* [11]).
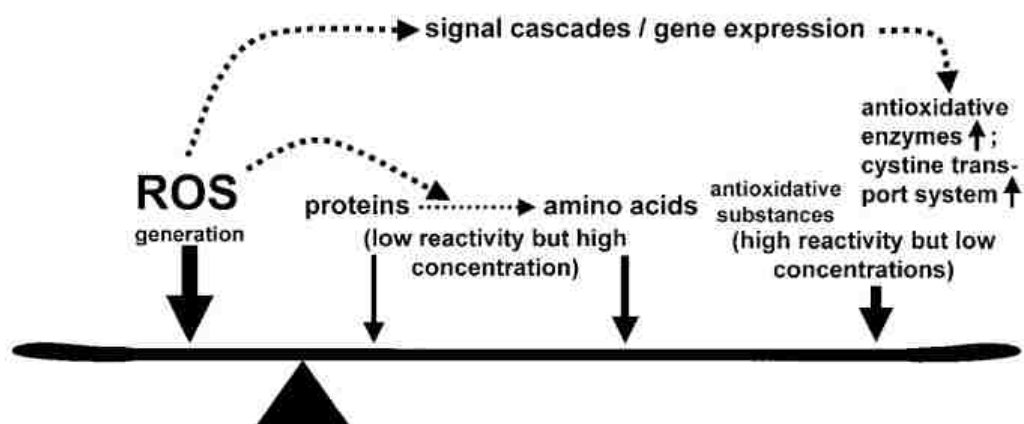


Figure 1.6 Mechanisms of redox homeostasis: balance between ROS production and various types of scavengers (adapted from Dröge, W. [3]).

| **Lungs:**<br>Asthma<br>Chronic bronchitis | **Kidneys:**<br>Glomerulonephritis<br>Chronic renal failure | **Fetus:**<br>Preeclampsia<br>IU growth restriction |
| **Joints:**<br>Arthritis<br>Rheumatism | **Oxidative Stress** | **Eyes:**<br>Cataract<br>Retinal diseases |
| **Brain:**<br>Alzheimer's<br>Parkinson's<br>Memory loss<br>Depression<br>Stroke | **Multi-organs:**<br>Cancer<br>Aging<br>Diabetes<br>Inflammation<br>Infection | **Heart-Vessels:**<br>Arteriosclerosis<br>Hypertension<br>Ischemia<br>Cardiomyopathy<br>Heart failure |

Figure 1.7 Oxidative stress-induced diseases in humans (adapted from Pham-Huy, L.A. *et al.* [4]).

**1.1.4. Oxidative Damage By-Products and Their Formation.** An excess of ROS, especially hydroxyl (HO$^•$) and peroxyl (ROO$^•$) radicals, hydrogen peroxide ($H_2O_2$), and superoxide radical anion ($O_2^{•-}$), is associated with oxidation-induced damage to DNA, proteins, and fatty acids. In this section, the formation of DNA oxidation by-products, protein carbonyls, and lipid peroxidation by-products will be discussed.

Lipid peroxidation is a free radical chain reaction in which free radicals attack the carbon-carbon double bonds of polyunsaturated fatty acids (PUFAs), generating lipid hydroperoxides and electrophilic α,β-unsaturated carbonyl derivatives of these lipids [19]. Lipid peroxidation consists of three steps: initiation, propagation, and termination (see Figure 1.8) [12, 20]. In the initiation step, a free radical (R$^•$) attacks the methylene bridge (-CH$_2$-) of an unsaturated fatty acid and abstracts hydrogen to produce a lipid radical (a carbon radical). A stable conjugated diene is formed after molecules are rearranged

(Figure 1.8, step 1). In the propagation step, the lipid radical (carbon radical) reacts with $O_2$ to form a new peroxyl radical (ROO$^\bullet$) (Figure 1.8, step 2), which abstracts H$^\bullet$ from an adjacent lipid, forming a lipid hydroperoxide (ROOH) plus a new lipid radical (Figure 1.8, step 3) that will then continue the chain reaction. In the termination step, an antioxidant donates hydrogen to the lipid peroxyl radical (ROO$^\bullet$), resulting in a non-radical product (Figure 1.8, step 4). Aldehydes, such as malondialdehyde (MDA) and 4-hydroxynonenal (4-HNE), (Figure 1.9, [21]) may also be formed during lipid peroxidation. MDA is mainly formed from the peroxidation of PUFAs with more than two double bonds, such as linolenic acid, arachidonic, and docosahexaenoic acid, whereas 4-HNE is formed during peroxidation of $\omega$-6 (omega-6) PUFAs, such as linolenic acid and arachidonic acid [22]. These by-products are associated with human tissue injury and disease [23].

DNA's localization in the nucleus affords it some protection from ROS, and it is relatively stable under physiological conditions. DNA is not very susceptible to direct oxidative damage from weak ROS, such as $O_2^{\bullet-}$, NO$^\bullet$, and $H_2O_2$ [24]. However, when DNA (or RNA) is exposed to highly reactive OH$^\bullet$, adducts may be generated. For example, OH$^\bullet$ can attack guanine at C-8 to form 8-hydroxyguanine (8-OH-dG) [6]. Figure 1.10 shows the modification of DNA bases by HO$^\bullet$ radicals [25]. In addition, electrophilic lipid peroxidation by-products (such as MDA and 4-HNE) can cause DNA damage. MDA can react with DNA at a physiological pH to form the adducts deoxyguanosine, deoxyadenosine, and deoxycytidine [26]. 4-HNE is the most genotoxic, while MDA is the most mutagenic, but both of them may contribute to human disease [27].
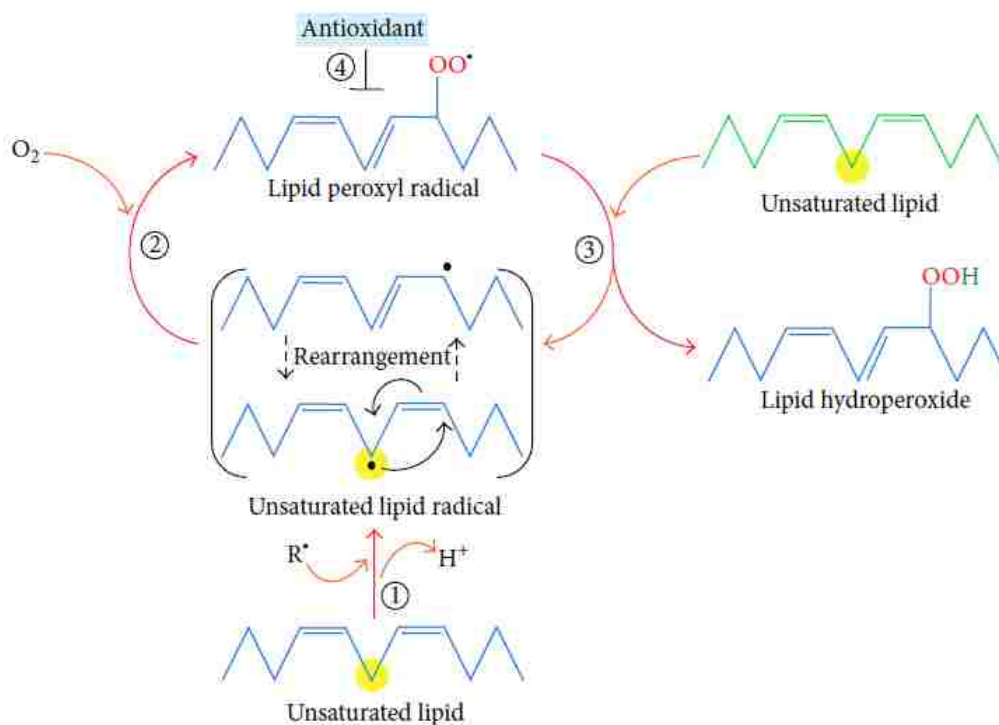
Figure 1.8 The four steps of lipid peroxidation (adapted from Ayala, A. et al [12]).
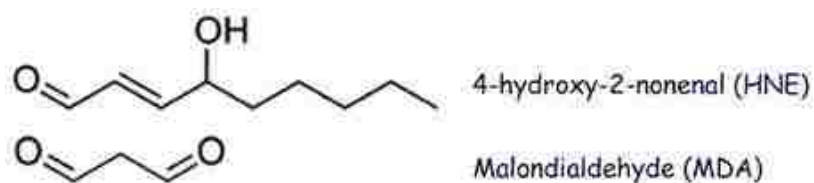


Figure 1.9 Chemical structures of 4-hydroxynonenal (4-hydroxy-*trans*-2-nonenal, 4-HNE) and malondialdehyde (MDA) (modified from Pizzimenti, S. *et al.* [21]).

There is a high abundance of protein in biological systems; therefore, proteins are often a target for oxidative damage. Proteins can be attacked by ROS directly or indirectly by lipid peroxidation by-products, and the resulting damaged proteins can affect enzyme activity or alter cellular functions [6]. Protein carbonyls are the most well-

known biomarkers for protein peroxidation and are associated with many human diseases, including diabetes, Alzheimer's disease, and chronic lung disease [28]. Table 1.1 lists the oxidants involved in protein oxidation and their major sites of reaction [29]. Direct protein carbonylation often happens on the side chains of proline, arginine, lysine and threonine residues. Figure 1.11 shows the structures of carbonyl derivative products of amino acid side chains: 2-pyrrolidone from prolyl residues, glutamic semialdehyde from arginyl and prolyl residues, α-aminoadipic semialdehyde from lysyl residues, and 2-amino-3-ketobutyric acid from threonyl residues [30].
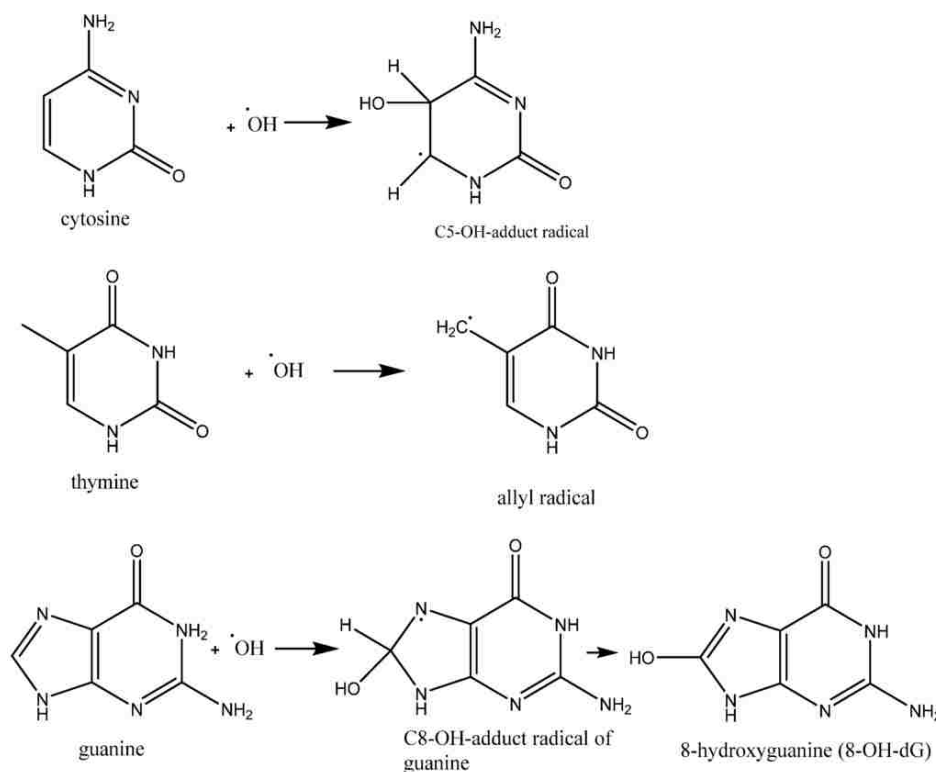


Figure 1.10 Reactions of hydroxyl radical with DNA bases and their major products (adapted from Dissanayake, N. *et al.* [25]).

Table 1.1 The summary of protein modifications induced by reactive oxidants

| Oxidant | Major sites of reaction |
| --- | --- |
| HO$^{\bullet}$ | All residues |
| RO$^{\bullet}$ | Most residues |
| ROO$^{\bullet}$ | Cys, Met, Trp, Tyr |
| NO$_2$$^{\bullet}$ | Cys, Tyr/Trp radicals |
| O$_2$$^{\bullet -}$ | Superoxide dismutase, some transition metal ions, Fe-S clusters, Tyr/Trp radicals |
| $^1$O$_2$ | Cys, Met, Trp, Tyr, His |
| HOCl/HOBr | Cys, Met, cysteine, His, Lys, Trp, α-amino group |
| Peroxynitrous acid (ONOOH) | Cys, Met, Tyr, Trp |
| Reactive aldehydes | Cys, Arg, Lys, His, α-amino group |
| UVB light | Trp, Tyr, cystine |
| H$_2$O$_2$ | Cys, selenocysteine |

**Cys**, Cysteine; **Met**, Methionine; **Trp**, Tryptophan; **Tyr**, Tyrosine; **His**, Histidine; **Lys**, Lysine; **Arg**, Arginine. (Table was modified from Davies, M. [29]).
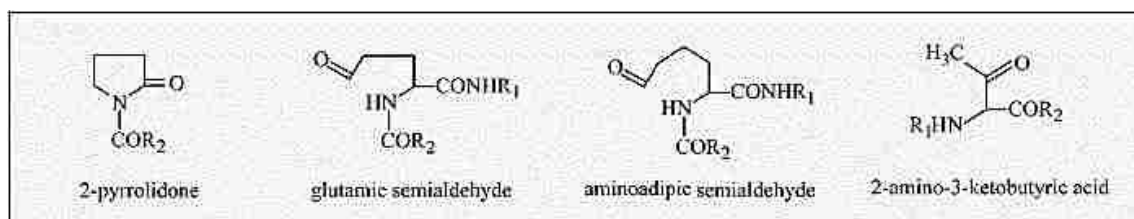


Figure 1.11 The structures of carbonyl derivatives produced by direct oxidation of amino acid side chains (adapted from Dalle-Donne, I. *et al.* [30]).

## 1.2. ANTIOXIDANTS

The primary role of antioxidants is to neutralize excess ROS, thereby protecting

the cell from their deleterious effects. Antioxidants can be classified as enzymatic or non-

enzymatic [4]. Superoxide dismutase (SOD), glutathione peroxidase (GPx), catalase, and

thioredoxin are examples of enzymatic antioxidants (Table 1.2) [31, 32]. The non-enzymatic

antioxidants can be further divided into metabolic antioxidants and nutrient antioxidants (Table 1.3) [31]. Glutathione (GSH), melatonin, and α-lipoic acid are metabolic antioxidants. Vitamin E, vitamin C, carotenoids, omega-3 and omega-6 fatty acids, trace metals (selenium, manganese, and zinc), and flavonoids are nutrient antioxidants. Oxidative stress occurs when oxidants and antioxidants are not balanced in a cell, leaving excess oxidants to damage cellular components.

Table 1.2 Enzymatic Antioxidant Defenses

| Enzymatic Antioxidants | Catalyzed Reaction |
| --- | --- |
| Superoxide dismutase (SOD) | $O_2^{\bullet-} + O_2^{\bullet-} + 2H^+ \rightarrow H_2O_2 + O_2$<br>$\text{Enzyme-Cu}^{2+} + O_2^{\bullet-} \rightarrow \text{Enzyme-Cu}^+ + O_2$<br>$\text{Enzyme-Cu}^+ + O_2^{\bullet-} + 2H^+ \rightarrow \text{Enzyme-Cu}^+ + H_2O_2$<br>$Mn(III) + O_2^{\bullet-} \leftrightarrows [\,Mn(III) - O_2^{\bullet-}\,] \rightarrow Mn^{2+} + O_2$<br>$Mn^{2+} + O_2^{\bullet-} \leftrightarrows [\,Mn^{2+} - O_2^{\bullet-}\,] + 2H^+ \rightarrow Mn(III) + H_2O_2$ |
| Catalase (CAT) | $2H_2O_2 \rightarrow O_2 + 2H_2O$<br>$\text{Catalase-Fe(III)} + H_2O_2 \rightarrow \text{Compound I} + H_2O$<br>$\text{Compound I} + H_2O_2 \rightarrow \text{Catalase-Fe(III)} + H_2O + O_2$ |
| Glutathione peroxidase (GPx) | $2GSH + H_2O_2 \rightarrow GSSG + 2H_2O$<br>$2GSH + ROOH \rightarrow GSSG + H_2O + ROH$ |
| Thioredoxin (TRX) | $\text{TRX-(SH)}_2 + \text{Protein-S}_2 \leftrightarrows \text{TRX-S}_2 + \text{Protein-(SH)}_2$ |
| Peroxiredoxin (PRX) | $2\,R'\text{-SH} + ROOH \leftrightarrows R'\text{-S-S-R} + H_2O + ROH$ |
| Glutathione transferase (GST) | $RX + GSH \rightarrow \text{R-S-GSH} + HX$ |

**RX**: halogenated hydrocarbons [33]. Table was modified from Birben, E. *et al.* [31].

Table 1.3 Non-Enzymatic Antioxidant Defenses

| Metabolic antioxidant |
| --- |
| Glutathione  |
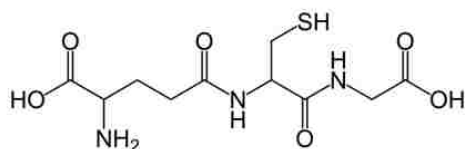
Table 1.3 Non-Enzymatic Antioxidant Defenses (Cont'd)

| Nutrient Antioxidant | | |
| --- | --- | --- |
| Vitamin A | | All trans retinol |
| Vitamin C | | Ascorbic acid |
| Vitamin E | | α-Tocopherol Ref [34] |
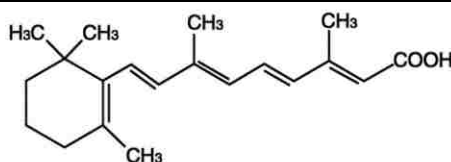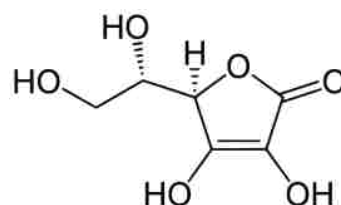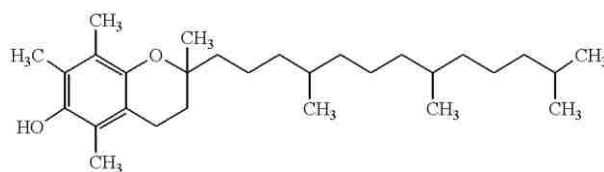
Tocopherol
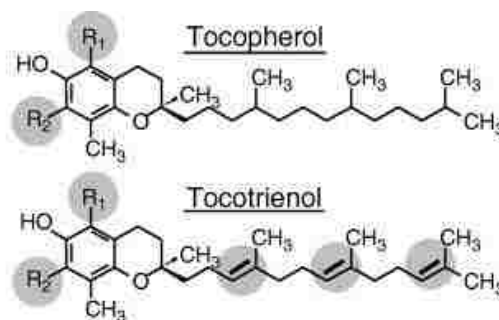
Tocotrienol

| Tocochromanol | R₁ | R₂ | Vitamin E activity(%) Tocopherol | Tocotrienol |
| --- | --- | --- | --- | --- |
| alpha | $CH_3$ | $CH_3$ | 100 | 21–50 |
| beta | $CH_3$ | H | 25–50 | 5 |
| gamma | H | $CH_3$ | 8–19 | nm |
| delta | H | H | <3 | nm |

β-Carotene
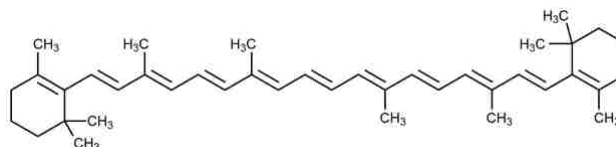
(Table was modified from Birben, E. *et al.* [31]).

**1.2.1.  Glutathione.** Glutathione (γ-glutamylcysteinylglycine, GSH) is a water-soluble endogenous tripeptide (structure in Figure 1.12) with γ-carboxyl groups that make this small peptide relatively more stable as compared to other peptides. GSH, the most abundant thiol present in mammalian cells, has concentrations of up to 10 mM [35].
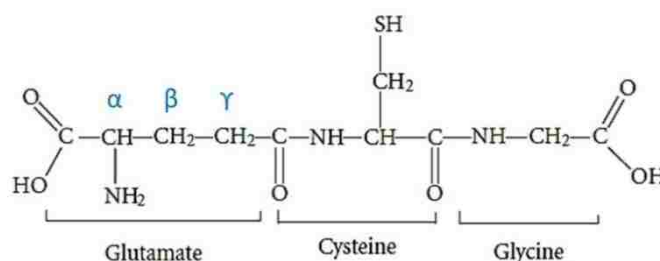


Figure 1.12 The structure of glutathione.

GSH cannot penetrate cell membranes; therefore, intracellular GSH must be synthesized through both *de novo* and salvage pathways (Figure 1.13, modified from [36, 37]). The first and rate-limiting step of *de novo* synthesis requires ATP and γ-glutamylcysteine ligase (also known as γ-glutamylcysteine synthetase (GCS) [38]. Then, the dipeptide is combined with glycine by glutathione synthetase. The salvage synthesis pathways of GSH proceed via three different routes: reduction from GSSG, formation from the products of GSH hydrolysis, or production from amino acids and dipeptides transported into the cell by γ-glutamyl transpeptidase (Figure 1.13). GSH can be broken down by γ-glutamyltransferase (GGT), which cleaves to the gamma linkage and generates cysteinylglycine.
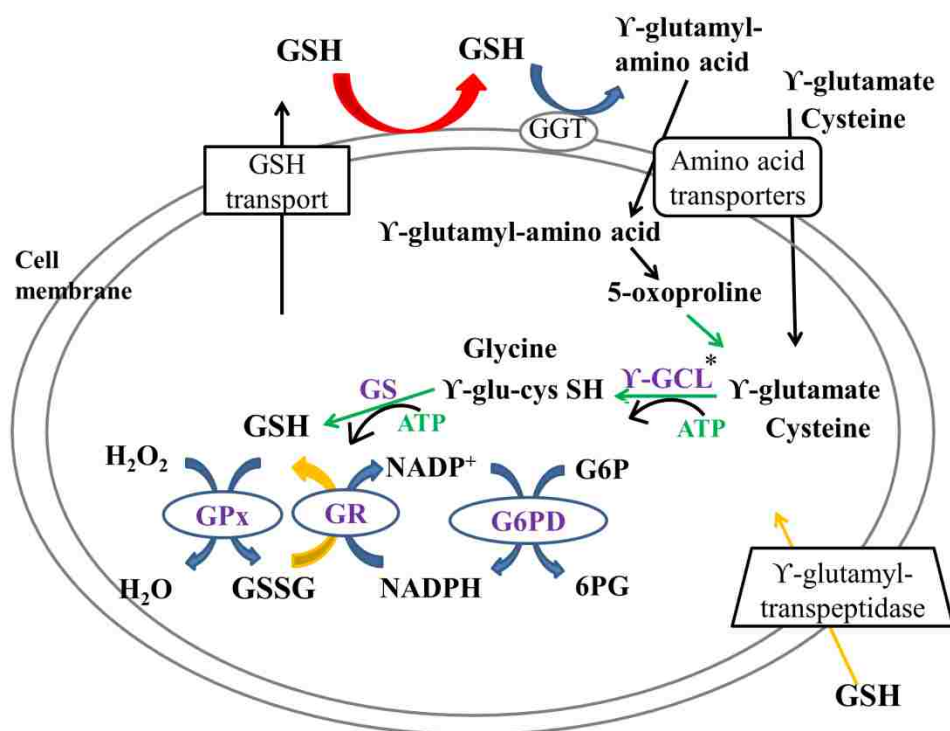
Figure 1.13 Glutathione synthesis and enzymes involved in GSH metabolite. **GCL**: γ-glutamylcysteine ligase, **GS**: Glutathione synthetase, **GGT**: γ-glutamyltransferase (or γ-glutamyltranspeptidase), **G6P**: glucose-6-phosphate, **G6PD**: glucose-6-phosphate dehydrogenase, **6PG**: 6-phosphogluconate, **NADPH**: nicotinamide adenine dinucleotide phosphate, **GR**: GSH reductase, **GPx**: GSH peroxidase.

The functions of GSH include antioxidant defense against reactive oxygen species (ROS) and electrophiles to maintain the cellular reducing environment, cysteine reservation, nitric oxide transportation, xenobiotic detoxification, and involvement in redox signaling-related transcription factor operations [36, 39]. In the xenobiotic detoxification pathway, GSH can directly interact with excess ROS or conjugate with electrophile metabolites, which are then exported from the cell. Figure 1.14 shows the role of GSH in detoxification of xenobiotics and ROS balance, processes that may lead

to pathological conditions if dysregulated [36]. The effects of an imbalance between

ROS and antioxidant defenses depend on the level of ROS production, as shown in

Figure 1.15 [8].
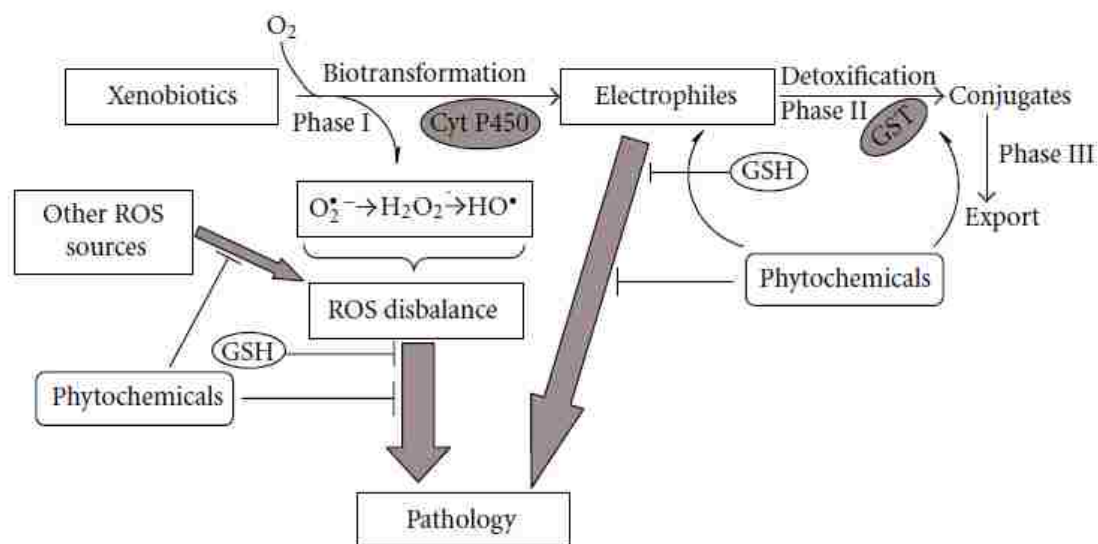


Figure 1.14 Relationship between GSH homeostasis and pathologies (adapted from Lushchak, V.I. [36])

**1.2.2. Glutathione Reductase.** GSH can be oxidized to glutathione disulfide

(GSSG) by glutathione peroxidase (GPx).The function of the enzyme glutathione

reductase (GR) is to reduce GSSG to GSH using NADPH generated by glucose-6-

phosphate dehydrogenase (G6PD) in the pentose phosphate pathway [38] (Figure 1.13).

Patients with age-related macular degeneration (AMD) show both lower glutathione

reductase activity and glutathione peroxidase activity in the blood, as compared to

controls [40, 41].
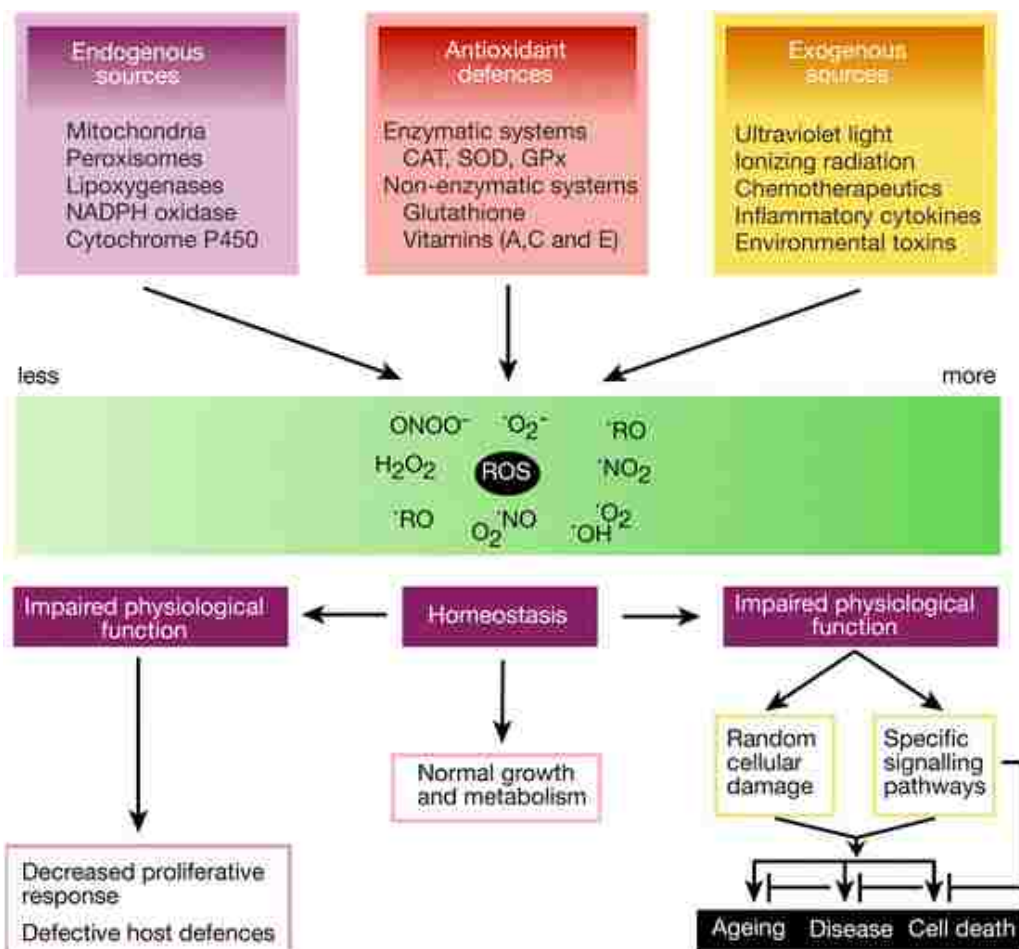
Figure 1.15 Sources of ROS, antioxidant defenses, and subsequent biological effects depending on the level of ROS production (adapted from Krumova, K. & Cosa, G. [8]).

**1.2.3. Glutathione Prodrugs and N-Acetylcysteine Amide (NACA).** Direct administration of GSH as a therapeutic agent is ineffective because of its unfavorable biochemical and pharmacokinetic properties that limit its entry into cells. However, GSH prodrugs are able to replenish intracellular GSH levels and have been used as antioxidants for treatment of conditions associated with reduced GSH levels [42]. There are two approaches for elevating intracellular GSH levels: GSH prodrugs or GSH co-

drugs. GSH prodrugs are compounds with better bioavailability that can directly or indirectly increase intracellular GSH levels. GSH co-drugs consist of GSH covalently linked to another compound that both improves bioavailability and acts synergistically with GSH to produce the desired therapeutic effect. [42]. GSH prodrugs can be divided into different categories: GSH esters, cysteinyl-modified GSH derivatives, and cysteine prodrugs [42]. The most promising GSH prodrugs are the cysteine prodrugs, N-acetylcysteine (NAC) and N-acetylcysteine amide (NACA) (their structures are shown in Figure 1.16). N-acetylcysteine (NAC), a thiol antioxidant, has been clinically used to treat various disorders and is already approved by the FDA (the U.S. Food and Drug Administration). However, NACA, the amide derivative of NAC, has been shown to be more effective because of its neutral charge, which increases its ability to permeate cell membranes and the blood-neural barrier [43]. The protective effect of NACA in eye-related research will be discussed in Section 1.4.5.

A                                                          B



N-Acetylcysteine                          N-Acetylcysteine amide
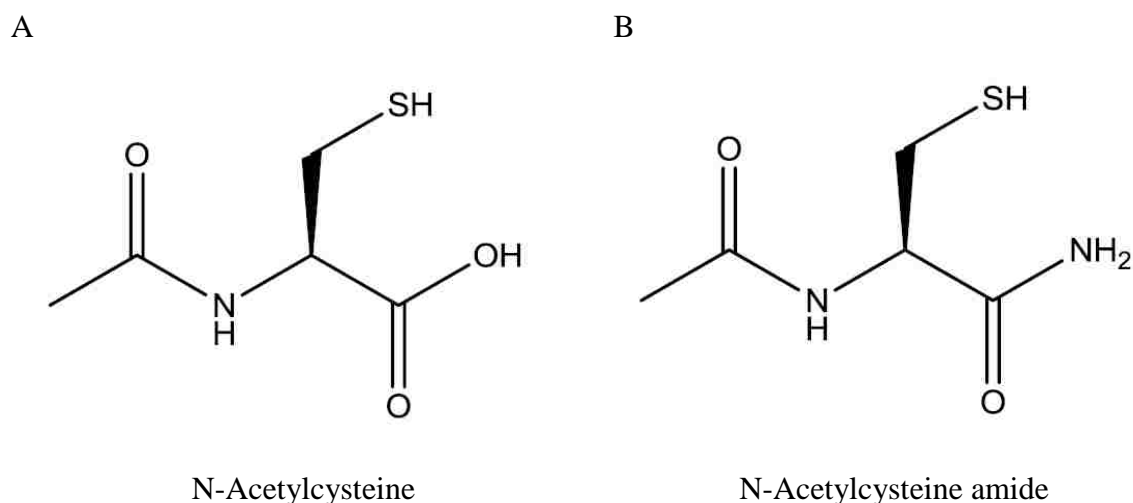
Figure 1.16 The structures of (A) N-acetylcysteine and (B) N-acetylcysteine amide (adapted from Tobwala, S. and Ercal, N. [44]).

## 1.3. EYE ANATOMY AND PHYSIOLOGY

**1.3.1. Eye Anatomy.** The eye is made up of three layers of tissues. The outermost layer is composed of the cornea and sclera. The middle layer contains the choroid, ciliary body, pigmented epithelium, and iris. The light-sensitive retina is the innermost layer. The lens focuses an image of the visual world on the retina, which acts like film in a camera. The macula lies near the center of the retina and is responsible for high-resolution color vision. The fovea is a small depression at the center of the macula and enables the highest-resolution vision. Figure 1.17 shows a horizontal section of the right eye [45]. Once the retina receives light focused by the lens, it converts the light into electrical signals and then sends these signals through the optic nerve to the brain. When the macula is damaged, the center of a visual image will be blurry or lost completely [46], which will affect a patient's daily activities, such as driving, reading, and recognizing faces.
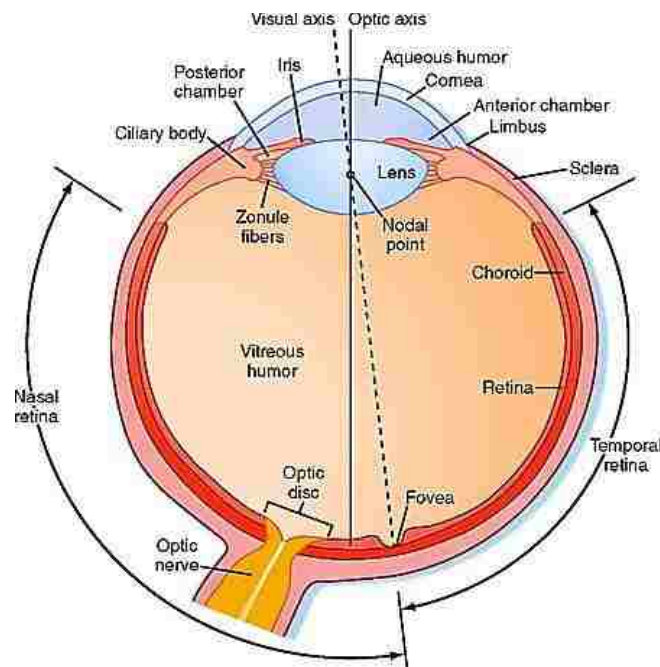


Figure 1.17 Horizontal section of the right eye (adapted from Basicmedicalkey [45]).

**1.3.2. Retina.** Histologically, the retina has three layers that contain nerve cell bodies and two layers of synapses (Figure 1.18) [47]. The three nerve cell body layers are the ganglion cell layer (GCL), inner nuclear layer (INL), and outer nuclear layer (ONL). These layers are interconnected by two synapses, the inner plexiform layer (IPL) and the outer plexiform layer (OPL). The GCL contains the bodies of ganglion cells and displaced amacrine cells; the INL contains the bodies of bipolar, horizontal, and amacrine cells; and the ONL contains cell bodies of the rods and cones. The IPL functions as a relay station for the vertical-information-carrying nerve cells, the bipolar cells, to connect with ganglion cells. In the OPL, rods and cones synapse with both horizontal cells and bipolar cells. The retinal pigment epithelium (RPE) is a single layer of hexagonal cells and contains the pigment melanin. The RPE connects retinal cells and the choroid and forms a part of the blood-retinal barrier. Figure 1.19 shows a color fundus photograph of a normal macula and a cross-section of macular layers [48].

## 1.4. AGE-RELATED MACULAR DEGENERATION

**1.4.1. What is AMD?** Age-related macular degeneration (AMD) is the leading cause of irreversible blindness in the industrialized world, and the third-leading cause worldwide [49, 50]. In the U.S, about 2.1 million people are affected by AMD, and the number of cases is projected to increase to 3.7 million by 2030 [51, 52]. Taking aging (the major risk factor) into consideration, the expected global prevalence of AMD is expected to be approximately 196 million by 2020, and rising to 288 million in 2040 [53]. The prevalence of AMD is close to that of invasive cancers and almost twice that of Alzheimer's [54]. This creates an annual direct health care cost of $4.6 billion in the U.S.[55]. Unfortunately, patients with AMD lose quality of life because they require assistance with simple daily tasks, such as walking, reading, or driving [56].
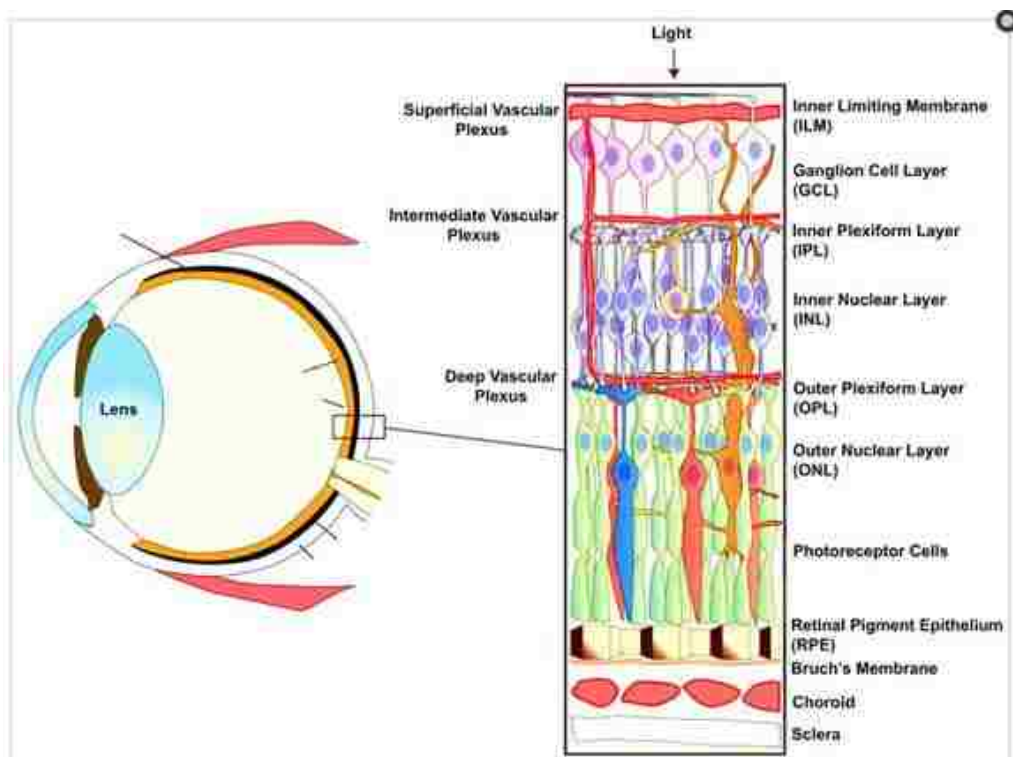
Figure 1.18  A cross-sectional diagram depicting the major structures of the eye is shown on the left, and an enlarged diagram of the neural retina, underlying the RPE, choroid, and sclera is shown on the right (adapted from Jarrett, S. and Boulton, M. [47]).

AMD is a degenerative condition that begins in Bruch's membrane and progresses to involve the RPE and ultimately the overlying photoreceptors [57]. The clinical hallmark of AMD is the presence of drusen. AMD is classified as dry (non-exudative, affecting an estimated 85-90% of patients) or wet (exudative, affecting an estimated 10-15% of patients) clinically. The non-exudative disease is characterized by RPE death, or geographic atrophy. Attenuation of the overlying photoreceptors, which are located in the outer nuclear layer, follows the demise of the RPE. The distinguishing feature of wet AMD is choroidal neovascularization, followed by exudation and hemorrhaging as the disease worsens. If left untreated, dry AMD may progress to wet [58,

[59]; however, this can be halted if a therapeutic intervention is initiated early enough during the course of the disease.

Currently, there is no FDA-approved treatment for dry AMD. The only available treatment to slow the progression of visual loss in dry AMD includes vitamin and micronutrient supplementation, cessation of smoking, and dietary modification [60, 61]. Figure 1.19A is a fundus photograph of the normal macula, and Figure 1.19B is a cross section of retina (after Haemotoxylin and Eosin staining) that shows the multilayer structure of the macula [48]. Figure 1.20 compares the pathophysiological classification of age-related macular degeneration [57, 62]. In early AMD, there are a few medium-sized soft drusen (63-124 microns in diameter) and retinal pigmentary abnormalities. In intermediate AMD, at least one large ($\geq$ 125 microns in diameter) and more medium-sized drusen are present, as well as geographic atrophy that does not involve the center of the macula. Advanced non-neovascular AMD is characterized by drusen and geographic atrophy that extends to the center of the macula. Advanced neovascular AMD is characterized by choroidal neovascularization and its consequences, including subretinal fluid, lipid deposition, hemorrhage, and retinal pigment epithelium (RPE) detachment.

**1.4.2. Risk Factors for AMD.** AMD is a multifactorial disease. The risk factors include tobacco smoking, white race, genetics (complement factor H), and light exposure (expecially blue light). AMD is also associated with hypertension, atherosclerosis, fat-rich diet, and obesity [63, 64]. Age is the most significant risk factor for AMD, due to the build-up of oxidation by-products and decrease in antioxidant capacity with age.
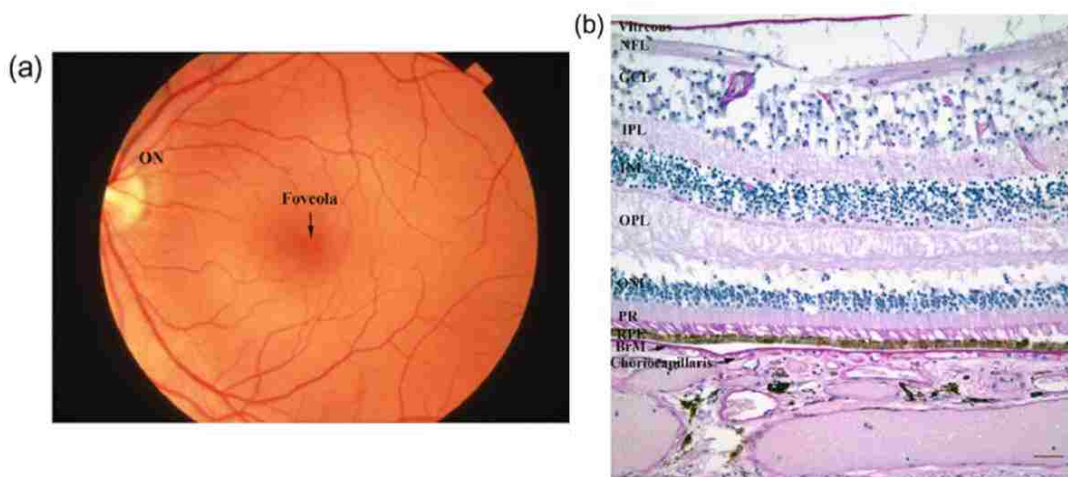
Figure 1.19 A normal macula (a) Color fundus photograph of a normal left macula. (b) Multilayer structure of a macula (adapted from Handa J.T. [48]).
From top to bottom**: NFL**, nerve fiber layer; **IPL**, inner plexiform layer; **INL**, inner nuclear layer; **OPL**, outer plexiform layer; **ONL**, outer nuclear layer; **PR**, photoreceptor layer; **RPE**, retinal pigment epithelium; **BrM**, Bruch's membrane.
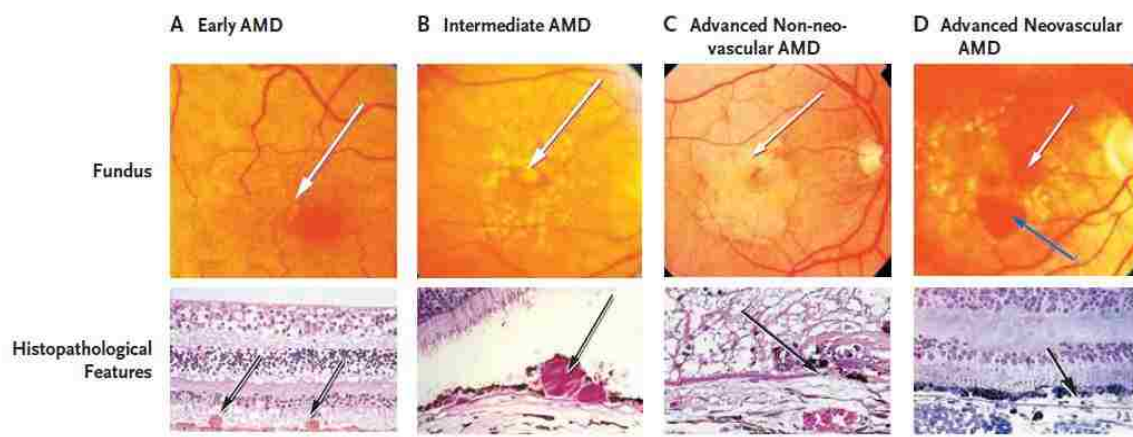


Figure 1.20 Fundus photographs and a cross section of H&E stain showing the histopathological features in different stages of age-related macular degeneration (AMD) (adapted and modified from Jager, R. D. *et al.* [57]).
The white arrow indicates the drusen and geographic atrophy; the black arrow indicates the drusen and Bruch's membrane degeneration; and the blue arrow shows the subretinal hemorrhage.

**1.4.3.  How Does Oxidative Stress Contribute to AMD?** The RPE is a monolayer of cuboidal and columnar cells which regulate ion and metabolite transport, phagocytose photoreceptor outer segments (OS), and metabolize the retinol. These cells also form the outer blood-retinal barrier and thus maintain the extracellular matrix [65]. This complex layer is subject to intense oxidative insult; therefore, oxidative stress plays an important role in the dysfunction of the RPE and other retinal cells in macular degeneration.

This level of exogenous oxidative stress is potentiated by the relative paucity of antioxidants, such as GSH, in an aging retina. Light-induced peroxidation of shed photoreceptor outer segments, that contain polyunsaturated fatty acids (PUFAs), leads to the formation of toxic reactive oxygen species (ROS) and lipofuscin. Lipofuscin contains a fluorescent mixture of lipid-protein complexes, by-products of vitamin A (bisretinoids) metabolism, and lipid peroxidation products. Lipofuscin is cytotoxic and can activate complement and increase oxidative stress in RPE. Accumulation of ROS-laden lipofuscin granules, elevated local oxygen tension, high PUFA content, light exposure, and secondary photosensitizing agents that accumulate with aging create a highly oxidizing environment for the RPE [52]. The peroxidation by-product of PUFAs, mainly is docosahexaenoic acid (DHA) to form carboxyethylpyrrole (CEP), can bind to protein. The CEP-protein adducts can further lead to activate complement and induce neo-angiogenesis. Figure 1.21 shows the resources of oxidative stress and outline the key role of oxidative stress in AMD pathogenesis [66].
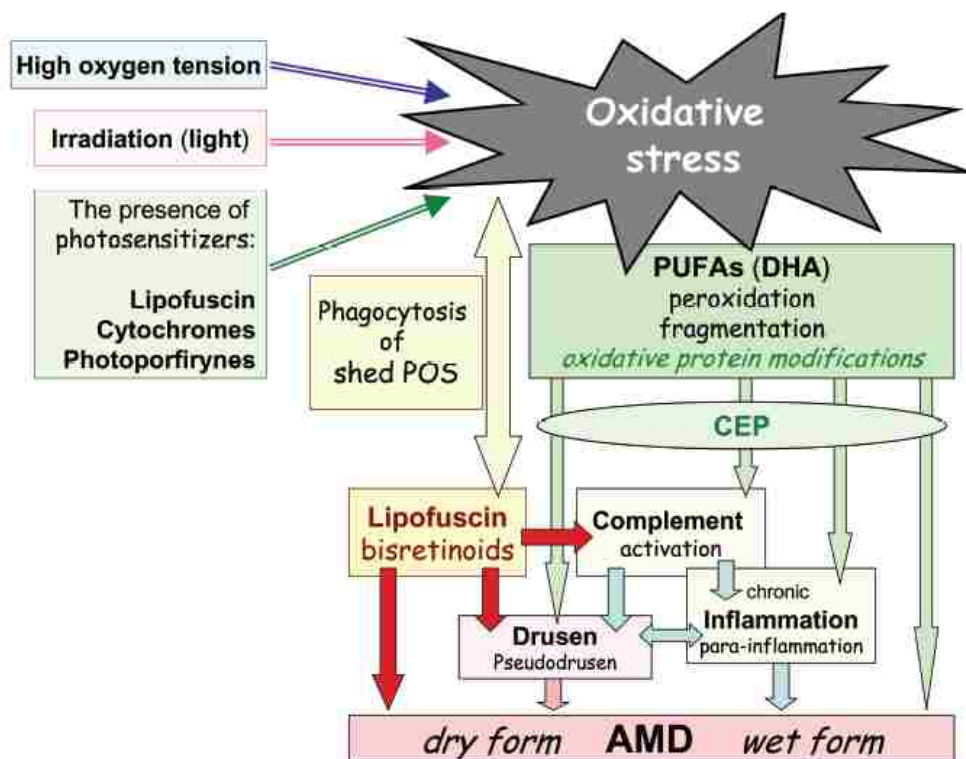
Figure 1.21 Key role of oxidative stress in AMD pathogenesis (adapted from Nowak, J.Z. [66]). **POS**, photoreceptor outer segment; **CEP**, carboxyethylpyrrole; **DHA**, docosahexaenoic acid.

### 1.4.4. Treatment and the Results of Age-Related Eye Disease Study

**(AREDS).** Treatment options for dry AMD are limited. Early AMD is asymptomatic and

often goes untreated until more severe symptoms manifest as the disease progresses. For

intermediate and late dry AMD, the only currently available treatments are aimed at

slowing the progression to advanced AMD and include vitamin and micronutrient

supplementation, cessation of smoking, and dietary modification [60, 61].

In prospective large trials, like the Age-Related Eye Disease Studies (AREDS and

AREDS2), conducted by the U.S. National Eye Institute, a wide variety of nutrients were

studied, including ω-3 fatty acids, antioxidants (β-carotene and vitamins C and E),

minerals (zinc and copper), and xanthophyll carotenoids (lutein and zeaxanthin) [67, 68].

The first AREDS trial was performed in 1990, and results showed that a combination of

vitamin C (500 mg/day), vitamin E (400 IU/day), β-carotene (25,000 IU)/day), zinc (zinc

oxide, 80 mg/day), and copper (cupric oxide, 2 mg/day) can reduce the risk of late AMD

by 25% [69]. The follow-up ARDES2 study was initiated in 2006, for a period of over 5

years, to evaluate the effects of adding lutein, zeaxanthin, and ω-3 fatty acids to the

original AREDS formulation on progression to advanced AMD. A further modification

of the original AREDS formulation was the elimination of β-carotene because of possible

pro-oxidant activity that could increase lung cancer risk in smokers. The AREDS2

formulas incorporated either lutein and zeaxanthin (10 mg/day and 2 mg/day) or DHA

and EPA (350 mg/day and 650 mg/day) [70]. Compared with results for participants

treated with the original formulation (with β-carotene, but neither lutein nor zeaxanthin),

those who were administered the AREDS2 formulation (with lutein and zeaxanthin but

no β-carotene) had an 18% lower risk of progressing to advanced AMD (95% CI, 0.69-

0.96; $P = 0.02$) [68, 71].

Exudative AMD is characterized by choroidal neovascular membrane formation.

The available treatments include anti-VEGF therapy (e.g., ranibizumab), macular thermal

laser photocoagulation, and photodynamic therapy (PDT, e.g., Visudyne®) to minimize or

block new blood vessels [72]. For dry AMD, however, there is currently no FDA-approved

treatment. Although numerous investigations of candidate treatments have been

conducted, the results of these studies are inconclusive. Therefore, there is a dire need for

an effective AMD treatment. An ideal therapeutic agent should be highly bioavailable,

non-toxic, easy to use, and economical. It should also limit oxidation, boost anti-

oxidative mechanisms, and even reverse existing damage.

**1.4.5.  The Protective Effect of NACA in Eye-Related Research.** For more

than a decade, our research group has been investigating the use of thiol antioxidants,

particularly N-acetylcysteine amide (NACA)[73-75], in oxidative stress-related eye

disorders such as cataracts and AMD [43, 76-80]. The immortalized ARPE-19 cell line and

primary cultures of RPE cells were used as *in vitro* models. ROS generation and lipid

peroxidation induced by *tert*-butyl hydroperoxide (TBHP) were reversed by pretreatment

with NACA. NACA also protected against TBHP-induced cell damage by increasing

cellular levels of GSH, increasing antioxidant enzyme glutathione peroxidase (GPx)

activity, and maintaining cellular integrity, as measured by transepithelial electrical

resistance (TEER). In an animal model, phototoxicity-induced photoreceptor cell death

and dysfunction were prevented by NACA [77].

**1.5.  OTHER OXIDATIVE-STRESS RELATED EYE DISORDERS**

Oxidative stress and ROS are involved in the pathogenesis of numerous eye

disorders [81, 82], especially in age-related cataract [83], age-related macular degeneration

(AMD), open-angle glaucoma [84], and diabetic retinopathy [85, 86]. They are also

implicated in autoimmune uveitis and pseudoexofoliation syndrome (PEX). Important

features of these diseases and the role of oxidative stress in each will be discussed briefly

in the following section. Table 1.4 summarizes the major risk factors and role of

oxidative damage in oxidative stress-related ocular diseases.

Table 1.4 Summary of the risk factors of oxidative-stress related ocular diseases and the role of oxidative stress in pathogenesis of each

| Ocular Disorders *-tissue affected* | Types | Major Risk Factors | Role of ROS & Oxidative Damage |
|---|---|---|---|
| Cataract *-lens* | Nuclear<br><br>Cortical<br><br>Subcapsular | Age<br>Sunlight (UV-B)<br>UV light<br>Diabetes<br>Microwave radiation<br>-ref: [87] | ↓ GSH,<br>↓Antioxidant enzymes<br>Internal $H_2O_2$<br>↓ Protein sulfhydryl<br>Crystalline cross-linkage |
| AMD - *Photoreceptor, RPE, Bruch's Membrane,; neovascularization* | Dry (Geographic Atrophic)<br><br>Wet (Choroidal neovascularization) | Age<br>Tobacco smoking<br>UV light<br>High fat diets<br>Cataract surgery<br>Complement H<br>-ref:[63, 88] | ↓ GSH,<br>↓Antioxidant enzymes<br>High oxygen tension<br>High metabolic activity<br>High energy light<br>Photo-oxidative damage<br>PUFA (↑4-HNE, CEP) |
| Glaucoma *-ganglion cells, optic nerve* | Open-Angle (Partially blocks the drainage)<br><br>Angle-Closure (Iris blocks the drainage angle) | High intraocular pressure<br>Family history<br>Age<br>Thin cornea<br>Eye surgery<br>Using corticosteroid<br>Farsightedness | TM oxidative stress<br>DNA damage (Mitochondria, TM)<br>Lipid peroxidation |
| Retinitis Pigmentosa (RP) - *photoreceptors* | Rod-cone dystrophy | Genetics | High oxygen tension<br>↓oxygen consumption |
| Diabetic retinopathy (DR) - *macula; neovascularization* | Non-Proliferative DR<br><br>Proliferative DR | Diabetes<br>Hyperglycemia<br>Hypertension<br>Dyslipidemia<br>-ref: [89] | Hyperglycemia<br>Polyol pathway<br>(↓ NADPH)<br>PKA activation |
| Autoimmune uveitis *-outer segment of retina* | | | PR DNA damage (mitochondria) |
| Pseudoexofoliation syndrome (PEX) - *systemic disease in the anterior segment of eye* | | Age | ↓GSH<br>↑MDA in lens epithelial cell |

**RPE**, retinal pigment epithelium; **NPDR**, non-proliferative diabetic retinopathy; **PDR**, proliferative diabetic retinopathy; **4-HNE**, 4-hydroxyl-2-nonenal; **CEP**, carboxyethylpyrrole; **TM**, trabecular meshwork.

**1.5.1. Cataract.** A cataract is the progressive opacification of the lens, resulting in blurred vision. Cataracts are the leading cause of blindness worldwide and account for 42% of all blindness [90]. While the primary cause of cataracts is age, they are also common in diabetes where superoxide levels in the mitochondria are elevated as a result of hyperglycemia [90]. Increased serum MDA levels and decreased blood levels of enzymatic antioxidants SOD and GPx are also indicators of oxidative stress observed in cataract patients [91]. α-Crystallin, a major protein family in the lens, is responsible for the maintenance of lens transparency. It has been demonstrated that exposure to UV light induces cross-linking of α-, β- and γ-crystallins [87]. α-Crystallins can also act as chaperons against photodamage from UV light [92]. Figure 1.22 shows how aging and diabetes affect the chaperone function of α-crystallins in cataract formation [92].
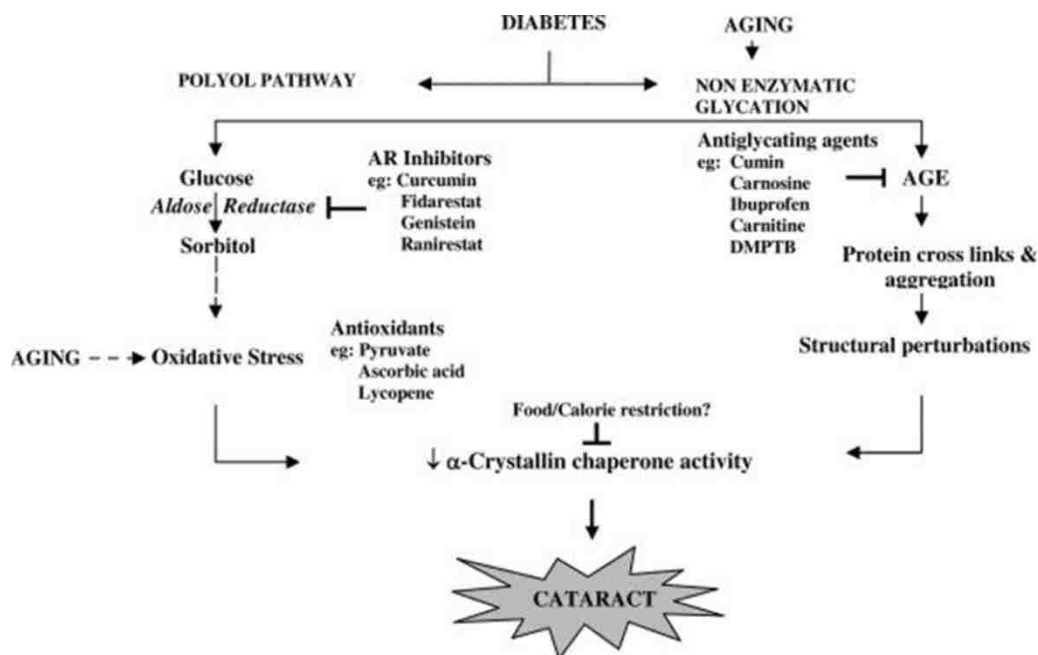


Figure 1.22 The possible molecular events affecting chaperone function of α-crystallins during aging and diabetes and potential target points for modulation α-crystallin chaperone function (adapted from Kumar, P & Reddy G. [92]).

**1.5.2. Glaucoma.** In this disease, fluid builds up in the anterior chamber of the eye, which increases intraocular pressure and results in retinal ganglion cell apoptosis and damage to the optic nerve. Glaucoma is the second most common cause of blindness worldwide [84]. The trabecular meshwork (TM) has fewer antioxidant defenses than the cornea and iris, thus making it the most sensitive tissue to oxidative insult in the anterior chamber of the eye. There are three key pieces of evidence that suggest TM cells are subject to a highly oxidizing environment [82, 84]. First, increased hydrogen peroxide ($H_2O_2$) measured in the aqueous humor outflow depletes glutathione [93]. Secondly, the antioxidant potential in TM tissue from open-angle glaucoma patients was lower than that in controls [94]. Finally, increased ROS levels ($H_2O_2$) have been shown to damage to mitochondrial DNA in the TM. Oxidative stress, occurring not only in the TM but also in retinal cells, appears to be involved in the neuronal cell degeneration affecting the optic nerve in open-angle glaucoma [82, 95]. The oxidation in the TM involved in the pathogenesis of open-angle glaucoma is shown in Figure 1.23.
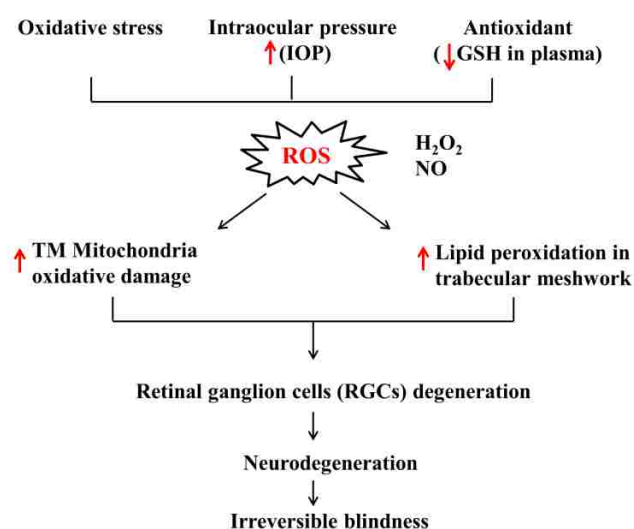


Figure 1.23 Key role of oxidative stress in glaucoma pathogenesis.

**1.5.3. Diabetic Retinopathy (DM).** Diabetic retinopathy is one of the most common microvascular complications in diabetes mellitus (DM) patients and is the leading cause of blindness and visual dysfunction in working-age populations [96, 97]. Hyperglycemia induces ROS production in mitochondria, leading to increased levels of reactive oxygen metabolites in type 2 DM patients [85]. Hyperglycemia upregulates the polyol pathway (also called the sorbitol-aldose reductase pathway), resulting in decreased NADPH available for GR-catalyzed regeneration of GSH from GSSG [86]. Hyperglycemia also activates PKC and contributes to ROS formation. Figure 1.24 shows the relationship between hyperglycemia and oxidative stress in the pathogenesis of diabetic retinopathy [86].
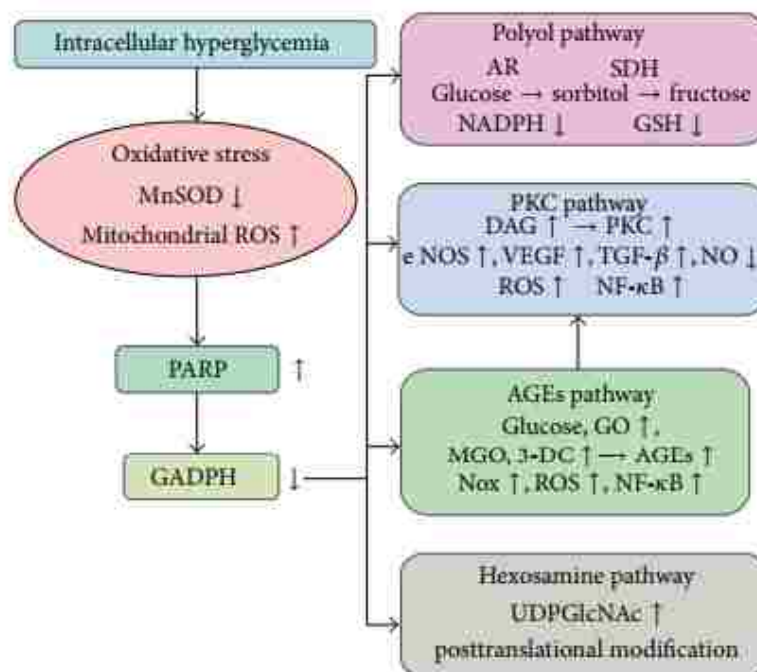


Figure 1.24 Relationship between hyperglycemia, oxidative stress, and pathways associated with the pathogenesis of diabetic retinopathy (adapted from Wu, Y. *et al.* [86]).

**1.5.4. Retinitis Pigmentosa (RP).** RP, also known as rod-cone dystrophy, is an inherited eye disorder that causes photoreceptor breakdown and retinal degeneration. Human ONL is composed of 95% rods and 5% cones. Oxidative damage is a major contributor to cone cell death. Oxygen utilization is greatly reduced after rods die, which eventually disturbs the oxygen balance in the outer retina. High oxygen tension and NADPH oxidase activation cause superoxide radical production in both mitochondria and cytoplasm in cones [98, 99].

**1.5.5. Autoimmune Uveitis.** The uvea is the layer located between the sclera and the retina that includes the iris, ciliary body, and choroid. Inflammation during uveitis is strongly correlated with ROS generation [100]. Oxidative stress caused by DNA damage in photoreceptor mitochondria likely initiates the pathological effects. Figure 1.25 shows the role of oxidative stress in autoimmune uveitis as well as the effect of antioxidants in preventing uveitis complications [100].

**1.5.6. Pseudoexfoliation Syndrome (PEX).** PEX is an age-related fibrillopathy of the eye. It is characterized by the accumulation of granular material on the anterior segment structures of the eye and is associated with glaucoma and cataract surgery complications [81, 101]. Decreased GSH levels and increased lipid peroxidation by-product malondialdehyde (MDA) levels were found in the lens epithelial cells of PEX patients, which may indicate oxidative stress involvement in the pathogenesis of this syndrome [102].
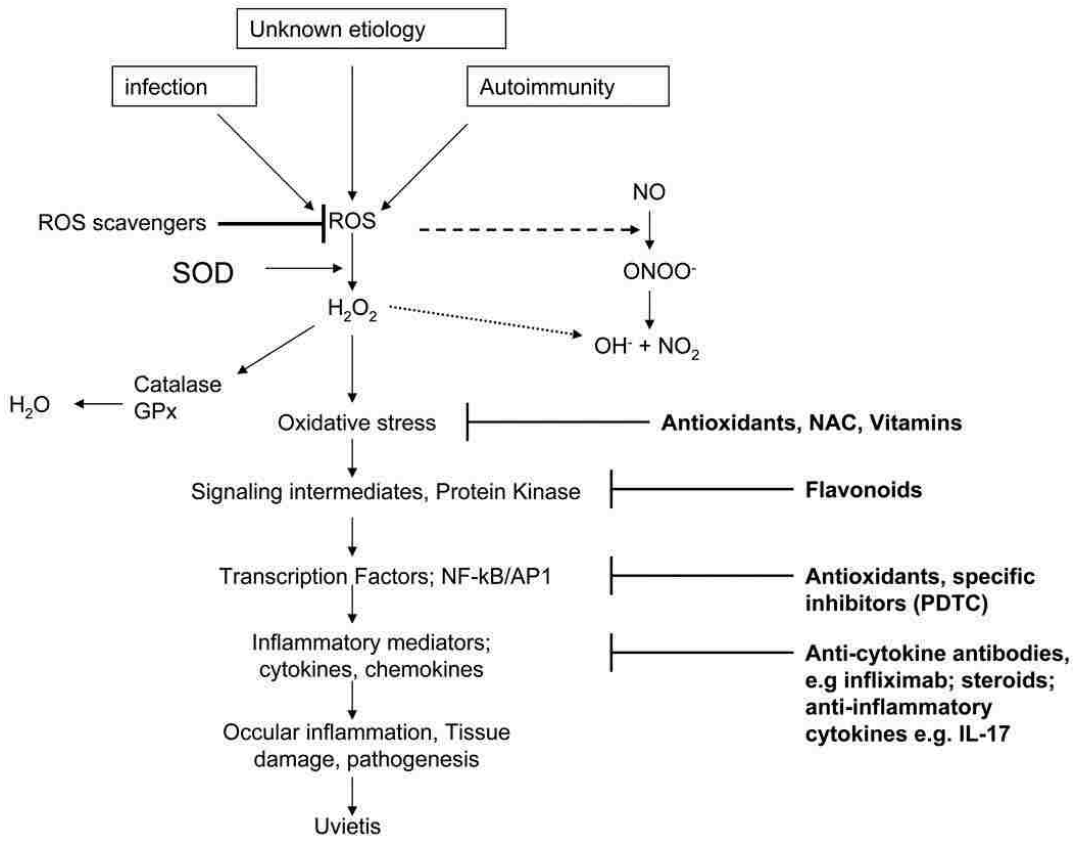
Figure 1.25 Effects of antioxidants in preventing uveitis (adapted from Gartaganis, S.P. *et al.* [102]).

## 2. EXPERIMENTAL DESIGN

Since oxidative stress is strongly implicated in the pathogenesis of AMD, we hypothesized that N-acetylcysteine amide (NACA), a novel thiol antioxidant, would impede the progression of oxidative stress-induced retinal degeneration. We designed an *in vitro* and an *in vivo* model to investigate the effectiveness of NACA in preventing retinal pigment epithelial cell and retinal cell damage.

In an *in vitro* model, we tested the ability of NACA to prevent oxidative stress induced by *tert*-butyl hydroperoxide in primary human retinal pigment epithelial cells (HRPEpiC) (Figure 2.1).

## Role of NACA in defending HRPEpiC against TBHP-induced oxidative stress
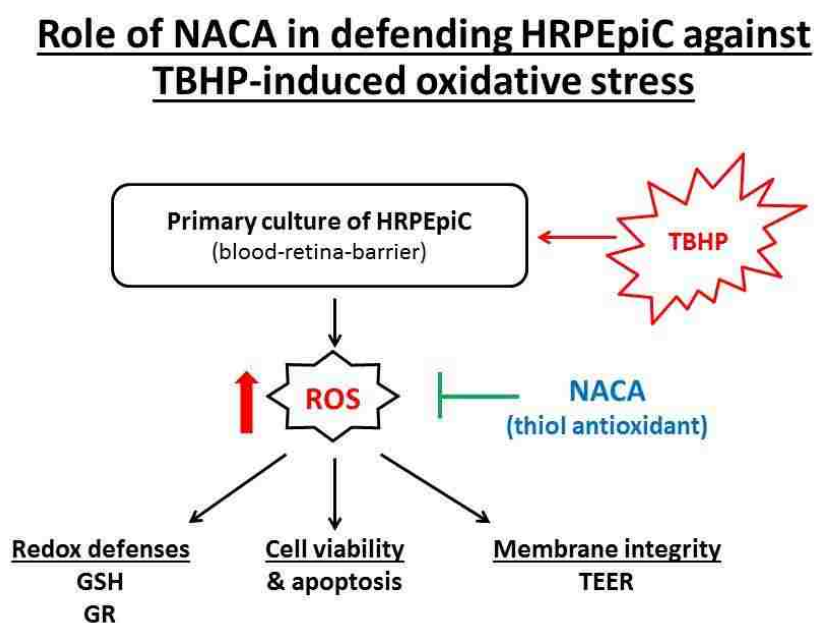
Figure 2.1 The experimental hypothesis of NACA's role in defending RPE cells against oxidative stress in a cell model.

In an animal model, we investigated the effectiveness of NACA eye drops in preventing and/or delaying photoreceptor loss and maintaining visual potential in sodium iodate-induced retinal degeneration in C57BL/6 mice (Figure 2.2).

## Role of NACA in defending against oxidative stress-related AMD

**Smoking**
**Exogenous sources (blue-light)**
**Endogenous source (mit.)**
**\* Oxidant (TBHP & NaIO$_3$)**

**Antioxidant enzyme (SOD, GPx, GR)**
**Free radical scavenger (GSH)**

↑ ROS ⊣ **NACA**
**(thiol antioxidant)**

↑inflammation  ↑Lipid & protein  ↓GSH
peroxidation

*Age-Related Macular Degeneration*

➢ peroxidation of PUFAs
➢ lipofuscin
➢ RPE cell death
➢ drusen formation
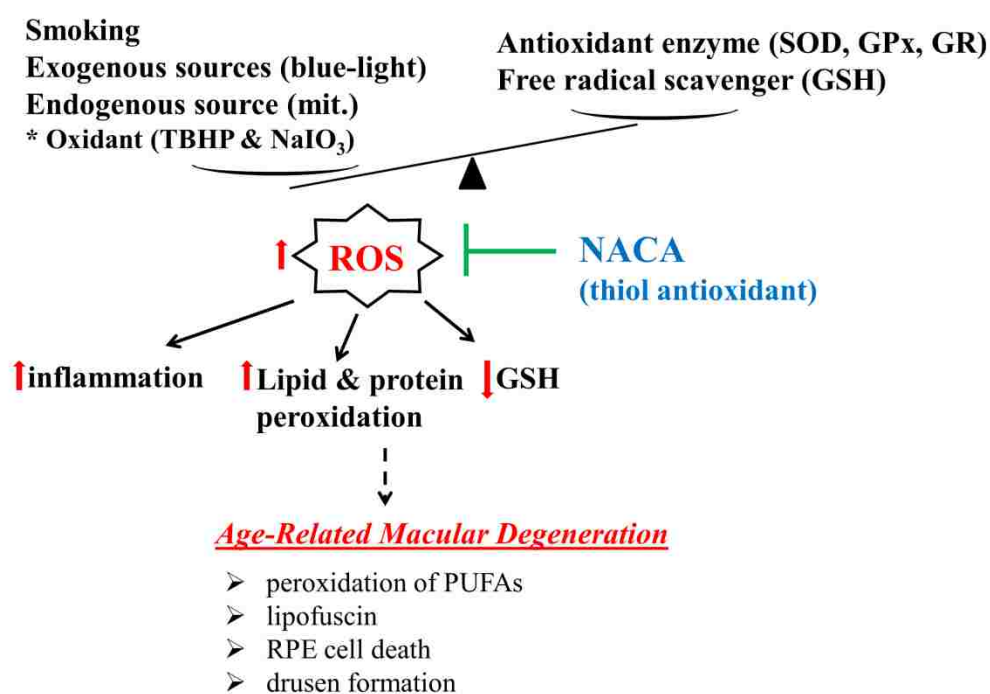
Figure 2.2 The experimental hypothesis of NACA's role in defending against sodium iodate-induced retinal degeneration in an animal model.

Sodium iodate was first used in 1941 to selectively induce retinal degeneration in rabbits. Systematic delivery of NaIO$_3$, a stable oxidizing agent, is an effective way to induce retinal degeneration, with loss of retinal function followed by local morphological changes in RPE cells and photoreceptors, and significant ONL thinning.

To study the effectiveness of NACA eye drops in preventing retinal degeneration, we utilized an animal model with sodium iodate-treated C57BL/6 mice. The details of the experimental design are outlined in Figure 2.3.

## Sodium iodate-induced retinal degeneration

C57BL/6 mice: 7-8 weeks old, male (Jackson Laboratory)

| Group | Eye drop | Injection (IP) |
|---|---|---|
| Control | Buffer* | Buffer |
| NACA only | 0.1% NACA | Buffer |
| $NaIO_3$ only | Buffer* | $NaIO_3$ |
| $NaIO_3$ + NACA | 0.1% NACA | $NaIO_3$ |

*25mM Phosphate buffer, pH=7.4

$NaIO_3$, IP (75 mg/kg )

7 weeks old

+1 wk    +4 wks    + 1wk

ERG base line

Eye drop
(20μL on both eyes twice a day
& every day for 4 wks)

@ 36hr recording ERG
@ Day 7 Sacrifice & collect
sample for GSH, ONL, 4-HNE
& Western blot
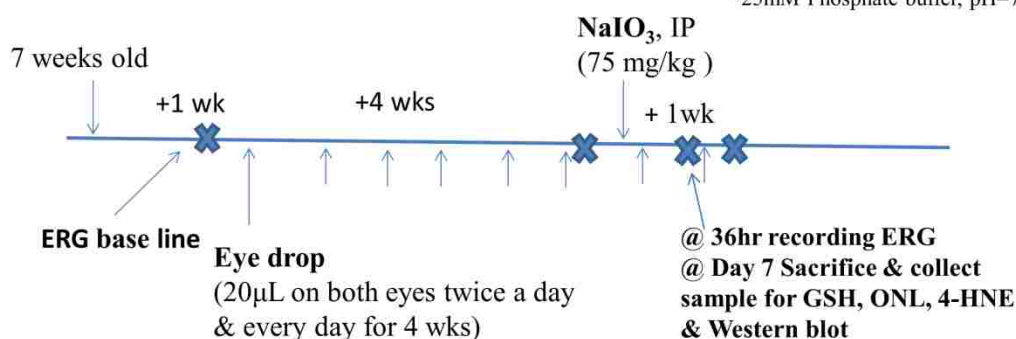
Figure 2.3 Experimental design for sodium iodate-induced retinal degeneration in C57BL/6 mice.

# 3. MATERIALS & METHODS

## 3.1. MATERIALS

N-acetylcysteine amide (NACA) was provided by Dr. Glenn Goldstein (David Pharmaceuticals, New York, NY, USA). C57BL/6 mice were obtained from the Jackson Laboratory (Bar Harbor, ME, USA). Other chemicals were ordered from Sigma (St. Louis, MO, USA), unless otherwise indicated.

Human retinal pigment epithelial cells (HRPEpiC, CAT # 6540) were purchased from ScienCell Research Laboratories (Carlsbad, CA, USA). HRPEpiC were grown as suggested by ScienCell, and all experiments were performed during passages 4 and 5.

## 3.2. CELL CULTURE CONDITIONS

HRPEpiC were grown in complete media and divided in to four groups (control, NACA, TBHP, and NACA+TBHP). Cells were pretreated with 2 mM NACA (in NACA and NACA+TBHP groups) or serum-free media (in control and TBHP groups). After 4 hours of incubation, the media was removed, and cells were washed with PBS and then dosed with 0.5 mM TBHP (in TBHP and NACA+TBHP groups) or serum free media (control and NACA groups) for 3 hours. For apoptosis assays, an alternative NACA and TBHP dosing protocol was used in addition to the one described above. This involved pretreatment with NACA for 1 hour (in NACA and NACA+TBHP groups) prior to TBHP exposure and addition of NACA (in NACA and NACA+TBHP groups) to the media for an additional 3 hours while TBHP was applied (i.e., cells were co-exposed to TBHP and NACA for 3 hours).

### 3.3.  CELL VIABILITY ASSAY

Calcein-AM is a cell-permeant dye that can be used to determine cell viability in most eukaryotic cells. In living cells, the non-fluorescent Calcein-AM is converted to green-fluorescent Calcein after acetoxymethyl ester hydrolysis by intracellular esterases. The structure of  Calcein-AM and its staining mechanism is illustrated in Figure 3.1[103].

Each well of 96-well plate contained $1 \times 10^4$ cells were grown in complete media for 24 hours before further dosing. After cells were rinsed with 1X PBS (37 °C), cells were treated as indicated in the experimental design. Each well of cells was replaced with 100 µL of 2 µM Calcein-AM (Biotium Inc., CA, USA) in 1X phosphate buffered saline (PBS), and cells were incubated for 30 min before measuring the fluorescence by a plate reader ($\lambda_{ex}$ = 485 nm and $\lambda_{em}$ = 530 nm) (FLUOstar Omega, BMG Labtech).
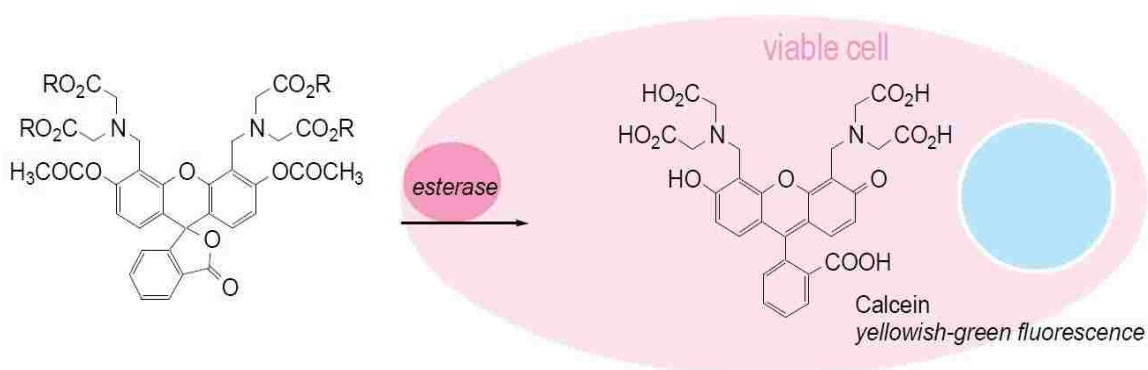


Figure 3.1 Calcein-AM staining mechanism (adapted from Dojindo Molecular Technologies, Inc. [103]).

### 3.4. INTRACELLULAR REACTIVE OXYGEN SPECIES (ROS) MEASUREMENT

Cellular ROS accumulation was measured using 5-(and-6)-chloromethyl-2′,7′-dichlorodihydrofluorescein diacetate, acetyl ester (CM-H$_2$DCFDA, Molecular Probes, Life Technologies) [104-106]. CM-H$_2$DCFDA is a chloromethyl derivative of H$_2$DCFDA (2′,7′-dichlorodihydrofluorescein diacetate; molecular formula: C$_{24}$H$_{16}$Cl$_2$O$_7$) and exhibits better retention in live cells than H$_2$DCFDA. CM-H$_2$DCFDA passively diffuses into cells, where its acetate groups are cleaved by intracellular esterases, and its thiol-reactive chloromethyl group reacts with intracellular glutathione and other thiols. Subsequent oxidation yields a fluorescent adduct that is trapped inside the cell and can therefore be detected for extended periods of time, making CM-H$_2$DCFDA a valuable tool for ROS quantification during a longer-term experimental design. The structure of CM-H$_2$DCFDA and the mechanism of ROS measurement are illustrated in Figure 3.2.

Each well of 96-well plate contained $1\times10^4$ cells were grown with complete media for 24 hours. CM-H$_2$DCFDA was freshly dissolved in dimethyl sulfoxide (DMSO) to make 10 mM stock solution, then further diluted in 1X PBS to make working solution and kept from light exposure. After the cells were rinsed with 1X PBS (37 °C), 100 μL of 10 μM CM-H$_2$DCFDA in 1X PBS (37 °C) were added to each well, and then plates were placed back to incubator for another 30 min. Each well was rinsed carefully with 1X PBS to remove extra CM-H$_2$DCFDA after incubation. Cells were dosed with NACA and/or TBHP in 100 μL of serum-free, phenol red-free media according to the experimental design. Fluorescence was measured after treatment by a plate reader ($\lambda_{ex}$ = 485 nm and $\lambda_{em}$ = 530 nm) (FLUOstar Omega, BMG Labtech).
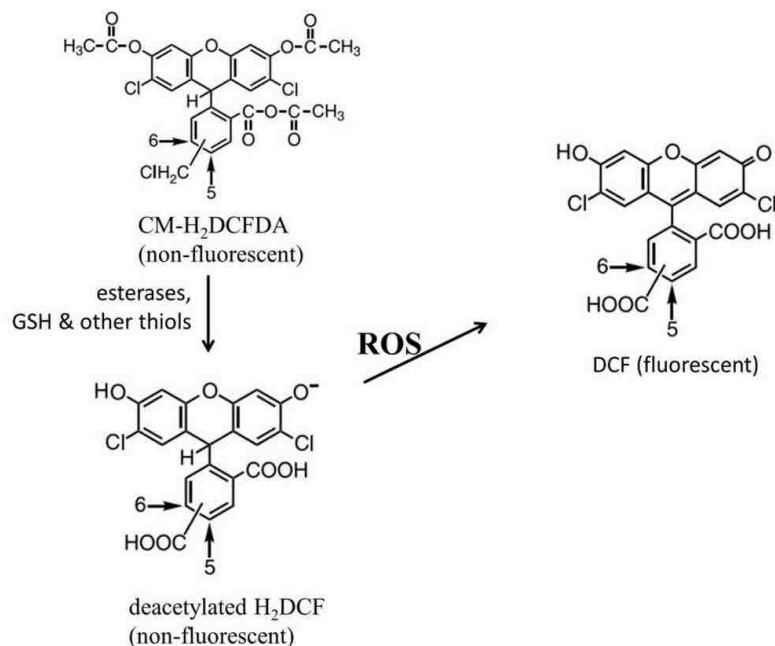
Figure 3.2 The measurement of ROS by CM-H₂DCFDA.

## 3.5. QUANTIFICATION OF INTRACELLULAR GLUTATHIONE (GSH) AND CYSTEINE LEVELS.

GSH is the primary endogenous antioxidant responsible for redox homeostasis in endothelial cells. Cells were grown at a density of $1.2 \times 10^6$ cells per 10-cm plate for 24 hours before further treatment. Cell pellets were homogenized in serine borate buffer (pH = 7.5). Supernatant fractions were collected after centrifugation at 1000 xg at 4 °C for 10 min. GSH was separated and quantified by HPLC with fluorescence detection (Finnigan Surveyor FL Plus, Thermo Scientific, USA) after derivatization of cell homogenates with N-(1-pyrenyl) maleimide (NPM) (Figure 3.3) [107-109]. The mobile phase gradient program used for analysis of cysteine and GSH is shown in Table 3.1.

For derivatization, retinas were homogenized in 230 μL of serine borate buffer (pH = 7.5). 50 μL of retina homogenate were mixed with 25 μL of serine borate buffer,

and 225 µL of NPM was added to derivatize at room temperature for 5 min. Finally, 3 µL

of 2 N HCl were added to quench the reaction. Representative separation of a mixed thiol

standards and a retina sample by HPLC are shown in Figures 3.4 and 3.5. GSH level is

then reported in units of nmol/mg protein.



$(\lambda_{ex} = 330 \text{ nm and } \lambda_{em} = 376 \text{ nm})$
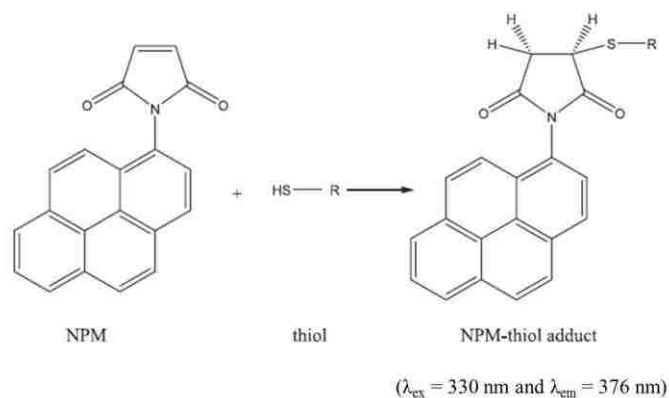
Figure 3.3 Formation of fluorescent NPM-thiol adduct (adapted from Wu, W. *et al.* [107]).

Table 3.1 Gradient program of mobile phase used in the HPLC separation

| Time (min) | Mobile phase A (%) | Mobile phase B (%) | Flow rate (mL/min) |
|---|---|---|---|
| 0.0 | 100 | | 0.7 |
| 6.0 | 100 | | 0.7 |
| 6.1 | | 100 | 1 |
| 20.0 | | 100 | 1 |
| 20.1 | 100 | | 0.7 |
| 25 | 100 | | 0.7 |

The mobile phase A was composed of 0.05% acetic acid in 70:30 acetonitrile–
HPLC-$H_2O$ (vol : vol) in 1 liter of mobile phase.
The mobile phase B was composed of 0.1% o-phosphoric acid and 0.1% acetic
acid in 70:30 acetonitrile–HPLC $H_2O$ (vol : vol) in 1 liter of mobile phase.
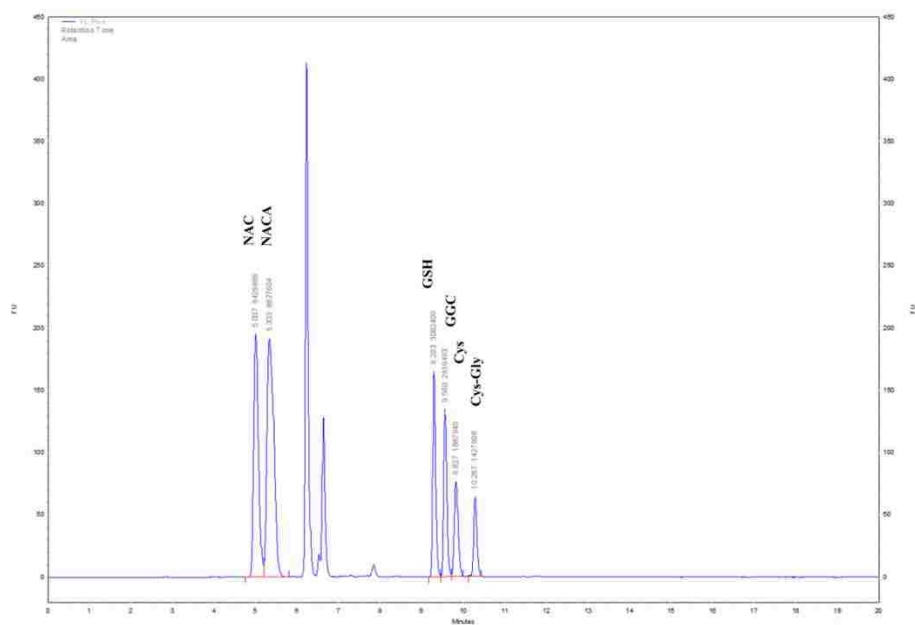
Figure 3.4 The above HPLC chromatogram showing the separation of a derivatized mixed thiol standard.
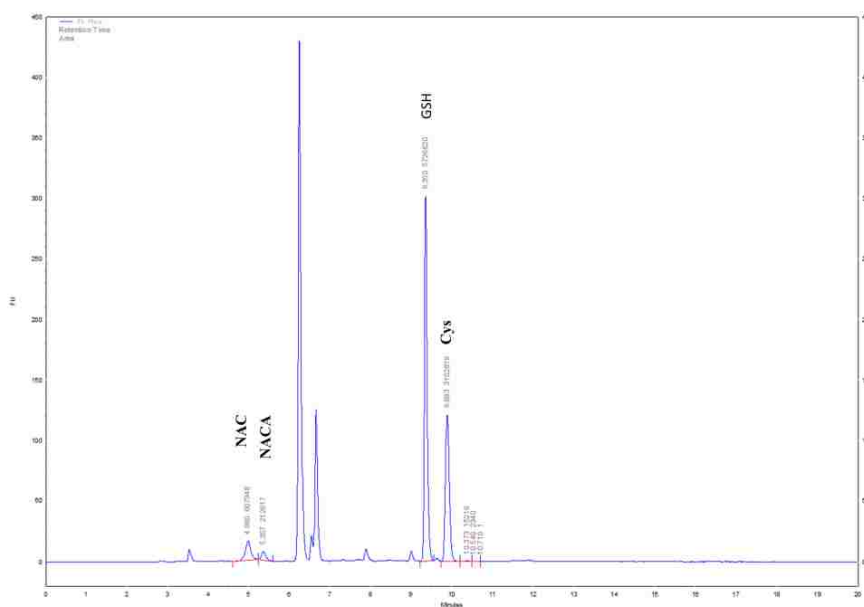


Figure 3.5 The above HPLC chromatogram showing the separation of a derivatized retina sample.

### 3.6.  GLUTATHIONE REDUCTASE (GR) ACTIVITY ASSAY.

Glutathione reductase (GR, EC 1.6.4.2) catalyzes the reduction of glutathione disulfide (GSSG) to GSH. This assay is based on the reduction of GSSG by NADPH in the presence of the enzyme. Cells were homogenized in 250 μL of 50 mM Tris-HCl (pH = 7.5) containing 1 mM EDTA. After centrifugation at 1000 xg for 15 min, the supernatant fractions were isolated. NADPH, which absorbs light at 340 nm, was added to each sample. The rate of its oxidation to NADP$^+$ by GR as GSSG is reduced to 2 GSH can be determined from the resulting decrease in absorbance at this wavelength over time [110, 111].

$$GSSG + NADPH + H^+ \xrightarrow{\text{Glutathione Reductase}} 2GSH + NADP^+$$
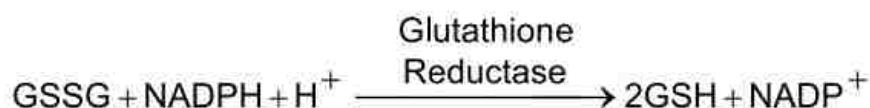
Reaction mixture:

800 μL of diluted supernatant + 40 μL of 25 mM GSSG + 160 μL of 1.25 mM NADPH (Proportion of supernatant should be increased if the rate of reduction in NADPH absorbance, $[-\Delta A]$/min is less than 30 mAbs/min).

GR activity calculation step by step:

The molar extinction coefficient ε for NADPH at 340 nm is 6220 M$^{-1}$cm$^{-1}$. The activity of GR can be calculated according to the Beer-Lambert law as follows:

Given: $\varepsilon = 6220$ M$^{-1}$cm$^{-1}$ when the path length = 1 cm;

$\varepsilon = 6.22 \times 10^{-3}$ (nmol/mL)$^{-1}$;

1 mU = 1 nmol/min (i.e., 1 mU GR reduces 1 nmol NADPH per min);

Then: mU/mL = $(\Delta A_{340}/\text{min})/\varepsilon$, or mU/mL = $[A_{340}/\text{min}]/[6.22 \times 10^{-3}$ mL/nmol];

mU/mg = (mU/mL)/(mg/mL protein)

GR activity is then reported in units of mU/mg protein.


## 3.7.  QUANTIFICATION OF TOTAL PROTEIN

Protein levels of the cell homogenates were measured by the Bradford method [112] (BioRad Laboratories, Inc., CA, USA) and BCA protein assay [113] (ThermoFisher Scientific, NY, USA). Bovine serum albumin was used as the protein standard. The protein concentration is reported in units of mg/mL protein.

The Bradford protein assay, which was performed using Coomassie® Brilliant Blue G-250, was used for total protein concentrations between 5 mg/mL to 50 mg/mL. After 20 μL of the protein was mixed with 1 mL of Coomassie® Brilliant Blue G-250 solution, the absorbance shifted from 465 nm to 595 nm when the protein was bound to the dye.

The bicinchoninic acid assay (BCA assay) was used for total protein quantification especially when samples with protein concentrations between 0.5 μg/mL to 1.5 mg/mL. The method involved reduction of $Cu^{2+}$ to $Cu^+$ by protein in an alkaline solution (Step 1 in Figure 3.6), and formed a purple-colored BCA-$Cu^+$ complex that absorbs light at 562 nm (Step 2 in Figure 3.6) [114].

Step 1    Protein + Cu$^{2+}$  $\xrightarrow{\text{OH}^-}$  Protein + Cu$^{1+}$

Step 2



**Bicinchoninic Acid (BCA) sodium salt**          **BCA-Copper Reaction**

**Purple at $\lambda_{562}$ nm**
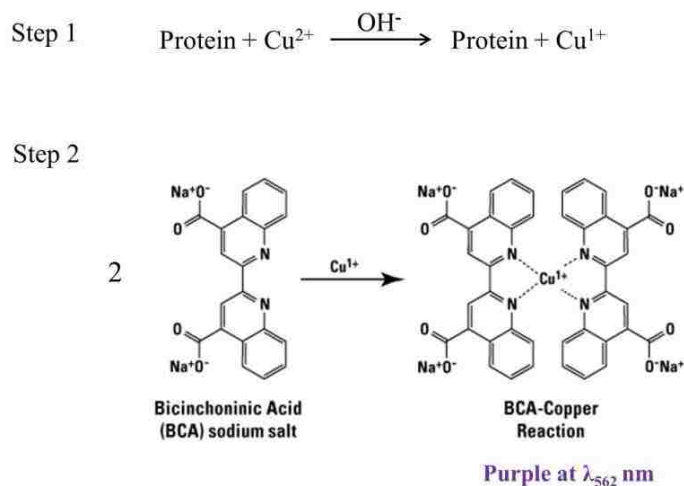
Figure 3.6 Reaction schematic for the BCA protein assay (adapted from ThermoFisher website [114]).

## 3.8. DEXTRAN PERMEABILITY AND TRANSEPITHELIAL ELECTRICAL RESISTANCE (TEER) MEASUREMENT

12-mm Transwell® (Product #3401) inserts were coated with poly-L-lysine for 1 hour prior to seeding with 0.5 mL of cell suspension at $1\times10^6$ cells/mL. Each well contained 1.5 mL of media, and cell growth was maintained for 5 days without disturbing the monolayer (Figure 3.7). Cells were treated with NACA and/or TBHP according to the experimental design. After an appropriate time, the treatment media in the insert was removed and replaced with 250 μL of serum-free, phenol red-free media. The insert was then relocated to a new plate containing 1.5 mL of fresh serum-free, phenol red-free media. Fluorescently labelled dextrans (FD4, 1 mg/mL in media, Sigma) were administered apically onto the insert after dosing. Fluorescence was read after 30 min ($\lambda_{ex}$ = 485 nm and $\lambda_{em}$ = 530 nm) (FLUOstar Omega, BMG Labtech, Cary, NC, USA). The inserts containing the monolayer were then transferred to new wells with 500 μL of

serum-free phenol, red-free media and used for TEER measurement. TEER readings
were recorded by an EVOM voltohmmeter (World Precision Instruments, Sarasota, FL,
USA) to assess the integrity of the HRPEpiC monolayer.

## Monolayer Integrity  Measurement
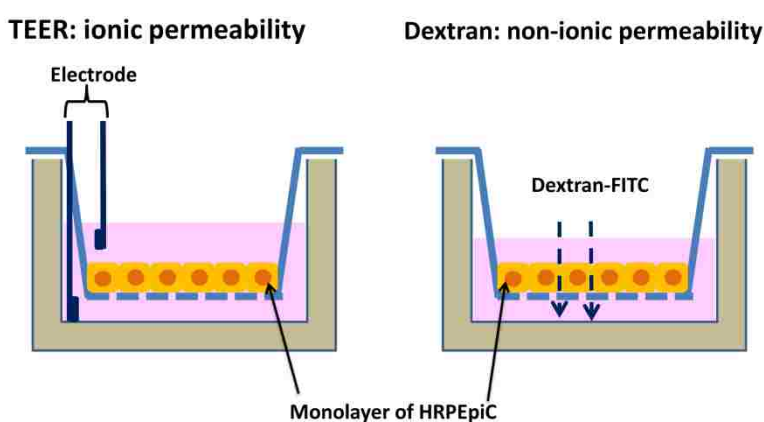


Figure 3.7 The monolayer integrity measurement (A) TEER and (B) Dextran
permeability.

## 3.9.  FLOW CYTOMETRY QUANTIFICATION OF APOPTOTIC CELLS

Cell suspension contained $6.5 \times 10^5$ cells were grown in each of 6-cm plates and
dosed as described by the experimental design. To conduct the apoptosis assay,
trypsinized cells were re-suspended in 100 μL of 1X binding buffer containing 5 μL of 7-
AAD and 5 μL of annexin V-FITC (BD Biosciences, San Jose, CA, USA). Cells were
incubated for 15 min at room temperature in the dark, followed by addition of 250 μL of
binding buffer. The cells were then analyzed using a Cell Lab Quanta SC flow cytometer
(Beckman Coulter, Fullerton, CA, USA).

## 3.10. ANIMAL MODEL AND EXPERIMENTAL DESIGN

Seven-week-old male C57BL/6 mice were received and housed in a temperature-
and humidity-controlled (about 22 °C and 55%, respectively) animal facility, with a 12-
hour light and dark cycle. The animals had free access to rodent chow and water; they
were acclimatized for 1 week before experiments were performed. All animal procedures
conformed to the ARVO Statement for the Use of Animals in Ophthalmic and Vision
Research and were approved by the Institutional Animal Care and Use Committee of
Missouri University of Science and Technology.

Eight-week-old C57BL/6 mice received 0.1% NACA eye drops (in 25 mM
phosphate buffer, pH 7.4) twice a day, on every other day for 4 weeks. After dosing with
NACA for 4 weeks, mice received one intraperitoneal (IP) injection of 75 mg/kg $NaIO_3$,
and then eye drops were continued for another week.

On the final day of the experiment, the mice were anesthetized by an IP injection
of ketamine (120 mg/kg) and xylazine (16 mg/kg) and cervical dislocation was used for
the secondary euthanasia method. Retinas were removed under a dissecting microscope
and immediately placed in liquid nitrogen immediately for further analysis.

## 3.11. ELECTRORETINOGRAPHY (ERG)

After adaptation in the dark for 10-12 hours, scotopic and photopic ERG were
recorded in mice under anesthesia induced by isoflurane (Butler Schein, Dublin OH)
(2.25% for induction and 1.25% maintenance). Proparacaine hydrochloride ophthalmic
solution and tropicamide (0.5%, Akorn Inc, IL, USA) were used for the topical anesthetic
and mydriatic, respectively. The recording electrode was placed in a drop of
methylcellulose on the surface of the cornea, a reference electrode was placed
subdermally at the vertex of the skull, and a ground electrode was placed subdermally at

the base of the tail (Figure 3.8). Scotopic and photopic ERGs [115, 116] were recorded using an HMsERG machine (OcuScience, Henderson, NV, USA). ERG procedures started with a scotopic intensity series from -3 to 1 log (cd·s/m$^2$). Photopic ERGs were recorded after light adaption (10000 mcd·s/m$^2$) for 5 min (mcd: millicandelas). The scotopic and photopic view program is illustrated in Figure 3.9. Signals obtained from corneal surfaces were amplified, digitized, and averaged using ERG View 2.5 software (Retvet Corp Ocuscience, Rolla, Missouri).

## The pictures in conducting electroretinography
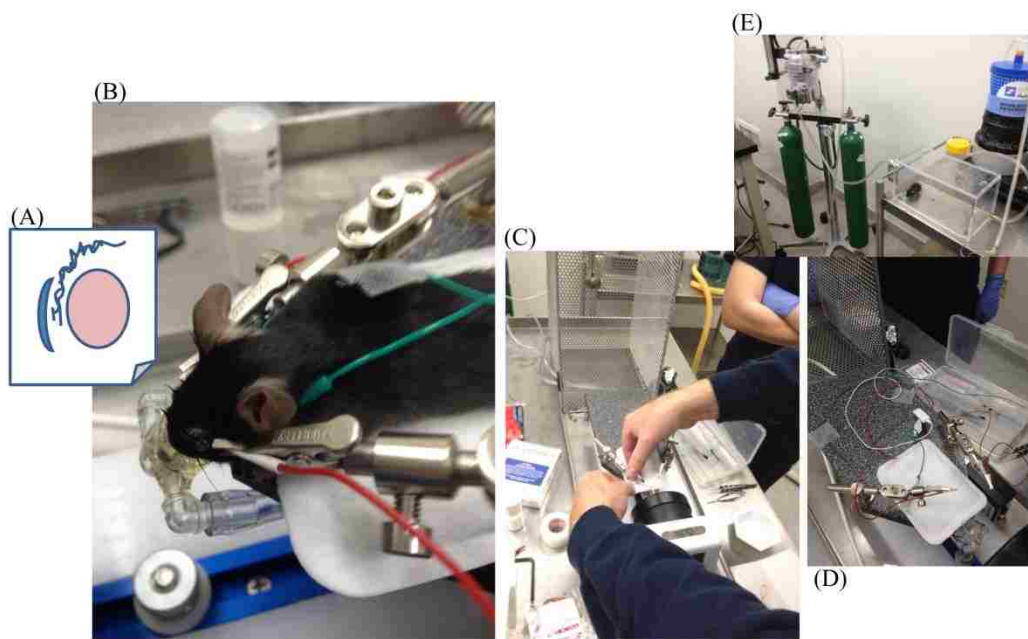


Figure 3.8 More pictures in conducting electroretinography. (A) The corneal electrode is placed between contact lenses and the cornea; (B) The placements of corneal electrode (red), skin electrode (green), and mask to introduce isoflurane; (C) and (D) The HMsERG system; (E) The isoflurane induction system.

| Scotopic/Photopic Subset | | | | | | | | | |
|---|---|---|---|---|---|---|---|---|---|
| | | | Flash Intensity | | | | | | |
| Step label | Action | | Log | mcd.s/m 2 | Number of Flashes Avg'd | Interval Seconds | Time Req. Seconds | Elapsed Time Seconds | response |
| | Test | 1 | -3 | 3 | 4 | 30 | 90 | 90 | |
| | Delay | | | | | | 30 | 120 | |
| | Test | 2 | -2 | 30 | 4 | 30 | 90 | 210 | |
| | Delay | | | | | | 30 | 240 | |
| | Test | 3 | -1 | 300 | 4 | 30 | 90 | 330 | rod only |
| | Delay | | | | | | 30 | 360 | |
| | Test | 4 | 0 | 3000 | 4 | 30 | 90 | 450 | mix |
| | Delay | | | | | | 30 | 480 | |
| | Test | 5 | 1 | 30000 | 4 | 30 | 90 | 570 | |
| Background Light Adaptation | | | | 10000 | | | 300 | 870 | |
| | Test | 6 | -0.25 | 2000 | 32 | 0.5 | 16 | 886 | |
| | Delay | | | | | | 2 | 888 | |
| | Test | 7 | -0.1 | 2500 | 32 | 0.5 | 16 | 904 | |
| | Delay | | | | | | 2 | 906 | |
| | Test | 8 | 0 | 3000 | 32 | 0.5 | 16 | 922 | |
| | Delay | | | | | | 2 | 924 | |
| | Test | 9 | 0.125 | 3500 | 32 | 0.5 | 16 | 940 | |
| | Delay | | | | | | 2 | 942 | |
| | Test | 10 | 0.25 | 4000 | 32 | 0.5 | 16 | 958 | |
| | Delay | | | | | | 2 | 960 | |
| | Test | 11 | 0.37 | 4500 | 32 | 0.5 | 16 | 976 | |
| | Delay | | | | | | 2 | 978 | |
| | Test | 12 | | 5000 | 32 | 0.5 | 16 | 994 | cone only |
| | Delay | | | | | | 2 | 996 | |
| | Test | 13 | 0.5 | 10000 | 32 | 0.5 | 16 | 1012 | |
| | Delay | | | | | | 2 | 1014 | |
| Flicker | Test | 14 | 0 | 3000 | 128 | 0.033 | 2 | 1016 | |
| Flicker | Test | 15 | 0.5 | 10000 | 128 | 0.033 | 2 | 1018 | |
| | | | | | Total Elapsed Time in Minutes | | | 16.97 | |

Figure 3.9 The program settings for the scotopic and photopic view in an ERG recording.

The ERG is a recording of a light-elicited diffuse electrical responses developed by cells within the retina [117]. Four different waveforms (a-wave, b-wave, c-wave and d-wave) may be observed, depending on the ERG program. The first negative peak was the a-wave, which was followed by a large, positive b-wave and a slower, positive c-wave. After termination of the stimulus, a d-wave developed. Figure 3.10 shows where the major components of the ERG originate. The ERG a-wave (called the "late receptor potential") originated from the photoreceptors, and the b-wave originated from the inner

retinal cells that are post-synaptic to the photoreceptors (Figure 3.10) [118]. The a-wave

and b-wave represented the health of the outer and inner retina, respectively. Analysis of

the ERG waveforms required measurement of the amplitude and the implicit time of each

wave (Figure 3.11) [118]. In the ERG program used for the investigations described here,

only the a-wave and b-wave were recorded and analyzed.
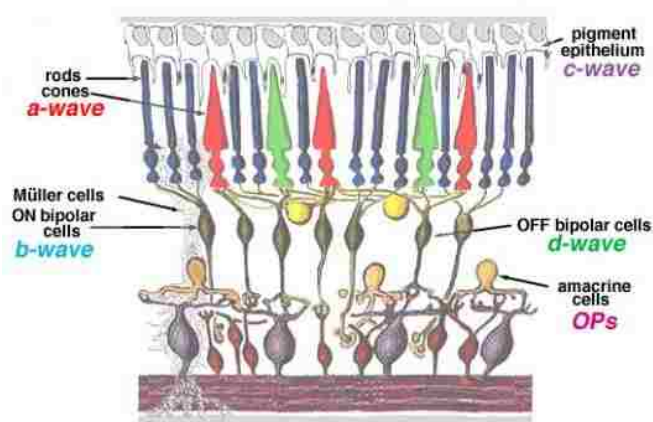


Figure 3.10 Diagram of the retina showing where the major components of the ERG originate (adapted from Creel, D.J. [115]). (OP, oscillation potential)
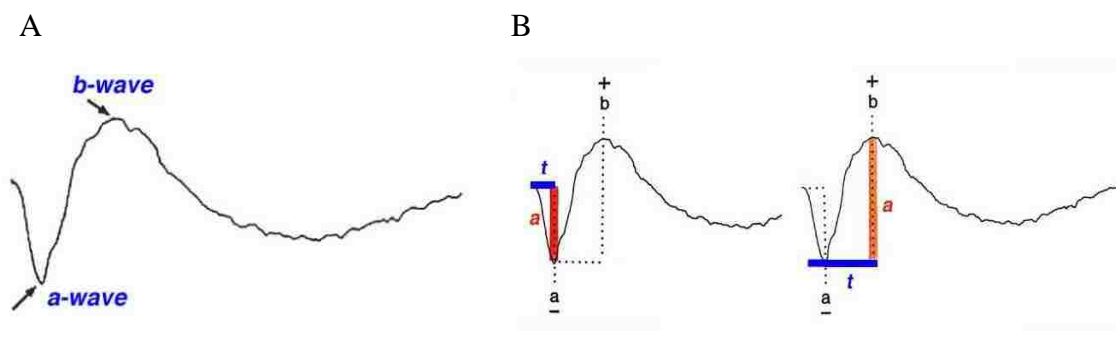


Figure 3.11 Electroretinogram (A) ERG waveform and (B) amplitude and implicit time measurement of the ERG waveform (adapted from Creel, D.J. [118]).

## 3.12. HEMATOXYLIN AND EOSIN (H&E) STAINING

Eyes were enucleated and fixed in 4% paraformaldehyde overnight. Briefly, the eyes were then embedded in paraffin, and serial 5-μm of sagittal sections of the whole eye were cut through the cornea to the optic nerve. Paraffin-embedded serial sections of the retina were deparaffinized with xylene and absolute ethanol, rehydrated with distilled water, stained with hematoxylin solution, and counterstained with eosin.

## 3.13. OUTER NUCLEAR LAYER (ONL) THICKNESS MEASUREMENT

In each fixed and H&E-stained eye ($n = 3$ mice), the ONL thickness was measured at 40-μm intervals across 400-μm sections of the parafoveal area located 500 μm from the optic nerve head. Images were analyzed at 20X objective magnification using ImageJ image processing software (Version 1.49, NIH). For every group, ONL thickness at each interval was averaged, and statistical analysis was performed.

## 3.14. 4-HYDROXYNONENAL (4-HNE) IMMUNOHISTOCHEMISTRY STAINING AND QUANTIFICATION

Briefly, serial sections adjacent to those designated for H&E staining were taken from paraffin-embedded eyes ($n = 3$ mice). Sections were deparaffinized, rehydrated, blocked, and incubated overnight at 4°C with an anti-4-HNE antibody (1:100 dilution; Abcam 46545, MA, USA) using 3,3'-diaminobenzidine (DAB) as the chromogen (which indicates the presence of 4-HNE as a dark brown stain) and hematoxylin as the counterstain. Images were examined at 100X objective magnification for quantification of 4-HNE levels, using ImageJ to determine the proportion of dark brown area to the total image area in the ONL.

## 3.15. SDS-PAGE AND WESTERN BLOT FOR PTEN AND PHOSPHO-PTEN (P-PTEN) ANALYSIS.

Protein levels of cell homogenates were measured using the bicinchoninic acid (BCA) protein assay. 25-µg of the protein samples ($n = 3$ mice) were separated in NuPage 12% Bis-Tris gels (Life Technologies, Grand Island, NY). Anti-PTEN (Cat # 9552) and anti-p-PTEN (Ser380/Thr382/383, Cat # 9554) (1:1000 dilutions; Cell Signaling, MA, USA) were used as the first antibodies, and GAPDH (1:1000 dilution; Cell Signaling) was used as the dominant housekeeping gene. SuperSignal Chemiluminescent substrate was used to visualize PTEN bands. The membrane was stripped after PTEN measurement, and the procedure was repeated for anti-p-PTEN. SuperSignal West Pico Chemiluminescent substrate and Restore Western blot stripping buffer were obtained from Thermo Scientific.

## 3.16. STATISTICAL ANALYSIS

All values are reported as mean ± SD. Statistical analysis was performed using GraphPad Prism 5 software (GraphPad, San Diego, CA, USA). Statistical significance was determined by one-way analysis of variance (ANOVA), followed by Tukey's multiple comparison tests. Values of $P < 0.05$ were considered significant. Each experiment was repeated at least three times, and each time $n \geq 3$.

# BIBLIOGRAPHY

1.  Sies H. Oxidative stress: oxidants and antioxidants. Exp Physiol. 1997;82.

2.  Reactive Oxigen Species [PowerPoint]  [cited 2017 2 Aug]; Available from: http://slideplayer.com/slide/5372691/.

3.  Dröge W. Free Radicals in the Physiological Control of Cell Function. Physiological Reviews. 2002;82:47.

4.  Pham-Huy LA, He H, and Pham-Huy C. Free radicals, antioxidants in disease and health. Int J Biomed Sci. 2008;4:89-96.

5.  Lushchak VI. Free radicals, reactive oxygen species, oxidative stress and its classification. Chem Biol Interact. 2014;224:164-75.

6.  Kohen R and Nyska A. Oxidation of biological systems: oxidative stress phenomena, antioxidants, redox reactions, and methods for their quantification. Toxicol Pathol. 2002;30:620-50.

7.  Mailloux RJ. Teaching the fundamentals of electron transfer reactions in mitochondria and the production and detection of reactive oxygen species. Redox Biol. 2015;4:381-98.

8.  Krumova K and Cosa G, Chapter 1 Overview of Reactive Oxygen Species, in Singlet Oxygen: Applications in Biosciences and Nanosciences, Volume 1. 2016, The Royal Society of Chemistry. 1-21.

9.  Finkel T and Holbrook NJ. Oxidants, oxidative stress and the biology of ageing. Nature. 2000;408:239-47.

10. Sabharwal SS and Schumacker PT. Mitochondrial ROS in cancer: initiators, amplifiers or an Achilles' heel? Nat Rev Cancer. 2014;14:709-21.

11. Ajuwon OR, Marnewick JL, and Davids LM, Rooibos (Aspalathus linearis) and its Major Flavonoids — Potential Against Oxidative Stress-Induced Conditions., in Basic Principles and Clinical Significance of Oxidative Stress, S.J.T. Gowder, Editor. 2015.

12. Ayala A, Munoz MF, and Arguelles S. Lipid peroxidation: production, metabolism, and signaling mechanisms of malondialdehyde and 4-hydroxy-2-nonenal. Oxid Med Cell Longev. 2014;2014:360438.

13. Yamamoto BK, Moszczynska A, and Gudelsky GA. Amphetamine toxicities Classical and emerging mechanisms. Annals of the New York Academy of Sciences. 2010;1187:101-21.

14.    Pubill D, Garcia-Ratés S, Camarasa J, and Escubedo E. Neuronal Nicotinic Receptors as New Targets for Amphetamine-Induced Oxidative Damage and Neurotoxicity. Pharmaceuticals. 2011;4:822-47.

15.    Jiang J, Briede JJ, Jennen DG, Van Summeren A, Saritas-Brauers K, Schaart G *et al*. Increased mitochondrial ROS formation by acetaminophen in human hepatic cells is associated with gene expression changes suggesting disruption of the mitochondrial electron transport chain. Toxicol Lett. 2015;234:139-50.

16.    Sarafian TA, Magallanes JA, Shau H, Tashkin D, and Roth MD. Oxidative stress produced by marijuana smoke. An adverse effect enhanced by cannabinoids. Am J Respir Cell Mol Biol. 1999;20:1286-93.

17.    Dixon SJ and Stockwell BR. The role of iron and reactive oxygen species in cell death. Nat Chem Biol. 2014;10:9-17.

18.    Stocker R and Keaney JF. Role of Oxidative Modifications in Atherosclerosis. Physiological Reviews. 2004;84:1381.

19.    LoPachin RM, Gavin T, Petersen DR, and Barber DS. Molecular mechanisms of 4-hydroxy-2-nonenal and acrolein toxicity: nucleophilic targets and adduct formation. Chem Res Toxicol. 2009;22:1499-508.

20.    Yin H, Xu L, and Porter NA. Free radical lipid peroxidation: mechanisms and analysis. Chem Rev. 2011;111:5944-72.

21.    Pizzimenti S, Ciamporcero E, Daga M, Pettazzoni P, Arcaro A, Cetrangolo G *et al*. Interaction of aldehydes derived from lipid peroxidation and membrane proteins. Front Physiol. 2013;4:242.

22.    Halliwell B and Gutteridge JMC, Free Radicals in Biology and Medicine. 4 ed. Cellular responses to oxidative stress: adaption, damage, repair, senescence and death. 2007: Oxford University Press. 851.

23.    Esterbauer H, Schaur RJ, and Zollner H. Chemistry and biochemistry of 4-hydroxynonenal, malonaldehyde and related aldehydes. Free Radical Biology and Medicine. 1991;11:81-128.

24.    Halliwell B and Gutteridge JMC, Free radicals in biology and medicine. fourth ed. 2007: oxford.

25.    Dissanayake N, Current K, and Obare S. Mutagenic Effects of Iron Oxide Nanoparticles on Biological Cells. International Journal of Molecular Sciences. 2015;16:23482.

26.    Marnett LJ. Oxy radicals, lipid peroxidation and DNA damage. Toxicology. 2002;181-182:219-22.

27.	Luczaj W and Skrzydlewska E. DNA damage caused by lipid peroxidation products. Cell Mol Biol Lett. 2003;8:391-413.

28.	Dalle-Donne I, Giustarini D, Colombo R, Rossi R, and Milzani A. Protein carbonylation in human diseases. Trends Mol Med. 2003;9:169-76.

29.	Davies MJ. Protein oxidation and peroxidation. Biochem J. 2016;473:805-25.

30.	Dalle-Donne I, Rossi R, Giustarini D, Milzani A, and Colombo R. Protein carbonyl groups as biomarkers of oxidative stress. Clinica Chimica Acta. 2003;329:23-38.

31.	Birben E, Sahiner UM, Sackesen C, Erzurum S, and Kalayci O. Oxidative Stress and Antioxidant Defense. The World Allergy Organization journal. 2012;5:9-19.

32.	Halliwell B and Gutteridge JMC, Free Radicals in Biology and Medicine 4ed. Antioxidant defences: endogenous and diet derived. 2007: Oxford University Press. 851.

33.	Dixon DP and Edwards R. Glutathione Transferases. The Arabidopsis Book / American Society of Plant Biologists. 2010;8:e0131.

34.	DellaPenna D. Progress in the dissection and manipulation of vitamin E synthesis. Trends in Plant Science. 2005;10:574-9.

35.	Meister A. Glutathione metabolism and its selective modification. J Biol Chem. 1988;263:17205-8.

36.	Lushchak VI. Glutathione homeostasis and functions: potential targets for medical interventions. J Amino Acids. 2012;2012:736837.

37.	Townsend DM, Tew KD, and Tapiero H. The importance of glutathione in human disease. Biomedicine & Pharmacotherapy. 2003;57:145-55.

38.	Ganea E and Harding JJ. Glutathione-related enzymes and the eye. Curr Eye Res. 2006;31:1-11.

39.	Halliwell B and Gutteridge JMC, Free radicals in biology and medicine. 1989: Clarendon Press.

40.	Cohen SM, Olin KL, Feuer WJ, Hjelmeland L, Keen CL, and Morse LS. Low glutathione reductase and peroxidase activity in age-related macular degeneration. Br J Ophthalmol. 1994;78:791-4.

41.	Venza I, Visalli M, Cucinotta M, Teti D, and Venza M. Association between oxidative stress and macromolecular damage in elderly patients with age-related macular degeneration. Aging Clinical and Experimental Research. 2012;24:21-7.

42.     Cacciatore I, Cornacchia C, Pinnen F, Mollica A, and Di Stefano A. Prodrug approach for increasing cellular glutathione levels. Molecules. 2010;15:1242-64.

43.     Sunitha K, Hemshekhar M, Thushara RM, Santhosh MS, Yariswamy M, Kemparaju K *et al*. N-Acetylcysteine amide: a derivative to fulfill the promises of N-Acetylcysteine. Free Radic Res. 2013;47:357-67.

44.     Tobwala S, Fan W, Stoeger T, and Ercal N. N-acetylcysteine amide, a thiol antioxidant, prevents bleomycin-induced toxicity in human alveolar basal epithelial cells (A549). Free Radic Res. 2013;47.

45.     Basicmediaclkey. The Special Senses May 17, 2016 [cited 2017 Aug. 3]; Available from: https://basicmedicalkey.com/the-special-senses-2/.

46.     Facts About Age-Related Macular Degeneration. September 2015 [cited 2017 March 14]; Available from: https://nei.nih.gov/health/maculardegen/armd_facts.

47.     Jarrett SG and Boulton ME. Consequences of oxidative stress in age-related macular degeneration. Mol Aspects Med. 2012;33:399-417.

48.     Handa JT. How Does the Macula Protect Itself from Oxidative Stress? Molecular Aspects of Medicine. 2012;33:418-35.

49.     Global data on visual impairments 2010. 2012: World Health Organization (WHO), Prevention of Blindness and Deafness Programme.

50.     Klein R, Klein BE, and Linton KL. Prevalence of age-related maculopathy. The Beaver Dam Eye Study. Ophthalmology. 1992;99:933-43.

51.     Age-Related Macular Degeneration (AMD). Projections for AMD (2010-2030-2050) 2016; Available from: https://nei.nih.gov/eyedata/amd.

52.     Tokarz P, Kaarniranta K, and Blasiak J. Role of antioxidant enzymes and small molecular weight antioxidants in the pathogenesis of age-related macular degeneration (AMD). Biogerontology. 2013;14:461-82.

53.     Wong WL, Su X, Li X, Cheung CM, Klein R, Cheng CY *et al*. Global prevalence of age-related macular degeneration and disease burden projection for 2020 and 2040: a systematic review and meta-analysis. Lancet Glob Health. 2014;2:e106-16.

54.     Pennington KL and DeAngelis MM. Epidemiology of age-related macular degeneration (AMD): associations with cardiovascular disease phenotypes and lipid factors. Eye and Vision. 2016;3:34.

55.     Wittenborn J and Rein D, Cost of Vision Problems: The Economic Burden of Vision Loss and Eye Disorders in the United States. 2013, NORC at the University of Chicago: Chicago, IL.

56. Arnold C, Winter L, Fröhlich K, and et al. Macular xanthophylls and ω-3 long-chain polyunsaturated fatty acids in age-related macular degeneration: A randomized trial. JAMA Ophthalmology. 2013;131:564-72.

57. Jager RD, Mieler WF, and Miller JW. Age-related macular degeneration. N Engl J Med. 2008;358:2606-17.

58. Fine SL, Berger JW, Maguire MG, and Ho AC. Age-Related Macular Degeneration. New England Journal of Medicine. 2000;342:483-92.

59. Hageman GS, Gehrs K, Johnson LV, and Anderson D, Age-Related Macular Degeneration (AMD), in Webvision: The Organization of the Retina and Visual System, H. Kolb, E. Fernandez, and R. Nelson, Editors. 1995: Salt Lake City (UT).

60. Zampatti S, Ricci F, Cusumano A, Marsella LT, Novelli G, and Giardina E. Review of nutrient actions on age-related macular degeneration. Nutrition Research. 2014;34:95-105.

61. Buschini E, Fea AM, Lavia CA, Nassisi M, Pignata G, Zola M *et al*. Recent developments in the management of dry age-related macular degeneration. Clin Ophthalmol. 2015;9:563-74.

62. Horton S and Guly C. Prevention and treatment of age-related macular degeneration. Prescriber. 2017;28:37-41.

63. Lambert NG, ElShelmani H, Singh MK, Mansergh FC, Wride MA, Padilla M *et al*. Risk factors and biomarkers of age-related macular degeneration. Prog Retin Eye Res. 2016;54:64-102.

64. Handa JT, Cano M, Wang L, Datta S, and Liu T. Lipids, oxidized lipids, oxidation-specific epitopes, and Age-related Macular Degeneration. Biochimica et Biophysica Acta (BBA) - Molecular and Cell Biology of Lipids. 2017;1862:430-40.

65. Simo R, Villarroel M, Corraliza L, Hernandez C, and Garcia-Ramirez M. The retinal pigment epithelium: something more than a constituent of the blood-retinal barrier--implications for the pathogenesis of diabetic retinopathy. J Biomed Biotechnol. 2010;2010:190724.

66. Nowak JZ. Oxidative stress, polyunsaturated fatty acids-derived oxidation products and bisretinoids as potential inducers of CNS diseases: focus on age-related macular degeneration. Pharmacol Rep. 2013;65:288-304.

67. Carneiro Â and Andrade JP. Nutritional and Lifestyle Interventions for Age-Related Macular Degeneration: A Review. Oxidative Medicine and Cellular Longevity. 2017;2017:13.

68. Gorusupudi A, Nelson K, and Bernstein PS. The Age-Related Eye Disease 2 Study: Micronutrients in the Treatment of Macular Degeneration. Adv Nutr. 2017;8:40-53.

69. A randomized, placebo-controlled, clinical trial of high-dose supplementation with vitamins C and E, beta carotene, and zinc for age-related macular degeneration and vision loss: AREDS report no. 8. Arch Ophthalmol. 2001;119:1417-36.

70. Bressler NM, Bressler SB, Congdon NG, Ferris FL, 3rd, Friedman DS, Klein R *et al*. Potential public health impact of Age-Related Eye Disease Study results: AREDS report no. 11. Arch Ophthalmol. 2003;121:1621-4.

71. Chew EY, Clemons TE, Sangiovanni JP, Danis RP, Ferris FL, 3rd, Elman MJ *et al*. Secondary analyses of the effects of lutein/zeaxanthin on age-related macular degeneration progression: AREDS2 report No. 3. JAMA Ophthalmol. 2014;132:142-9.

72. Voleti VB and Hubschman JP. Age-related eye disease. Maturitas. 2013;75:29-33.

73. Goldstein GA, N-acetylcysteine amide (nac amide) for the treatment of diseases and conditions associated with oxidative stress. 2006, Google Patents.

74. Goldstein GA, N-acetylcysteine amide (NAC amide) for the treatment of diseases and conditions associated with oxidative stress. 2013, Google Patents.

75. Goldstein GA, N-acetylcysteine amide (NAC amide) in the treatment of diseases and conditions associated with oxidative stress. 2015, Google Patents.

76. Chen W, Ercal N, Huynh T, Volkov A, and Chusuei CC. Characterizing N-acetylcysteine (NAC) and N-acetylcysteine amide (NACA) binding for lead poisoning treatment. J Colloid Interface Sci. 2012;371:144-9.

77. Schimel AM, Abraham L, Cox D, Sene A, Kraus C, Dace DS *et al*. N-acetylcysteine amide (NACA) prevents retinal degeneration by up-regulating reduced glutathione production and reversing lipid peroxidation. Am J Pathol. 2011;178:2032-43.

78. Carey JW, Pinarci EY, Penugonda S, Karacal H, and Ercal N. In vivo inhibition of l-buthionine-(S,R)-sulfoximine-induced cataracts by a novel antioxidant, N-acetylcysteine amide. Free Radic Biol Med. 2011;50:722-9.

79. Wnag H, Huang Y, Tobwala S, Pfaff A, Aronstam R, and Ercal N. The role of N-acetylcysteine amide in defending primary human retinal pigment epithelial cells against tert-butyl hydroperoxide-induced oxidative stress. Free Radicals and Antioxidants. 2017;7:172-7.

80. Maddirala Y, Tobwala S, Karacal H, and Ercal N. Prevention and reversal of selenite-induced cataracts by N-acetylcysteine amide in Wistar rats. BMC Ophthalmology. 2017;17:54.

81. Oduntan OA and Masige KP, A review of the role of oxidative stress in the pathogenesis of eye diseases. 2011. 2011.

82. Nita M and Grzybowski A. The Role of the Reactive Oxygen Species and Oxidative Stress in the Pathomechanism of the Age-Related Ocular Diseases and Other Pathologies of the Anterior and Posterior Eye Segments in Adults. Oxid Med Cell Longev. 2016;2016:3164734.

83. Truscott RJW. Age-related nuclear cataract—oxidation is the key. Experimental Eye Research. 2005;80:709-25.

84. Izzotti A, Bagnis A, and Sacca SC. The role of oxidative stress in glaucoma. Mutat Res. 2006;612:105-14.

85. Naruse R, Suetsugu M, Terasawa T, Ito K, Hara K, Takebayashi K *et al*. Oxidative stress and antioxidative potency are closely associated with diabetic retinopathy and nephropathy in patients with type 2 diabetes. Saudi Med J. 2013;34:135-41.

86. Wu Y, Tang L, and Chen B. Oxidative Stress: Implications for the Development of Diabetic Retinopathy and Antioxidant Therapeutic Perspectives. Oxidative Medicine and Cellular Longevity. 2014;2014:12.

87. Ho M-C, Peng Y-J, Chen S-J, and Chiou S-H. Senile cataracts and oxidative stress. Journal of Clinical Gerontology and Geriatrics. 2010;1:17-21.

88. Chakravarthy U, Wong TY, Fletcher A, Piault E, Evans C, Zlateva G *et al*. Clinical risk factors for age-related macular degeneration: a systematic review and meta-analysis. BMC Ophthalmol. 2010;10:31.

89. Yau JWY, Rogers SL, Kawasaki R, Lamoureux EL, Kowalski JW, Bek T *et al*. Global Prevalence and Major Risk Factors of Diabetic Retinopathy. Diabetes Care. 2012;35:556-64.

90. Vinson JA. Oxidative stress in cataracts. Pathophysiology. 2006;13:151-62.

91. Kaur J, Kukreja S, Kaur A, Malhotra N, and Kaur R. The Oxidative Stress in Cataract Patients. Journal of Clinical and Diagnostic Research : JCDR. 2012;6:1629-32.

92. Kumar PA and Reddy GB. Modulation of α-crystallin chaperone activity: A target to prevent or delay cataract? IUBMB Life. 2009;61:485-95.

93. Ferreira SM, Lerner SF, Brunzini R, Evelson PA, and Llesuy SF. Oxidative stress markers in aqueous humor of glaucoma patients. Am J Ophthalmol. 2004;137:62-9.

94. Gherghel D, Griffiths HR, Hilton EJ, Cunliffe IA, and Hosking SL. Systemic reduction in glutathione levels occurs in patients with primary open-angle glaucoma. Invest Ophthalmol Vis Sci. 2005;46:877-83.

95. Sacca SC and Izzotti A. Oxidative stress and glaucoma: injury in the anterior segment of the eye. Prog Brain Res. 2008;173:385-407.

96. Calderon GD, Juarez OH, Hernandez GE, Punzo SM, and De la Cruz ZD. Oxidative stress and diabetic retinopathy: development and treatment. Eye. 2017.

97. Kobrin Klein BE. Overview of Epidemiologic Studies of Diabetic Retinopathy. Ophthalmic Epidemiology. 2007;14:179-83.

98. Campochiaro PA, Strauss RW, Lu L, Hafiz G, Wolfson Y, Shah SM *et al*. Is There Excess Oxidative Stress and Damage in Eyes of Patients with Retinitis Pigmentosa? Antioxidants & Redox Signaling. 2015;23:643-8.

99. Usui S, Oveson BC, Lee SY, Jo YJ, Yoshida T, Miki A *et al*. NADPH oxidase plays a central role in cone cell death in retinitis pigmentosa. J Neurochem. 2009;110:1028-37.

100. Yadav UCS, Kalariya NM, and Ramana KV. Emerging Role of Antioxidants in the Protection of Uveitis Complications. Current medicinal chemistry. 2011;18:931-42.

101. Andrikopoulos GK, Alexopoulos DK, and Gartaganis SP. Pseudoexfoliation syndrome and cardiovascular diseases. World Journal of Cardiology. 2014;6:847-54.

102. Gartaganis SP, Patsoukis NE, Nikolopoulos DK, and Georgiou CD. Evidence for oxidative stress in lens epithelial cells in pseudoexfoliation syndrome. Eye. 2006;21:1406-11.

103. Cellstain-Calcein-AM. [web] 2017; Available from: http://www.dojindo.com/store/p/160-Cellstain-Calcein-AM.html.

104. Gomes A, Fernandes E, and Lima JL. Fluorescence probes used for detection of reactive oxygen species. J Biochem Biophys Methods. 2005;65:45-80.

105. Kalyanaraman B, Darley-Usmar V, Davies KJ, Dennery PA, Forman HJ, Grisham MB *et al*. Measuring reactive oxygen and nitrogen species with fluorescent probes: challenges and limitations. Free Radic Biol Med. 2012;52:1-6.

106. Wojtala A, Bonora M, Malinska D, Pinton P, Duszynski J, and Wieckowski MR. Methods to monitor ROS production by fluorescence microscopy and fluorometry. Methods Enzymol. 2014;542:243-62.

107. Wu W, Goldstein G, Adams C, Matthews RH, and Ercal N. Separation and quantification of N-acetyl-l-cysteine and N-acetyl-cysteine-amide by HPLC with fluorescence detection. Biomed Chromatogr. 2006;20:415-22.

108. Tobwala S, Wang H-J, Carey J, Banks W, and Ercal N. Effects of Lead and Cadmium on Brain Endothelial Cell Survival, Monolayer Permeability, and Crucial Oxidative Stress Markers in an in Vitro Model of the Blood-Brain Barrier. Toxics. 2014;2:258.

109. Winters RA, Zukowski J, Ercal N, Matthews RH, and Spitz DR. Analysis of glutathione, glutathione disulfide, cysteine, homocysteine, and other biological thiols by high-performance liquid chromatography following derivatization by n-(1-pyrenyl)maleimide. Anal Biochem. 1995;227:14-21.

110. Carlberg I and Mannervik B. Glutathione reductase. Methods Enzymol. 1985;113:484-90.

111. Mavis RD and Stellwagen E. Purification and subunit structure of glutathione reductase from bakers' yeast. J Biol Chem. 1968;243:809-14.

112. Bradford MM. A rapid and sensitive method for the quantitation of microgram quantities of protein utilizing the principle of protein-dye binding. Anal Biochem. 1976;72:248-54.

113. Smith PK, Krohn RI, Hermanson GT, Mallia AK, Gartner FH, Provenzano MD *et al*. Measurement of protein using bicinchoninic acid. Anal Biochem. 1985;150:76-85.

114. Bicinchoninic Acid (BCA) protein assays. Chemistry of protein assay [Web Page] [cited 2017 Aug 8]; Available from: https://www.thermofisher.com/us/en/home/life-science/protein-biology/protein-biology-learning-center/protein-biology-resource-library/pierce-protein-methods/chemistry-protein-assays.html.

115. Maleki S, Gopalakrishnan S, Ghanian Z, Sepehr R, Schmitt H, Eells J *et al*. Optical imaging of mitochondrial redox state in rodent model of retinitis pigmentosa. J Biomed Opt. 2013;18:16004.

116. Woodward WR, Choi D, Grose J, Malmin B, Hurst S, Pang J *et al*. Isoflurane is an effective alternative to ketamine/xylazine/acepromazine as an anesthetic agent for the mouse electroretinogram. Doc Ophthalmol. 2007;115:187-201.

117. Fishman GA. Basic principles of clinical electroretinography. Retina. 1985;5:123-6.

118. Creel DJ. The Electroretinogram and Electro-oculogram: Clinical Applications by Donnell J. Creel. [cited 2017 Aug 4]; Available from: http://webvision.med.utah.edu/book/electrophysiology/the-electroretinogram-clinical-applications/.

**PAPER**

# I. THE ROLE OF N-ACETYLCYSTEINE AMIDE IN DEFENDING PRIMARY HUMAN RETINAL PIGMENT EPITHELIAL CELLS AGAINST TERT-BUTYL HYDROPEROXIDE-INDUCED OXIDATIVE STRESS

Hsiu-Jen Wang[1], Yue-Wern Huang[2], Shakila Tobwala[1], Annalise Pfaff[1], Robert Aronstam[3], Nuran Ercal[1*]

1. Department of Chemistry, Missouri University of Science and Technology, Rolla MO, USA

2. Department of Biological Sciences, Missouri University of Science and Technology, Rolla MO, USA

3. College of Science and Technology, Bloomsburg University, Bloomsburg PA, USA

\* **Corresponding author**

Nuran Ercal

Chemistry department, Missouri University of Science and Technology

400 W. 11th street, Rolla, MO 65409, USA

Phone: +1-(573) 341-6950

Fax: +1-(573) 341-6033

Email address: nercal@mst.edu

**Keywords:** N-acetylcysteine amide; thiol antioxidant; oxidative free radical damage; retinal pigment epithelium

**Key Messages:** NACA defends RPE against oxidative stress in an in vitro model of AMD.

# ABSTRACT

**Background**: Age-related macular degeneration (AMD) is a leading cause of blindness in the United States among adults age 60 and older. While oxidative stress is implicated in the pathogenesis of AMD, dietary antioxidants have been shown to delay AMD progression in clinical studies. We hypothesized that N-acetylcysteine amide (NACA), a thiol antioxidant, would protect retinal pigment epithelium and impede progression of retinal degeneration.

**Methods**: *tert*-Butyl hydroperoxide (TBHP) was used to induce oxidative stress in cell cultures. The goal was to evaluate the efficacy of NACA in an in vitro model of AMD in primary human retinal pigment epithelial cells (HRPEpiC).

**Results**: Our data indicates that TBHP generated reactive oxygen species (ROS), which reduced cell viability, depleted glutathione (GSH) levels, and compromised glutathione reductase (GR) activity. Pretreatment with NACA significantly reduced ROS generation, restored GSH levels and GR activity, and recovered transepithelial electrical resistance. Pretreatment with NACA did not decrease the number of dying cells, as determined by flow cytometry analysis. However, survival was significantly improved when cells were co-exposed to NACA and TBHP after a shortened pretreatment period.

**Conclusions**: Our data suggest that pretreatment with NACA reduces sublethal but not lethal effects of TBHP in HRPEpiC. NACA significantly improved cell survival when administered prior to and during oxidative damage similar to that observed in the development of dry AMD. These results indicate that continuation of a thiol antioxidant regimen for treatment of AMD is beneficial throughout the course of the disease, and that NACA is a potent antioxidant that should be further evaluated for this purpose.

# 1. INTRODUCTION

Age-related macular degeneration (AMD) accounts for 8.7% of blindness worldwide, and is a leading cause of blindness in the United States among adults age 60 and older [1-3]. Globally, about 1 in 32 visual impairments and 1 in 15 cases of blindness are due to macular disease [4]. Dry AMD is a degenerative condition that begins in Bruch's membrane and progresses to the retinal pigment epithelium (RPE) and the overlying photoreceptors resulting in loss of central vision. The RPE is a single layer of pigment cells lying between the photoreceptors and choriocapillaris. Its functions include light absorption, epithelial transport, phagocytosis, secretion, and immune modulation. All of these functions are important for maintaining and supporting the photoreceptors. A high blood flow rate and high $O_2$ saturation in the choriocapillaris render the RPE more exposed to oxidative stress [5]. Oxidative stress seems to play a major role in the pathogenesis of dry AMD and retinal degeneration, although the pathophysiology of dry AMD is complex [5, 6]. The macula is subject to increased levels of photo-oxidative stress because of its elevated metabolic rate and high proportion of polyunsaturated fatty acids, which are highly susceptible to lipid peroxidation. As the RPE cells of the macula age, the oxidation of lipids and other cellular components result in an accumulation of indigestible lipofuscin in the lysosomes. The accumulation of lipofuscin granules closely parallels drusen formation in time and distribution in the retina. Oxidative damage to the mitochondrial DNA in RPE cells has also been implicated in the development of AMD. Levels of antioxidants in retinal tissue, glutathione (GSH) in particular, decrease with aging, making the macula even more vulnerable to progressive oxidative damage [7, 8].

Endogenous antioxidants, such as GSH, cannot be directly replaced. Instead, compounds that can easily enter cells and increase intracellular antioxidant levels are preferred. Dietary antioxidants have been shown to slow the progression of retinal degeneration and halt progression of AMD in human clinical trials.[9, 10] GSH and its amino acid precursors protect RPE cells from oxidative injury and oxidant-induced apoptosis *in vitro*. N-acetylcysteine amide (NACA), a GSH prodrug, is a promising candidate for use as an antioxidant-based treatment for AMD. It has demonstrated efficacy in numerous *in vitro* and animal models of other oxidative stress-related conditions, including drug-induced RPE damage and cataracts [11-15]. Our lab has demonstrated that NACA prevented retinal degeneration *in vitro* and in animal models [14]. The immortalized ARPE-19 cell line was used as an *in vitro* model because primary human RPE cells were not available at the time. ROS generation and lipid peroxidation induced by *tert*-butyl hydroperoxide (TBHP) were reversed by pretreatment with NACA. NACA also protected against TBHP-induced cell damage by increasing cellular levels of GSH, and maintaining cellular integrity, as measured by transepithelial electrical resistance (TEER). In an animal model, phototoxicity-induced photoreceptor cell death and photoreceptor dysfunction were prevented by NACA [14].

The experiments reported here utilized primary cultures of human retinal pigment epithelial cells (HRPEpiC), the best available *in vitro* model for studying RPE-related disorders. Because we attempted to mimic a human disease and provide a solution using a "disease-in-the-dish" model, choosing the most representative cell model was critical. Thus, we decided to determine whether the beneficial effects of NACA observed in ARPE-19 cells could also be observed in the HRPEpiC. Our goals were to investigate the

following: (1) the sub-lethal and lethal effects of TBHP in HRPEpiC and (2) the protective effects of NACA pretreatment against TBHP-induced oxidative damage. Sublethal effects included changes in redox status (ROS generation, GSH levels and GR activity) and monolayer integrity (TEER and dextran permeability). Lethal effects were determined with cell viability and apoptosis assays.

## 2. MATERIALS AND METHODS

### 2.1. MATERIALS

N-acetylcysteine amide (NACA) was provided by Dr. Glenn Goldstein (David Pharmaceuticals, New York, NY, USA). Human retinal pigment epithelial cells (HRPEpiC) were purchased from ScienCell Research Laboratories (Carlsbad, CA, USA). Other chemicals were ordered from Sigma (St. Louis, MO, USA), unless otherwise indicated.

### 2.2. HRPEPIC CULTURE AND EXPERIMENTAL DESIGN

HRPEpiC were grown in complete media and divided in to four groups (control, NACA, TBHP and NACA+TBHP). Cells were pretreated with 2 mM NACA (in NACA and NACA+TBHP groups) or serum-free media (in control and TBHP groups). After 4 hours incubation, the media was removed, and followed by dosing with 0.5 mM TBHP for 3 hours. For apoptosis assays, an alternative NACA and TBHP dosing protocol was used in addition to the one described above. This involved pretreatment with NACA for 1 h prior to TBHP exposure and the addition of NACA for another 3 hours (i.e., the NACA+TBHP group cells were co-exposed to TBHP and NACA for 3 hours).

## 2.3. CELL VIABILITY ASSAY

Cell suspension contained $1\times10^4$ cells per well were seeded in a 96-well plate for 24 hours before further dosing. After cells were treated as indicated in the experimental design, 2 μM Calcein-AM (Biotium Inc., CA) were added to each well, and cells were incubated for 30 min before measuring the fluorescence by a plate reader ($\lambda_{ex}$ = 485 nm and $\lambda_{em}$ = 530 nm) (FLUOstar Omega, BMG Labtech).

## 2.4. INTRACELLULAR ROS MEASUREMENT

10 μM of CM-H$_2$DCFDA (Molecular Probes, Life Technologies) were loaded prior to dosing according to the experimental design. Fluorescence was measured after treatment ($\lambda_{ex}$ = 485 nm and $\lambda_{em}$ = 530 nm).

## 2.5. QUANTIFICATION OF INTRACELLULAR GLUTATHIONE (GSH) LEVELS

Cells were grown at a density of $1.2\times10^6$ in a 10-cm plate for 24 h before further treatment. GSH was separated and quantified by HPLC with fluorescence detection (Finnigan Surveyor FL Plus, Thermo Scientific) after derivatization of cell homogenates with N-(1-pyrenyl)maleimide (NPM) [16].

## 2.6. GLUTATHIONE REDUCTASE (GR) ACTIVITY ASSAY

Cells were homogenized in 250 μl of 50 mM Tris-HCl (pH = 7.5) containing 1 mM EDTA. NADPH, which absorbs light at 340 nm, was added to each sample. The rate of its oxidation to NADP$^+$ by GR as GSSG is reduced to 2 GSH can be determined from the resulting decrease in absorbance at this wavelength over time [17].

## 2.7. DETERMINATION OF PROTEIN

Protein levels of the cell homogenates were measured by the Bradford method (BioRad Laboratories, Inc., CA). Bovine serum albumin was used as the protein standard.

## 2.8. DEXTRAN PERMEABILITY AND TRANSEPITHELIAL ELECTRICAL RESISTANCE (TEER) MEASUREMENT

12-mm Transwell inserts were coated with poly-L-lysine for 1 h prior to seeding 0.5 ml at $1\times10^6$ cells/ml. Cell growth was maintained for 5 days without disturbing the monolayer. Fluorescently labelled dextrans (FD4, 1 mg/ml) were administered apically onto the insert after dosing. Fluorescence was read after 30 min ($\lambda_{ex}$ =485 nm and $\lambda_{em}$ = 530 nm). The inserts containing the monolayer were then transferred to a new well with serum-free phenol red-free media and used for TEER measurement with an EVOM voltohmmeter (World Precision Instrument, Sarasota, FL, USA) to assess the integrity of the HRPEpiC monolayer.

## 2.9. FLOW CYTOMETRY QUANTIFICATION OF APOPTOTIC CELLS

Cells were grown in 6-cm plates and dosed as described by the experiment design. Trypsinized cells were re-suspended in binding buffer containing 7-AAD and annexin V-FITC (BD Biosciences, San Jose, CA, USA). Cells were incubated for 15 minutes at room temperature in the dark then analyzed by Cell Lab Quanta SC flow cytometry (Beckman Coulter, Fullerton, CA, USA).

## 2.10. STATISTICAL ANALYSIS

All values were reported as mean ± SD ($n$ = 3 to 10). Statistical analysis was performed using GraphPad Prism 5 software (GraphPad, San Diego, CA, USA). Statistical significance was determined by one-way analysis of variance (ANOVA), followed by Tukey's multiple comparison tests. #, ##, and ### represent $P < 0.05$, 0.01 and 0.001, respectively, as compared to control; *, **, and ***, which represent $P < 0.05$, 0.01 and 0.001, respectively, compared to TBHP group.

# 3. RESULTS

## 3.1. TBHP INCREASED INTRACELLULAR ROS LEVELS IN HRPEPIC, AND NACA PREVENTED ROS GENERATION

To investigate ROS generation in response to TBHP treatment, ROS levels were measured after exposing cells to TBHP for 3 hours. TBHP induced ROS generation in a dose-dependent manner (Figure 1A). ROS levels in TBHP-treated cells were 177% of those observed in the control group ($P < 0.001$). Pretreatment with NACA decreased ROS levels to 126% of those observed in the control group ($P < 0.001$ compared to TBHP group) (Figure 1B).
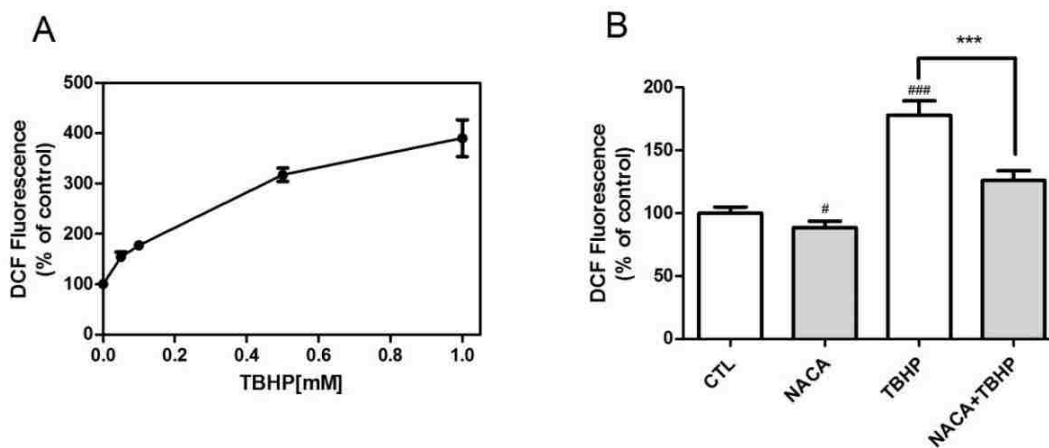


Figure 1. Intracellular ROS levels were measured using DCF fluorescence.
(A) TBHP induced ROS generation in a dose-dependent manner. (B) NACA prevented TBHP-induced ROS generation.

### 3.2. DOSE-DEPENDENT GSH DEPLETION BY TBHP AND PREVENTION BY PRETREATMENT WITH NACA

To elucidate the consequences of elevated ROS in HRPEpiC, GSH levels were measured after treatment for 3 hours with various concentrations of the TBHP. TBHP decreased cellular GSH levels in a dose-dependent manner: the average GSH levels in cells treated with 0, 0.5, 1, 25 and 50 mM of TBHP were $33.4 \pm 5.0$, $25.1 \pm 1.5$, $18.9 \pm 0.7$, $8.8 \pm 1.9$ and $6.2 \pm 1.3$ nmol/mg protein, respectively ($P < 0.001$ compared to control) (Figure 2A). The protective effect of NACA on GSH depletion in cells treated with TBHP was also investigated (Figure 2B). GSH is the major antioxidant in a cell and NACA is a GSH precursor, providing cysteine for GSH synthesis. The average GSH level in the control group was $31.7 \pm 2.3$ nmol/mg protein. The GSH level was increased after NACA incubation ($55.1 \pm 7.3$ nmol/mg protein, $P < 0.001$ compared to control). The average GSH level of the TBHP group was $25.1 \pm 1.5$ nmol/mg protein ($P < 0.01$ compared to control), but the NACA+TBHP group had an average GSH level of $30.5 \pm 2.5$ nmol/mg protein ($P < 0.05$, compared to the TBHP group).
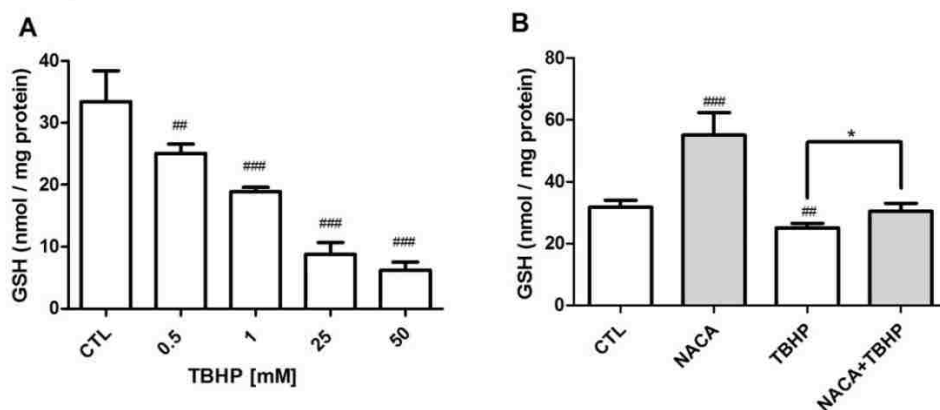


Figure 2. Intracellular GSH levels in HRPEpiC.
(A) TBHP depleted GSH levels in a dose-dependent manner. (B) NACA dramatically increased intracellular GSH levels and prevented GSH depletion by TBHP.

## 3.3. PRESERVATION OF GLUTATHIONE REDUCTASE ACTIVITY BY PRETREATMENT WITH NACA

Glutathione reductase (GR), an enzyme that reduces glutathione disulfide to GSH, is important in restoring intracellular levels of GSH. GR activity was reduced in the TBHP group ($33.5 \pm 3.2$ versus $21.9 \pm 2.2$ mU/mg protein in the control group; $P < 0.01$) (Figure 3). NACA-pretreated cells exhibited increased GR activity ($33.5 \pm 5.2$ mU/mg protein; $P < 0.01$ compared to the TBHP group).
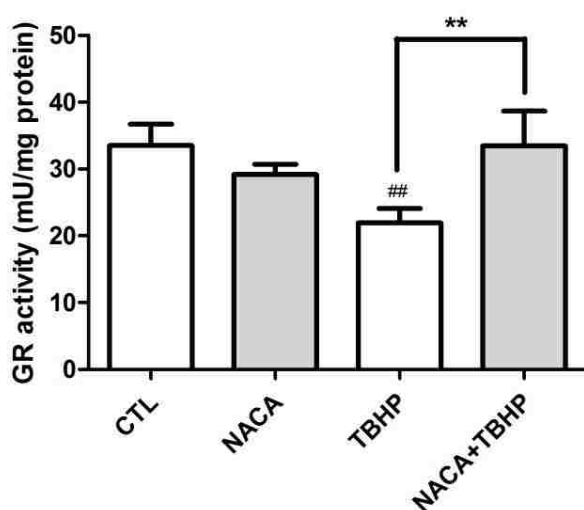
Figure 3. Preservation of glutathione reductase activity by NACA.

## 3.4. EFFECTS OF OXIDATIVE STRESS ON HRPEPIC MONOLAYER PARACELLULAR PERMEABILITY AND CONTRIBUTION OF NACA TO MONOLAYER FUNCTIONAL HOMEOSTASIS

RPE paracellular permeability was assessed in a HRPEpiC grown on a polycarbonate insert, which formed a monolayer similar to that of the blood-retina barrier

*in vivo*. Transepithelial electrical resistance (TEER) was used as a measure of paracellular permeability to ions, where lower electrical resistance was evidence of decreased membrane integrity of a  HRPEpiC in the monolayer. Permeability to non-ionic molecules was determined based on the amount of dextran that passed through the monolayer within 30 min. Compared to the TBHP group, the NACA+TBHP group exhibited significantly greater electrical resistance (Figure 4A). Dextran permeability in the TBHP group was significantly higher than that of the control ($P < 0.05$) (Figure 4B).
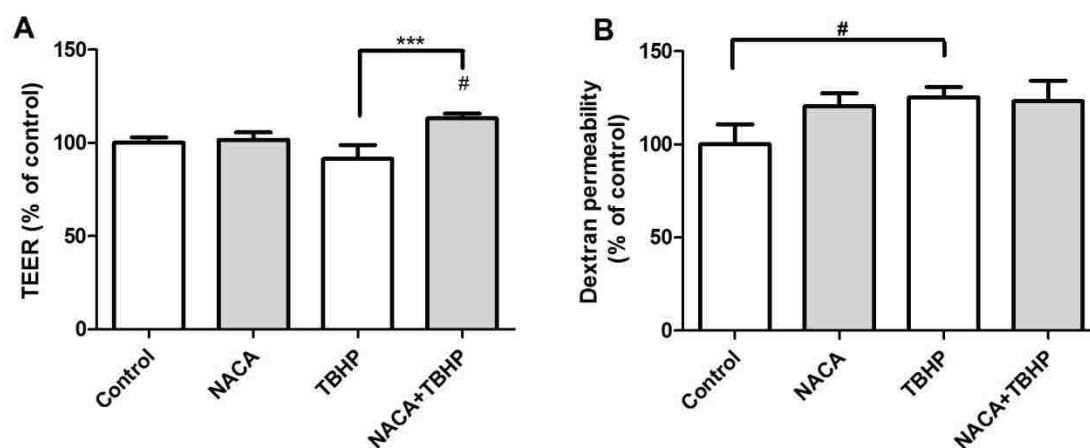


Figure 4. Protective effects of NACA on paracellular permeability in HRPEpiC. (A) Results of TEER measurement. (B) Results of dextran permeability assays.

## 3.5. CELL VIABILITY AND LETHAL EFFECTS OF TBHP ON HRPEPIC

To investigate cell survival in response to ROS generation, cell viability assays were performed after treatment (Figure 5). Pretreatment with NACA alone did not affect cell viability ($91.1 \pm 4.5\%$), as compared to control ($100.0 \pm 10.1\%$). Cell viability was

reduced in the TBHP group ($52.2 \pm 5.5\%$, $P < 0.001$). Pretreatment with NACA provided

slight but not statistically significant protection against TBHP-induced cell death.
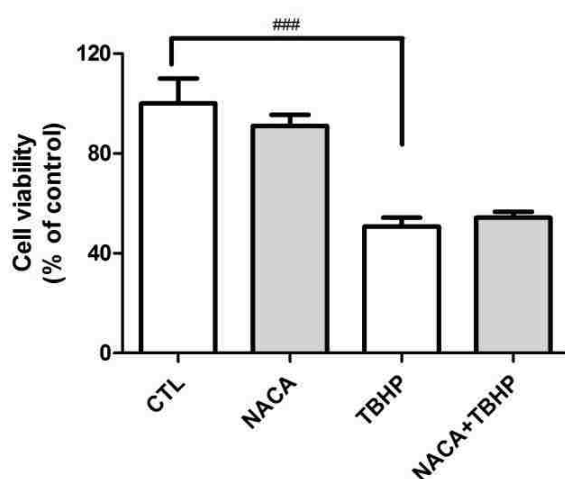


Figure 5. Effects of NACA and TBHP on HRPEpiC cell viability.

### 3.6. ANNEXIN V-FITC AND 7-AMINOACTINOMYCIN-D (7-AAD) DETECTION OF APOPTOSIS BY FLOW CYTOMETRY

NACA has multiple antioxidant properties. It is a well-known GSH prodrug and a

free radical scavenger [18-20]. In cell-free systems, NACA can non-enzymatically restore

GSH through thiol-disulfide exchange with the oxidized form, GSSG [21]. An annexin

V-FITC and 7-AAD double staining assay was performed. Cells in the early apoptotic

stages only bound annexin V-FITC, while cells in late apoptotic stages bound both

annexin-V-FITC and 7-AAD. Dead/necrotic cells may only exhibit 7-AAD fluorescence,

due to membrane disintegration and subsequent loss of phosphatidylserine. Table 1

summarizes the percent distribution of viable cells and cells in the early and late stages of

apoptosis. The percentages of viable cells in the TBHP and NACA+TBHP groups were very similar (64.0 ± 4.9 % versus 67.8 ± 9.9 %). There was no significant difference in the number of dying cells (defined as the total of early- and late-stage apoptotic cells) between the TBHP and the NACA+TBHP groups (20.5 ± 6.1% versus 20.8 ± 4.8%). Because no significant improvement was observed in the cells pretreated with NACA, the dosing protocol was modified slightly without changing the total NACA exposure time (see Methods). Results of the modified treatment protocol are shown in Figure 6 and Table 2.  In the NACA+TBHP (co-exposed) group, the percentage of viable cells (88.6 ± 0.1%) was significantly higher than that in the TBHP group (48.5 ± 5.1%, $P < 0.001$). The percentages of dying cells in the TBHP group and the NACA+TBHP co-exposure group were 16.5 ± 3.6% and 5.5 ± 0.8%, respectively.

Table 1. Percent distribution of viable cells and cells in the early and late stages of apoptosis after 4 hours of pretreatment with NACA followed by 3 hours of TBHP exposure.

| Groups | Control | 2 mM NACA | 0.5 mM TBHP | NACA+TBHP |
|---|---|---|---|---|
| Viable cells | 94.8 ± 1.3 | 93.7 ± 0.5 | 64.0 ± 4.9 | 67.8 ± 9.9 |
| Early apoptotic cells | 1.3 ± 0.6 | 3.0 ± 1.1 | 1.8 ± 0.8 | 2.1 ± 0.4 |
| Late apoptotic cells | 1.9 ± 0.2 | 2.1 ± 0.5 | 18.8 ± 5.4 | 18.6 ± 4.9 |

The results are shown as mean % of total cells ± SD
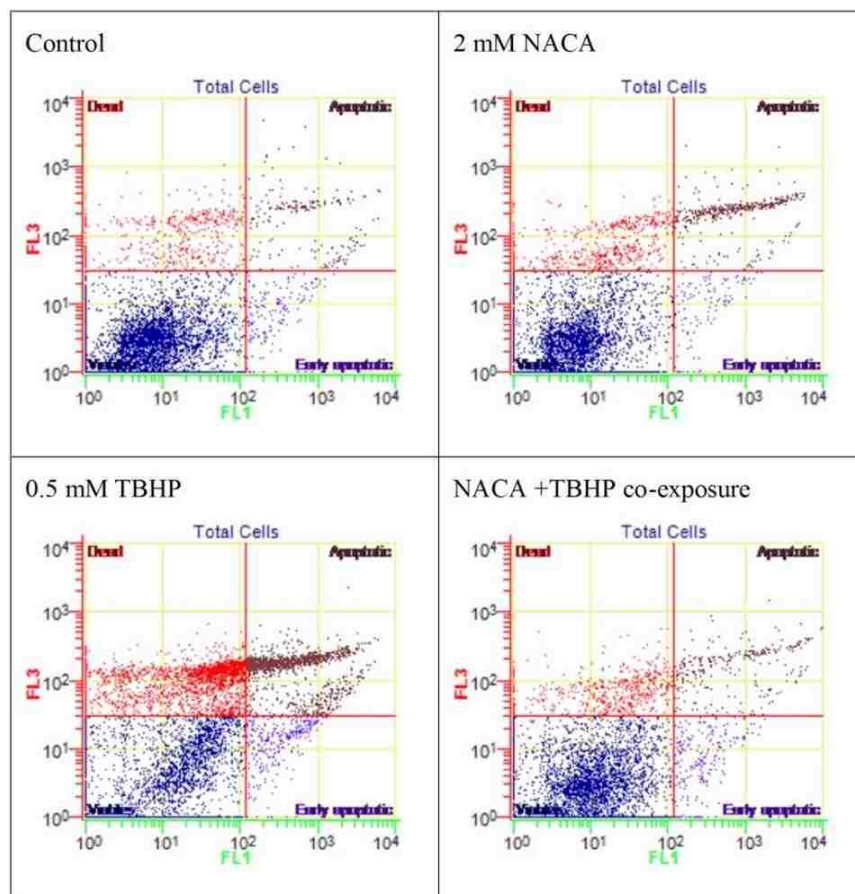
Figure 6. Flow cytometry analysis of apoptotic cells following the modified (co-exposure) protocol with NACA and TBHP.
The dot plots show a two-parameter analysis of fluorescence intensity of annexin-V FITC (FL1) and 7-AAD (FL3).

Table 2. Percent distribution of viable cells and cells in the early and late stages of apoptosis from Figure 6.

| Groups | Control | 2 mM NACA | 0.5 mM TBHP | NACA+TBHP |
|---|---|---|---|---|
| Viable cells | $90.4 \pm 1.2$ | $84.8 \pm 4.2$ | $48.5 \pm 5.1^{a}$ | $88.6 \pm 0.0^{b}$ |
| Early apoptotic cells | $2.2 \pm 0.3$ | $1.7 \pm 0.9$ | $2.2 \pm 1.0$ | $2.3 \pm 0.3$ |
| Late apoptotic cells | $2.5 \pm 0.4$ | $4.4 \pm 0.2$ | $14.3 \pm 3.5$ | $3.1 \pm 0.5$ |

The results are shown as mean % of total cells $\pm$ SD. (a, $P < 0.001$ compared to control group; b, $P < 0.001$ compared to TBHP group).

# 4. DISCUSSION

In this study, we evaluated the potential of NACA to prevent oxidative stress-related damage *in vitro* in HRPEpiC. This allowed for evaluation of NACA as a defense against TBHP-induced oxidative injury. Selection of the best *in vitro* analogue to RPE in AMD patients was vital to the clinical relevance of our results. Currently, there are three cell models being used to study the effects of oxidative stress on the RPE: ARPE-19, fetal human RPE cells (fhRPE) and primary culture adult human RPE (e.g., HRPEpiC). ARPE-19 is a spontaneously arising retinal pigment epithelia cell line derived from normal eyes. The fhRPE and HRPEpiC are primary cultures of fetal and adult human RPE cells, respectively. When compared to ARPE-19, the fhRPE cells were healthier; however, adult human RPE were more physiologically representative of the mature function of RPE than fhRPE [21, 22]. Thus, an adult human primary RPE cell model was used for the experiments detailed here.

The RPE of the macula is particularly vulnerable to oxidative damage due to increased $O_2$ exposure, photo-oxidation, elevated metabolic activity, and high proportion of polyunsaturated fatty acids [5]. Our data demonstrates that TBHP increased ROS levels in a dose-dependent manner, leading to severe oxidative stress in the HRPEpiC cultures, and that NACA pre-incubation prevented TBHP-induced ROS production in HRPEpiC. It has been shown that accumulation of ROS induces severe oxidative stress in RPE cells, which is manifested by a significant reduction in levels of GSH (the most critical antioxidant and redox buffer of the cell) [23, 24]. Results from our study showed a significant decrease in GSH levels in the HRPEpiC, when compared to those of the control group (Figure 2). Pretreatment with NACA significantly increased GSH levels,

which may indicate that NACA replenished GSH levels, leading to a reversal of oxidative stress. The protective effects of NACA are probably mediated by a number of pathways, which may include supplying cysteine for GSH biosynthesis, reducing extracellular cystine to cysteine, and converting GSSG to GSH by the action of GR and by non-enzymatic thiol disulfide exchange [12, 25-27]. Our results are in agreement with previous studies which reported an increase in GSH levels after NACA incubation and a decrease in GSH levels upon TBHP treatment in an ARPE cell line [11, 14].

Importantly, changes in GR activity were also observed. GR regenerates GSH from GSSG and plays an important role in GSH homeostasis [28]. NACA treatment increased the levels of GSH and restored GR activity (Figure 3). Our results are in line with another study that reported inhibition of GR activity in HepG2 upon TBHP treatment [29].

In the retina, the RPE forms the blood-retinal barrier (BRB) with tight junctions that control the exchange of nutrients and metabolites between the retina and the underlying choriocapillaris. It is thought that oxidative stress may induce changes in the BRB, which may contribute to the pathogenesis of retinal degeneration. To investigate and determine the ability of NACA to preserve the BRB function, membrane integrity after TBHP exposure was evaluated using dextran permeability and TEER assays [30]. NACA prevented TBHP-induced reduction in TEER, verifying its ability to protect cellular homeostasis and outer BRB integrity under severe oxidative stress conditions. A similar decrease in TEER has been reported in another study, where human embryonic stem cell (hESC)-derived RPE cells and ARPE-19 cells were exposed to hydrogen peroxide [30, 31]. These results are also in agreement with a previous study performed in

our laboratory using the ARPE-19 [14]. However, we did not observe any significant difference in dextran permeability upon NACA treatment, which could be due to a lower sensitivity of dextran permeability when compared with TEER [32].

The decline in GSH observed created a redox imbalance that enhanced cell susceptibility to injury and ROS-induced apoptosis. Altering the redox state to a more reduced environment by addition of GSH has been shown to decrease sensitivity of RPE cells to apoptosis from ROS [33, 34]. We initially investigated the protective effect of NACA pretreatment by studying cell viability. However, no significant improvement was noted by either the Calcein-AM or flow cytometry assay in cell survival. Therefore, we modified our study design to co-exposure along with pre-incubation and dramatically improved cell survival (Figure 6). It is possible that pretreatment alone is not sufficient to address multiple oxidative stress-related apoptotic mechanisms. Oxidants, such as TBHP, may induce apoptosis through two different pathways: (1) Fas-Fas ligand activation and (2) mitochondrial damage and subsequent release of cytochrome c [35]. Because the interplay between these two pathways is complex, it is plausible that antioxidant treatments, while producing a more favorable redox status in a cell, may not fully address both apoptotic pathways. In addition, the concentrations of TBHP (0.5 mM) and NACA (2 mM), used in our investigation, may have been too high and low, respectively, so that pretreatment with NACA did not provide any significant cytoprotection. Our previous studies with ARPE-19 indicated that up to 10 mM of NACA may be used for beneficial effect as a pretreatment for 0.4 mM tBHP exposure [14].

# 5. CONCLUSION

This study demonstrated that treatment of retinal pigment epithelium with NACA protects against oxidative stress-induced cellular injury. NACA also inhibited oxidative stress-related breakdown of the blood-retinal barrier as measured by TEER. The proposed mechanism of action involves NACA scavenging existing reactive oxygen species and increasing levels of reduced glutathione. With the prevalence of AMD and other retinal degeneration disorders that are expected to double in the coming decades, the development of more effective therapies to prevent their progression is imperative. Our results indicate that NACA has the potential to become an effective therapeutic agent by enhancing antioxidant defenses while removing pathologically relevant ROS.

## ACKNOWLEDEMENTS

## CONFLICT OF INTEREST

The authors have no financial, consulting, or personal conflicts of interest pertaining to this work.

## ABBREVIATIONS

**AMD**, Age-related macular degeneration; **7-AAD**, 7-aminoactinomycin-D; **AREDs**, age-related eye diseases; **GPx**, glutathione peroxidase; **GR**, glutathione reductase; **GSH**, glutathione; **GSSG**, reduces glutathione disulfide; **HRPEpiC**, primary human retinal pigment epithelial cells; **NACA**, N-acetylcysteine amide; **NPM**, N-(1-pyrenyl)-maleimide; **ROS**, reactive oxygen species; **RPE**, retinal pigment epithelium; **TBHP**, *tert*-butyl hydroperoxide; **TEER**, transepithelial electrical resistance.

## SUMMARY

1. TBHP increased intracellular ROS levels in HRPEpiC, and NACA prevented ROS generation.

2. Dose-dependent GSH depletion by TBHP was prevented by pretreatment with NACA.

3. Pretreatment with NACA preserved of GR activity.

4. NACA inhibited oxidative stress-related breakdown of HRPEpiC monolayer paracellular permeability.

5. NACA significantly improved cell survival when administered prior to and during oxidative damage.

# REFERENCES

1.      Congdon N, O'Colmain B, Klaver CC, Klein R, Munoz B, Friedman DS et al. Causes and prevalence of visual impairment among adults in the United States. Arch Ophthalmol. 2004;122:477-85.

2.      Pascolini D, Mariotti SP, Pokharel GP, Pararajasegaram R, Etya'ale D, Negrel AD et al. 2002 global update of available data on visual impairment: a compilation of population-based prevalence studies. Ophthalmic Epidemiol. 2004;11:67-115.

3.      Wong WL, Su X, Li X, Cheung CM, Klein R, Cheng CY et al. Global prevalence of age-related macular degeneration and disease burden projection for 2020 and 2040: a systematic review and meta-analysis. Lancet Glob Health. 2014;2:e106-16.

4.      Jonas JB, Bourne RR, White RA, Flaxman SR, Keeffe J, Leasher J et al. Visual impairment and blindness due to macular diseases globally: a systematic review and meta-analysis. Am J Ophthalmol. 2014;158:808-15.

5.      Plafker SM, O'Mealey GB, and Szweda LI. Mechanisms for countering oxidative stress and damage in retinal pigment epithelium. Int Rev Cell Mol Biol. 2012;298:135-77.

6.      Ambati J and Fowler BJ. Mechanisms of age-related macular degeneration. Neuron. 2012;75:26-39.

7.      Lang CA, Naryshkin S, Schneider DL, Mills BJ, and Lindeman RD. Low blood glutathione levels in healthy aging adults. J Lab Clin Med. 1992;120:720-5.

8.      Paasche G, Huster D, and Reichenbach A. The glutathione content of retinal Muller (glial) cells: the effects of aging and of application of free-radical scavengers. Ophthalmic Res. 1998;30:351-60.

9.      Cai J, Nelson KC, Wu M, Sternberg P, Jr., and Jones DP. Oxidative damage and protection of the RPE. Prog Retin Eye Res. 2000;19:205-21.

10.     A randomized, placebo-controlled, clinical trial of high-dose supplementation with vitamins C and E, beta carotene, and zinc for age-related macular degeneration and vision loss: AREDS report no. 8. Arch Ophthalmol. 2001;119:1417-36.

11.     Carey JW, Tobwala S, Zhang X, Banerjee A, Ercal N, Pinarci EY et al. N-acetyl-L-cysteine amide protects retinal pigment epithelium against methamphetamine-induced oxidative stress. Journal of Biophysical Chemistry. 2012;Vol.03No.02:10.

12. Carey JW, Pinarci EY, Penugonda S, Karacal H, and Ercal N. In vivo inhibition of l-buthionine-(S,R)-sulfoximine-induced cataracts by a novel antioxidant, N-acetylcysteine amide. Free Radic Biol Med. 2011;50:722-9.

13. Tobwala S, Pinarci EY, Maddirala Y, and Ercal N. N-acetylcysteine amide protects against dexamethasone-induced cataract related changes in cultured rat lenses. Advances in Biological Chemistry. 2014;Vol.04No.01:9.

14. Schimel AM, Abraham L, Cox D, Sene A, Kraus C, Dace DS et al. N-acetylcysteine amide (NACA) prevents retinal degeneration by up-regulating reduced glutathione production and reversing lipid peroxidation. Am J Pathol. 2011;178:2032-43.

15. Maddirala Y, Tobwala S, Karacal H, and Ercall N. Prevention and reversal of selenite-induced cataracts by N-acetylcysteine amide in Wistar rats. in Acta Ophthalmologica. 2016.

16. Winters RA, Zukowski J, Ercal N, Matthews RH, and Spitz DR. Analysis of glutathione, glutathione disulfide, cysteine, homocysteine, and other biological thiols by high-performance liquid chromatography following derivatization by n-(1-pyrenyl)maleimide. Anal Biochem. 1995;227:14-21.

17. Carlberg I and Mannervik B. Glutathione reductase. Methods Enzymol. 1985;113:484-90.

18. Tobwala S and Ercal N, N-Acetylcysteine Amide (NACA), a Novel GSH Prodrug: Its metabolism and Implications in Health, in Glutathione: Biochemistry, Mechanisms of Action and Biotechnological Implications, N. Labrou and E. Flemetakis, Editors. 2013, Nova Science Publishers, Inc. 111-42.

19. Ates B, Abraham L, and Ercal N. Antioxidant and free radical scavenging properties of N-acetylcysteine amide (NACA) and comparison with N-acetylcysteine (NAC). Free Radic Res. 2008;42:372-7.

20. Martinez A, Galano A, and Vargas R. Free radical scavenger properties of alpha-mangostin: thermodynamics and kinetics of HAT and RAF mechanisms. J Phys Chem B. 2011;115:12591-8.

21. Ablonczy Z, Dahrouj M, Tang PH, Liu Y, Sambamurti K, Marmorstein AD et al. Human retinal pigment epithelium cells as functional models for the RPE in vivo. Invest Ophthalmol Vis Sci. 2011;52:8614-20.

22. Blenkinsop TA, Saini JS, Maminishkis A, Bharti K, Wan Q, Banzon T et al. Human Adult Retinal Pigment Epithelial Stem Cell-Derived RPE Monolayers Exhibit Key Physiological Characteristics of Native Tissue. Invest Ophthalmol Vis Sci. 2015;56:7085-99.

23. Finkel T and Holbrook NJ. Oxidants, oxidative stress and the biology of ageing. Nature. 2000;408:239-47.

24. Sternberg P, Jr., Davidson PC, Jones DP, Hagen TM, Reed RL, and Drews-Botsch C. Protection of retinal pigment epithelium from oxidative injury by glutathione and precursors. Invest Ophthalmol Vis Sci. 1993;34:3661-8.

25. Grinberg L, Fibach E, Amer J, and Atlas D. N-acetylcysteine amide, a novel cell-permeating thiol, restores cellular glutathione and protects human red blood cells from oxidative stress. Free Radic Biol Med. 2005;38:136-45.

26. Penugonda S, Mare S, Goldstein G, Banks WA, and Ercal N. Effects of N-acetylcysteine amide (NACA), a novel thiol antioxidant against glutamate-induced cytotoxicity in neuronal cell line PC12. Brain Res. 2005;1056:132-8.

27. Issels RD, Nagele A, Eckert KG, and Wilmanns W. Promotion of cystine uptake and its utilization for glutathione biosynthesis induced by cysteamine and N-acetylcysteine. Biochem Pharmacol. 1988;37:881-8.

28. Tokarz P, Kaarniranta K, and Blasiak J. Role of antioxidant enzymes and small molecular weight antioxidants in the pathogenesis of age-related macular degeneration (AMD). Biogerontology. 2013;14:461-82.

29. Shivananjappa MM, Mhasavade D, and Joshi MK. Aqueous extract of Terminalia arjuna attenuates tert-butyl hydroperoxide-induced oxidative stress in HepG2 cell model. Cell Biochem Funct. 2013;31:129-35.

30. Omatsu T, Naito Y, Handa O, Hayashi N, Mizushima K, Qin Y et al. Involvement of reactive oxygen species in indomethacin-induced apoptosis of small intestinal epithelial cells. J Gastroenterol. 2009;44 Suppl 19:30-4.

31. Geiger RC, Waters CM, Kamp DW, and Glucksberg MR. KGF prevents oxygen-mediated damage in ARPE-19 cells. Invest Ophthalmol Vis Sci. 2005;46:3435-42.

32. Campa C. Effect of VEGF and anti-VEGF compounds on retinal pigment epithelium permeability: an in vitro study. Eur J Ophthalmol. 2013;23:690-6.

33. Zou X, Feng Z, Li Y, Wang Y, Wertz K, Weber P et al. Stimulation of GSH synthesis to prevent oxidative stress-induced apoptosis by hydroxytyrosol in human retinal pigment epithelial cells: activation of Nrf2 and JNK-p62/SQSTM1 pathways. J Nutr Biochem. 2012;23:994-1006.

34. Nelson KC, Armstrong JS, Moriarty S, Cai J, Wu MW, Sternberg P, Jr. et al. Protection of retinal pigment epithelial cells from oxidative damage by oltipraz, a cancer chemopreventive agent. Invest Ophthalmol Vis Sci. 2002;43:3550-4.

35.    Jiang S, Wu MW, Sternberg P, and Jones DP. Fas mediates apoptosis and oxidant-induced cell death in cultured hRPE cells. Invest Ophthalmol Vis Sci. 2000;41:645-55.

# II. N-ACETYLCYSTEINE AMIDE (NACA) EYE DROPS PARTIALLY PREVENT THE LOSS OF VISUAL FUNCTION AND RETINAL DAMAGE IN A CHEMICALLY-INDUCED RETINAL DEGENERATION ANIMAL MODEL

Hsiu-Jen Wang[1], Shakila Banu Tobwala[1], Annalise Pfaff[1], Daniel Lindgren[2], Robert S. Aronstam[3], Humeyra Karacal[4], and Nuran Ercal[5]*

1. Department of Chemistry, Missouri University of Science and Technology, Rolla MO, USA

2. OcuScience, Henderson NV, USA

3. College of Science and Technology, Bloomsburg University, Bloomsburg PA, USA

4. Ophthalmology & Visual Sciences, Washington University School of Medicine, St. Louis MO, USA

5. Richard K. Vitek/FCR Endowed Chair in Biochemistry, Missouri University of Science and Technology, Rolla MO, USA

*Corresponding author

Dr. Nuran Ercal

Chemistry department, Missouri University of Science and Technology,

400 W. 11th street, Rolla, MO 65409, USA

Phone: +1 (573) 341-6950

Fax: +1 (573) 341-6033

Email address: nercal@mst.edu

Keywords: AMD, sodium iodate, thiol antioxidant, and NACA

**ABSTRACT**

Oxidative stress is considered to be a major factor in the development of age-related macular degeneration (AMD), and the neuroretina is more sensitive to oxidative insult when compared to the retinal pigment epithelium (RPE). We hypothesized that N-acetylcysteine amide (NACA) would protect the neuroretina and retard progression of retinal degeneration. Sodium iodate ($NaIO_3$)-treated C57BL/6 mice were used to evaluate the therapeutic potential of NACA eye drops by assessing visual and photoreceptor function through electroretinogram (ERG) and measurements of the outer nuclear layer (ONL) thickness, the phosphatase and tensin homolog deleted on chromosome ten (PTEN), and oxidative stress parameters (such as glutathione (GSH), cysteine, and 4-hydroxynenal (4-HNE) levels). Our results indicated that NACA eye drops partially prevented the reduction in the ERG waveform peak amplitudes measured 36 hours after $NaIO_3$ injection. Furthermore, NACA eye drops prevented reduction in ONL thickness. Significant increases in GSH, cysteine, 4-HNE, and PTEN were observed, but were reversed upon treatment with NACA eye drops in this animal model. These results illustrated that NACA eye drops partially prevent photoreceptor degeneration and loss of visual potential 36 hours after $NaIO_3$ injection. Accordingly investigations of this potent antioxidant as a treatment for AMD should definitely be continued.

# 1. INTRODUCTION

Age-related macular degeneration (AMD) is the leading cause of irreversible blindness in the industrialized world and the third leading cause worldwide [1]. This creates an annual direct health care cost of $4.6 billion in the U.S. [2]. Unfortunately, patients with AMD lose quality of life, as they need assistance in their daily tasks of simply walking, reading, or driving [3].

AMD is a complex disease affected by senescence, genetic predisposition, environmental factor, and oxidative stress, all of which may contribute to its pathogenesis [4, 5]. AMD preferentially affects the macula—the central region of the retina. Due to its high oxygen tension, high metabolic rate, and a greater proportion of polyunsaturated fatty acids (PUFAs), the macula is subject to increased levels of photo-oxidative stress [6-9]. The endogenous antioxidants, such as GSH, in the retinal tissue support the redox balance that is crucial to maintaining healthy retinal pigment epithelial (RPE) cells and normal function of the eye [10]. Exogenous oxidative stress is potentiated by the relative paucity of antioxidants in an aging retina. Light-induced peroxidation of shed photoreceptor outer segments containing PUFAs leads to the formation of toxic reactive oxygen species (ROS) and lipofuscin [11-13]. AMD is classified as dry (non-exudative) or wet (exudative) clinically. Non-exudative disease is characterized by RPE death, or geographic atrophy. Attenuation of the overlying photoreceptors, which are located in the outer nuclear layer, follows retinal pigment epithelial demise. The distinguishing feature of wet AMD is choroidal neovascularization, followed by exudation and hemorrhaging as the disease worsens. If left untreated, dry AMD may progress to wet [14, 15]; however, this

can be halted if a therapeutic intervention is initiated early enough during the course of the disease.

Research efforts, using antioxidants to treat AMD, are plentiful because oxidative stress is one of the most important causes of AMD [16, 17]. Currently, the only available treatment to slow the progression of visual loss in dry AMD includes vitamin and micronutrient supplementation, cessation of smoking, and dietary modification [18, 19]. In large prospective trials, like the Age-Related Eye Disease Study (AREDS), a wide variety of nutrients, such as vitamins, ω-3 fatty acids, antioxidants (β-carotene and vitamins C and E), zinc, lutein, and zeaxanthin were studied [5, 20]. The results of these studies were inconclusive; therefore, there is a dire need to develop an effective treatment for AMD.

An ideal therapeutic agent should be highly bioavailable, non-toxic, easy to use, economical, and should limit oxidation, boost anti-oxidative mechanisms, and even reverse existing damage. One such candidate is N-acetylcysteine amide (NACA), a thiol antioxidant that has demonstrated beneficial effects on oxidative-stress related eye disorders [21-25]. Because AMD has a multifactorial etiology, no single animal model can fully recapitulate all of its pathologic features. Sodium iodate ($NaIO_3$), a stable oxidizing agent, was first used in a model of retinal degeneration by Sorsby in 1941 [26]. Since then, the systemic exposure of $NaIO_3$ has been an effective way to induce retinal degeneration and retinal pigment epithelium atrophy. Thus this model was a very appropriate model to use for evaluating therapeutic approaches to retinal degeneration [27]. $NaIO_3$ induces both retinal pigment epithelium degeneration and altered neurosensory function via separate cell-death pathways: necrosis in RPE and caspase-dependent apoptosis in photoreceptors [28-30]. Surprisingly, the photoreceptors seemed more vulnerable to oxidative insult, as

compared to RPE [29]. Other studies have suggested that necroptosis is a major mechanism for RPE cell death in response to oxidative stress in the AMD and apoptosis is the major mechanism for photoreceptor cell death in response to oxidative stress [31, 32]. Because the pathogenic mechanism of the AMD still remains unclear, antioxidants have garnered much interest in laboratory and clinical studies [18, 33, 34].

The tumor suppressor PTEN (phosphatase and tensin homolog deleted on chromosome 10) has three primary functions: cell adhesion and lipid phosphatase as well as protein phosphatase activities. PTEN plays a critical role in the organization of RPE cell junctions and adhesion [35]. The phosphatase activity of PTEN can recover junctional β-catenin and can suppress the epithelial-to-mesenchymal transition, thereby inhibiting the cell migration associated with the onset of retinal degeneration. The catalytic activity of PTEN is modulated by ROS. The presence of oxidants in the cellular environment can lead to inactivation of PTEN by phosphorylation, which disturbs the RPE adhesion structure and initiates RPE degeneration. In an advanced tumor cell, free fatty acid-induced oxidative stress is mediated by phosphorylates PTEN and suppression of PTEN monoubiquitination, which results in nuclear export of PTEN [36]. PTEN inactivation and the resulting Akt activation are inhibited by antioxidant treatment [37]. PTEN also regulates retinal interneuron morphogenesis and synaptic layer formation [38]. In summary, PTEN is strongly linked with ROS and PI3K/Akt cell survival signaling pathways.

Ercal's group has extensively investigated the use of thiol antioxidants, particularly NACA, in oxidative stress-related eye disorders including cataracts and light-induced retinal degeneration [21-23, 25, 39]. Their results showed that NACA restored GSH

levels and activities of glutathione reductase (GR), glutathione peroxidase (GPx) and catalase in L-buthionine-(S, R)-sulfoximine (BSO)-induced cataracts in rats [21]. NACA maintained outer nuclear layer thickness and RPE cell integrity in mice exposed phototoxic light [23]. In previous eye-related investigations, NACA was given as an injection; however, an eye drop formulation would be more desirable and more conveniently administered in both a clinical setting and by patients themselves. Accordingly, this study was designed to formulate a type of NACA eye drops that can be more conveniently administered in real-life cases, to protect the neuroretina against oxidative stress-induced damage. An understanding of the protective role of NACA would help in development of NACA eye drops for treatment of oxidative stress-related retinal diseases.

## 2. MATERIALS AND METHODS

### 2.1. MATERIALS

N-acetylcysteine amide (NACA) was provided by Dr. Glenn Goldstein (David Pharmaceuticals, New York, NY, USA). C57BL/6 mice were obtained from the Jackson Laboratory (Bar Harbor, ME, USA). Other chemicals were ordered from Sigma (St. Louis, MO, USA), unless otherwise indicated.

### 2.2. ANIMAL MODEL AND EXPERIMENTAL DESIGN

Seven-week-old male C57BL/6 mice were received and housed in a temperature- and humidity-controlled (about 22°C and 55%) animal facility, with a 12-hour light and dark cycle. The animals had free access to rodent chow and water, and animals were

acclimatized for 1 week before experiments were performed. All animal procedures conformed to the ARVO Statement for the Use of Animals in Ophthalmic and Vision Research and were approved by the Institutional Animal Care and Use Committee of Missouri University of Science and Technology.

Eight-week-old C57BL/6 mice received 0.1% NACA eye drops (in 25 mM phosphate buffer, pH = 7.4) or phosphate buffer bilaterally twice a day, every other day for 4 weeks. After dosing with NACA for 4 weeks, the mice received one intraperitoneal (IP) injection of 75 mg/kg $NaIO_3$, and then eye drops were continued for another week.

On the final day of the experiment, mice were anesthetized by an IP injection of ketamine (120 mg/kg) and xylazine (16 mg/kg), and cervical dislocation was used for the secondary euthanasia method. Retinas were removed under a dissecting microscope and immediately placed in liquid nitrogen for further analysis.

## 2.3. ELECTRORETINOGRAPHY (ERG)

After adaptation for 10-12 hours in the dark, ERGs were recorded in mice under anesthesia induced by isoflurane [40] (Butler Schein, Dublin OH) (2.25% for induction and 1.25% maintenance). Mice were placed on a heating pad to maintain their body temperature during anesthesia. Proparacaine hydrochloride ophthalmic solution and tropicamide (0.5%, Akorn Inc, IL, USA) were used as the topical anesthetic and mydriatic, respectively. The recording electrode was placed in a drop of methylcellulose on the surface of the cornea, a reference electrode was placed subdermally at the vertex of the skull, and a ground electrode was placed subdermally at the base of the tail. Scotopic and photopic ERGs were recorded and processed using a HMsERG LAB system and ERGView 2.5 analytical software [41] (OcuScience, Henderson, NV, USA).

ERG procedures started with a scotopic intensity series from -3 to 1 log (cd·s/m$^2$).

Photopic ERGs were recorded after light adaption (10000 mcd·s/m$^2$) for 5 min (mcd:

millicandelas).

## 2.4. HEMATOXYLIN AND EOSIN (H&E) STAINING

Eyes were enucleated and fixed in 4% paraformaldehyde overnight. Briefly, the

eyes were then embedded in paraffin, and serial 5 μm sagittal sections of the whole eye

were cut through the cornea to the optic nerve. Paraffin-embedded serial sections of

retina were deparaffinized with xylene and absolute ethanol, rehydrated with distilled

water, stained with hematoxylin solution, and counterstained with eosin.

## 2.5. OUTER NUCLEAR LAYER (ONL) THICKNESS MEASUREMENT

In each fixed and H&E-stained eye ($n = 3$ mice), ONL thickness was measured at

40-μm intervals across 400-μm sections of the parafoveal area, located 500 μm from the

optic nerve head. Images were analyzed at 20X objective magnification using ImageJ

image processing software (Version 1.49, NIH). For every group, ONL thickness at each

interval was averaged, and statistical analysis was performed.

## 2.6. 4-HYDROXYNONENAL (4-HNE) IMMUNOHISTOCHEMISTRY STAINING AND QUANTIFICATION

Briefly, serial sections adjacent to those designated for H&E staining were taken

from paraffin-embedded eyes ($n = 3$ mice). Sections were deparaffinized, rehydrated,

blocked, and incubated overnight at 4°C with anti-4HNE antibody (1:100 dilution;

ab46545, Abcam, MA, USA) using 3,3'-Diaminobenzidine (DAB) as the chromogen

(which indicates the presence of 4-HNE as a dark brown stain) and hematoxylin as the

counterstain. Images were examined at 100X objective magnification for quantification

of 4-HNE levels, using ImageJ to determine the proportion of dark brown area to the total image area in the ONL.

## 2.7. MEASUREMENT OF INTRACELLULAR GLUTATHIONE (GSH) AND CYSTEINE LEVELS

Mice ($n = 5$) were sacrificed and eyes were enucleated and dissected under a dissection microscope to verify isolation of the retina without RPE contamination. The retinas were homogenized in 250 μL of cold serine borate buffer (pH 7.5). GSH and cysteine were separated and quantified by HPLC with fluorescence detection (Finnigan Surveyor FL Plus, Thermo Scientific, USA) after derivatization with N-(1-pyrenyl)maleimide (NPM) [42-44]. Protein levels of the homogenates were measured by the Bradford method [45] (BioRad Laboratories, Inc., CA, USA).

## 2.8. SDS-PAGE AND WESTERN BLOT FOR PTEN AND PHOSPHO-PTEN (P-PTEN) ANALYSIS

Protein levels of the cell homogenates were measured by bicinchoninic acid (BCA) protein assay. 25 μg protein samples (n=3 mice) were separated in NuPage 12% Bis-Tris gels (Life Technologies, Grand Island, NY). Anti-PTEN (Cat # 9552) and anti-p-PTEN (Ser380/Thr382/383; 1000 dilutions; Cat # 95541, Cell Signaling, MA, USA) were used as the first antibody, and GAPDH (glyceraldehyde-3-phosphate dehydrogenase) (1:1000 dilutions; Cell Signaling) was used as the dominant housekeeping gene. SuperSignal Chemiluminescent Substrate was used to visualize PTEN bands. Membrane was stripped after PTEN measurement, and the procedure was repeated for anti-p-PTEN. SuperSignal West Pico Chemiluminescent Substrate and Restore Western blot stripping buffer were obtained from Thermo Scientific.

## 2.9. STATISTICAL ANALYSIS

All reported values were represented as the mean $\pm$ SD ($n \geq 3$). Statistical analysis was performed using GraphPad Prism 5.01 software (GraphPad Software Inc., La Jolla, CA). Statistical significance was ascertained by one-way analysis of variance (ANOVA) and Tukey's multiple comparison tests. Statistical significance was set at $P < 0.05$ (*, $P < 0.05$; **, $P < 0.01$; ***, $P < 0.001$).

## 3. RESULTS

## 3.1. PARTIAL PREVENTION OF SODIUM IODATE-INDUCED VISUAL LOSS BY NACA

In order to investigate the effect of NACA on $NaIO_3$-induced retinal dysfunction, electroretinography was performed 36 hours and 6 days after a $NaIO_3$ injection. Figure 1 is a subset of data in scotopic view at 3000 mcd·s/m$^2$ showing the mixed rod and cone response. Figure 1A is the average of the subset ERG data obtained 36 hours after $NaIO_3$ IP injection. Figure 1B-1F shows the data from day 6. The first negative peak was the a-wave, which was followed by the large, positive b-wave. The a-wave and b-wave represent the health of outer and inner retina, respectively. The a- and b-wave amplitude were attenuated and the implicit time prolonged in the aged eye. The average a-wave amplitudes in the control and NACA groups were 220.0 μV and 187.5 μV, respectively. Application of $NaIO_3$ led to a significant reduction in all ERG waveform peak amplitudes and increased a-wave implicit time. The average a-wave amplitude in the $NaIO_3$ group was 12.4 μV. In contrast, the mean a-wave amplitude measured in the NACA+$NaIO_3$

group was 181.7 µV. However, the a-wave implicit times were increased in both $NaIO_3$

and $NACA+NaIO_3$ groups. On day 6, the a-wave amplitude in the control, NACA, $NaIO_3$

and $NACA+NaIO_3$ group were $203.5 \pm 28.7$, $261.3 \pm 26.3$, $43.9 \pm 17.6$ and $27.4 \pm 11.0$

µV, respectively. The b-wave amplitude in the control, NACA, $NaIO_3$ and $NACA+NaIO_3$

group were $377.0 \pm 54.7$, $501.7 \pm 80.7$, $47.2 \pm 21.8$ and $19.0 \pm 4.7$ µV, respectively. The

average of a- and b-wave amplitude and implicit time are shown in Figure 1C-1F.

## 3.2. NACA PREVENTS OXIDATIVE DAMAGE AND OUTER NUCLEAR LAYER (ONL) THINNING

To investigate the ability of NACA eye drops to prevent photoreceptor death, the

thickness of the ONL, which contains rod and cone cell bodies, was measured.

Representative images of H&E-stained retinal sections are shown in Figure 2A, and the

averaged ONL thickness is shown in Figure 2B. In the $NaIO_3$ group, significant loss of

RPE and associated photoreceptor disorganization were observed. The outer segment

layer of rods and cones was markedly reduced, and the boundary between the inner and

outer segments (IS and OS) was lost. ONL folding and thinning were also detected. The

averages of the ONL thickness in the control and NACA groups were $54.48 \pm 3.32$ and

$55.7 \pm 4.97$ µm, respectively. The ONL thickness was significantly reduced in the $NaIO_3$

group ($32.96 \pm 4.12$ µm) as compared to the control group, but NACA eye drops

significantly prevented ONL thinning ($43.87 \pm 7.89$ µm) (***, $P < 0.001$).

## 3.3. EFFECTS OF $NAIO_3$-INJECTION AND NACA EYE DROPS ON RETINAL GSH AND CYSTEINE LEVELS

To determine the effects of oxidative stress, retinal tissues ($n = 5$) were dissected

and collected on day 7 after injection of $NaIO_3$ in order to measure GSH and cysteine

levels. GSH levels (Figure 3A) in the sodium iodate group were slightly increased ($26.0 \pm$

1.1 nmol/mg protein) compared to the control group ($23.5 \pm 0.9$ nmol/mg protein) ($P <$

0.001).  The GSH levels in the NACA group were $22.4 \pm 1.1$ nmol/mg protein, which was close to the control group. The cysteine levels (Figure 3B) in the control, NACA, $NaIO_3$ and the $NACA+NaIO_3$ groups were $0.6 \pm 0.1$, $0.5 \pm 0.1$, $5.6 \pm 1.1$ and $4.0 \pm 1.2$ nmol/mg protein, respectively. The cysteine levels in the $NaIO_3$ group were significantly higher than in both the control and NACA groups ($P < 0.001$).
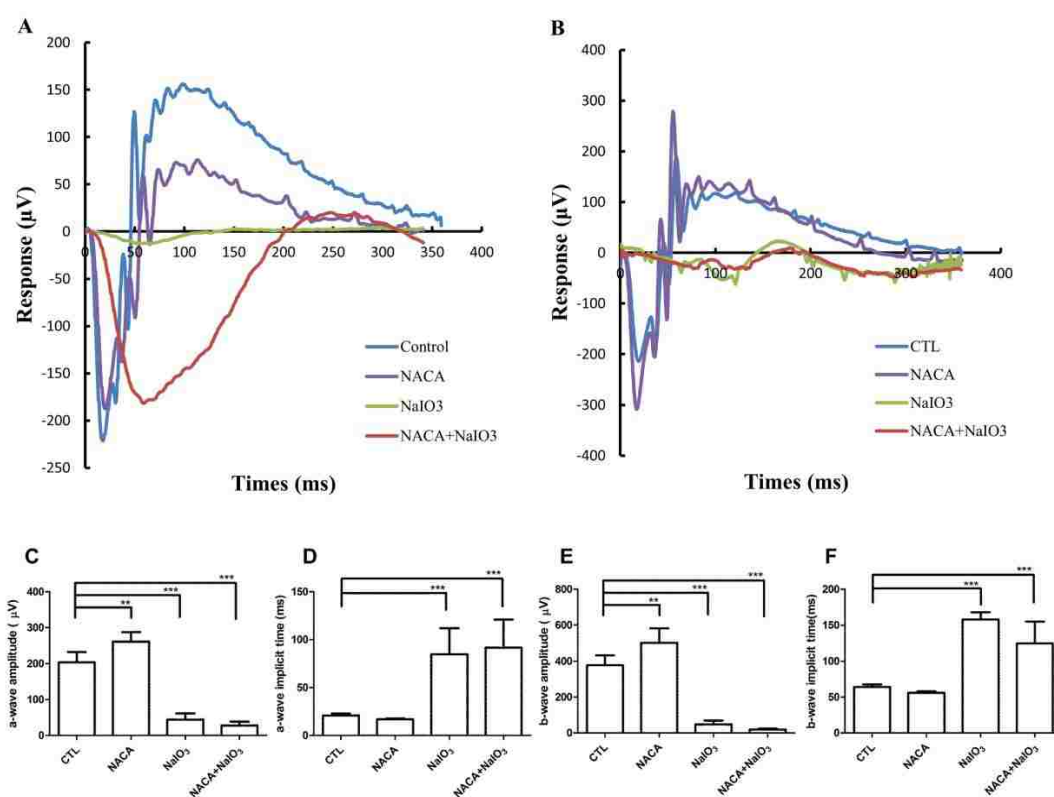


Figure 1. Partial prevention of sodium iodate-induced retinal dysfunction.
A represents ERG subset data in scotopic view at 3000 mcd·s/m$^2$ showing mixed rod and cone response ($n = 4$-6). A) ERG data were obtained 36 hours after $NaIO_3$ IP injection. The a-wave and b-wave amplitudes were decreased and the implicit time was prolonged in the $NaIO_3$-only group. Pretreatment with NACA eye drop partially prevented reductions in all ERG waveform peak amplitudes when compared to the $NaIO_3$-treated group. B) ERG data were collected on day 6 after $NaIO_3$ injection (one day before sacrifice). A-wave and b-wave are attenuated in the $NaIO_3$ group. (C-F) Data analysis of (B): (C) a-wave amplitude. (D) a-wave implicit time. (E) b-wave amplitude. (F) b-wave implicit time. NACA eye drops failed to protect photoreceptor function at day 6.
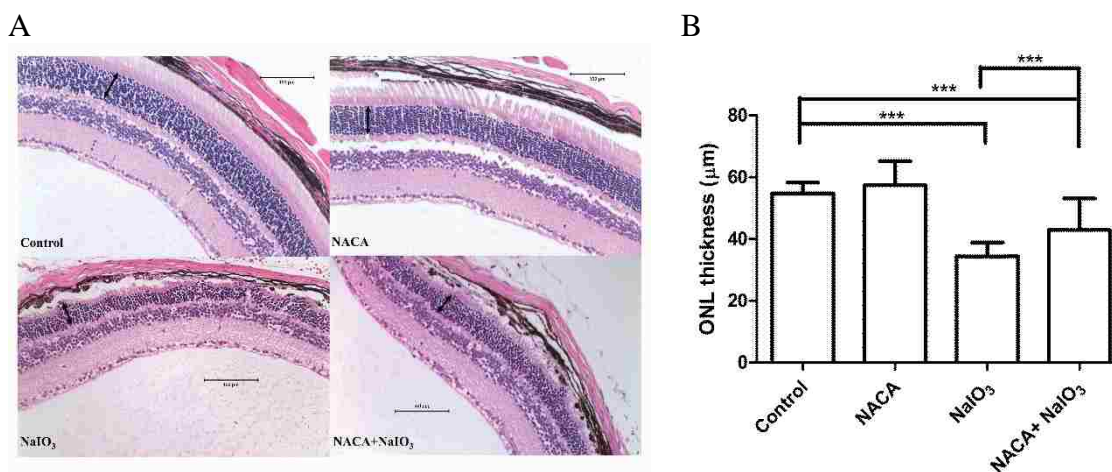
Figure 2. NACA prevents oxidative damage and outer nuclear layer thinning.
(A) A representative image of H&E staining for retinal sections showing prevention of ONL thinning by NACA eye drop (A double-headed arrow indicates the ONL).
(B) Average ONL thickness for each treatment group ($n = 3$ mice).
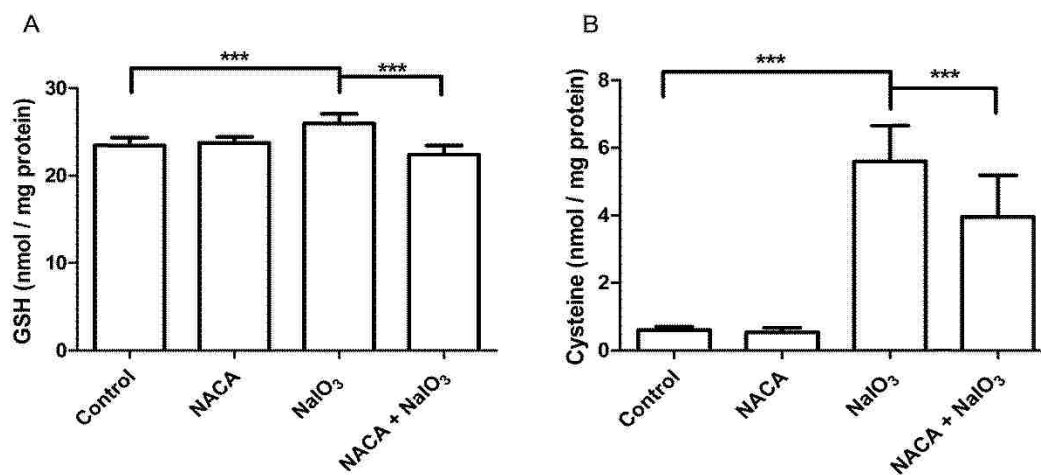


Figure 3. Thiol levels in retina.
(A) GSH levels ($n = 5$)  (B) Cysteine levels ($n = 5$)

## 3.4. REDUCTION OF LIPID PEROXIDATION BY-PRODUCT 4-HNE BY NACA IN ONL

To evaluate the ability of NACA to prevent lipid peroxidation, retinal samples were stained for 4-HNE adducts by immunohistochemistry. A representative image of the 4-HNE stain is shown in Figure 4A. A greater proportion of brown color in a given area indicated more 4-HNE adduct formation as demonstrated in Figure 4B. The averages ($n = 4$) of 4-HNE adduct-stained areas relative to the total stained area in each group were as follows: $0.49 \pm 0.03$ in the control group, $0.47 \pm 0.05$ in the NACA group, $0.67 \pm 0.03$ in the NaIO$_3$ group, and $0.5 6\pm 0.05$ in the NACA+NaIO$_3$ group. The 4-HNE levels were significantly increased in the NaIO$_3$ group ($P < 0.01$, compared to control) and decreased in the NACA+NaIO$_3$ group ($P < 0.05$, compared to NaIO$_3$ group).

A                                                                 B
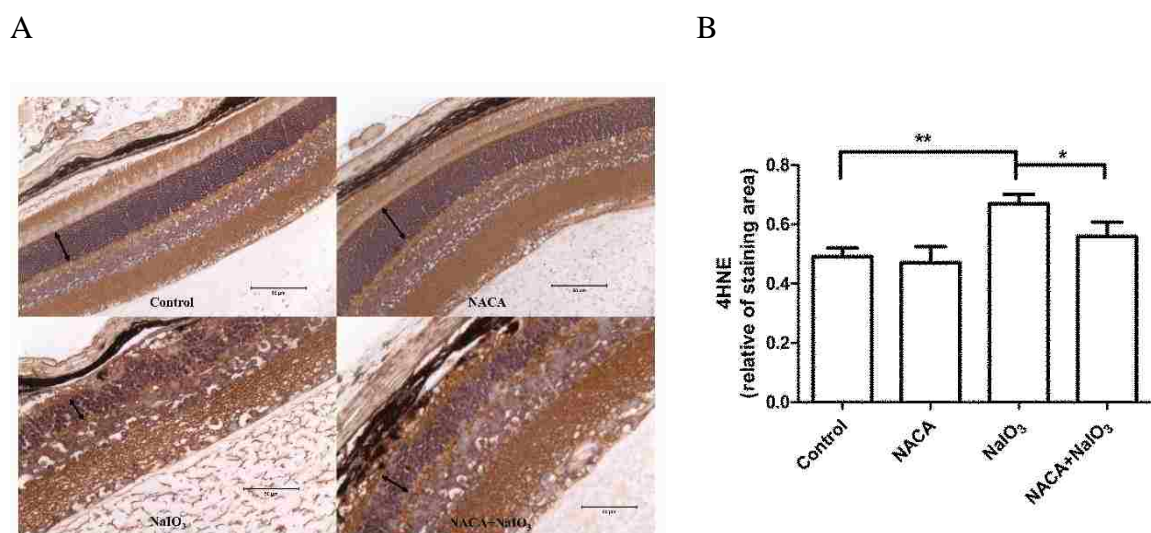


Figure 4. Reduction of lipid peroxidation by-product formation in ONL
(A) Immunohistochemical detection of 4-HNE adducts in retina (40X objective).
(B) Quantification of 4-HNE levels in ONL (A double-headed arrow indicates the ONL) ($n = 3$).

## 3.5. PTEN AND PHOSPHORYLATED-PTEN (P-PTEN) IN THE RETINA

In order to evaluate the PTEN and phosphorylated PTEN (p-PTEN) levels in the retina of mice treated with $NaIO_3$, PTEN and p-PTEN were analyzed using the Western blot. Figure 5A and 5B show the Western blot and the quantitated results for PTEN and p-PTEN, respectively. The calculated PTEN/p-PTEN ratio is shown in Figure 5C.

PTEN levels in the $NaIO_3$ group were 1.22 times greater than the control, and the $NACA+NaIO_3$ group PTEN levels were 1.07 times greater than the control. The p-PTEN levels were increased in the $NaIO_3$-injected group but not significantly when compared with the control group; however, p-PTEN levels were significantly lower in the $NACA+NaIO_3$ group ($P < 0.05$). The average of PTEN/p-PTEN ratio in control, NACA, $NaIO_3$ and $NACA+NaIO_3$ group were 1.003, 0.98, 1.12 and 1.23, respectively. The PTEN/p-PTEN ratio in the $NACA+NaIO_3$ group was significantly higher ($P < 0.05$).
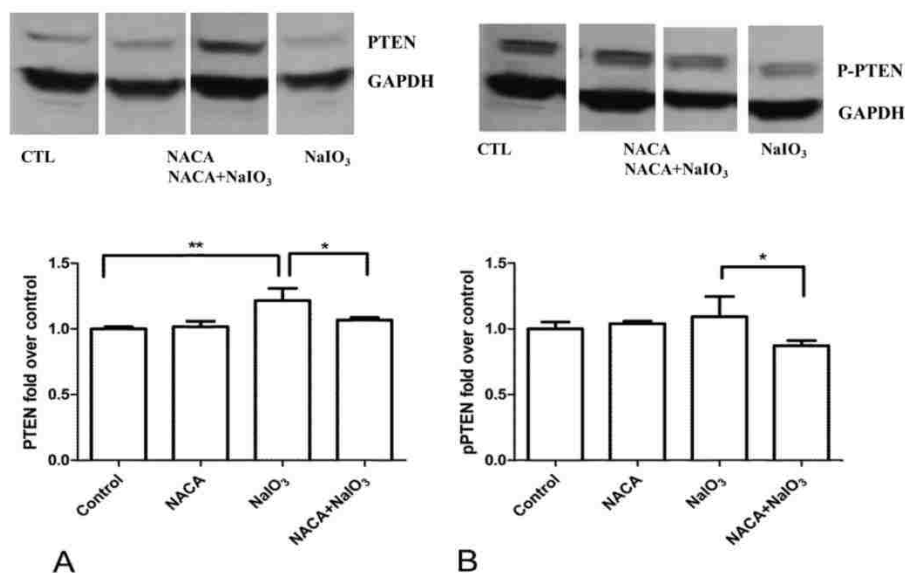


Figure 5. PTEN and phosphorylated-PTEN (p-PTEN) in the retina.
Western blots and quantitated results for PTEN (A), p-PTEN (B). (**, $P < 0.01$ and *, $P < 0.05$) ($n = 3$).
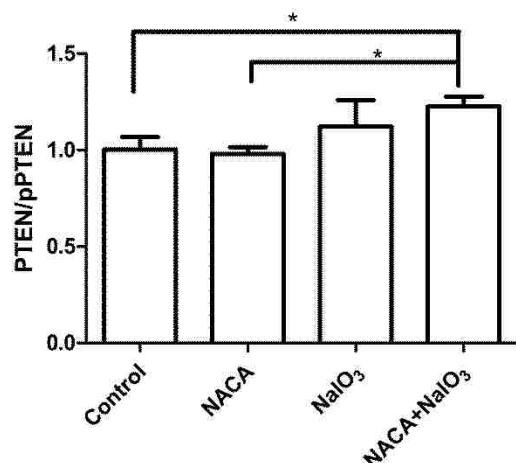
Figure 6 The calculated PTEN/p-PTEN ratio from Figure 5.

## 4. DISCUSSION

$NaIO_3$-induced retinal degeneration in a C57BL/6 mouse model was used to investigate the effects of NACA eye drops as treatment for oxidative stress-induced retinal degeneration. $NaIO_3$ is a stable oxidizing agent that has been employed in many retinal degeneration studies, and systemic administration has been reported to selectively impair the RPE, which leads to loss of photoreceptors [46]. However, $NaIO_3$ can also directly impair the neuroretina *in vitro* and *in vivo* models [29, 47], and the neuroretina seems to be more vulnerable to $NaIO_3$-induced damage compared to the RPE *in vivo* [29]. The underlying molecular mechanisms of $NaIO_3$ toxicity include activation of Akt, reduction in RPE-specific protein (RPE65), accumulation of ROS in mitochondria, impairment of Nrf2 signalling, and inactivation of PTEN in cell adhesion [27, 29, 35]. In a C57BL/6 model, systemic exposure to $NaIO_3$ at low concentrations can induce rapid dysregulation of phototransduction genes in the neuroretina, including *Rho, OPn1mw*,

and *Pde6b*, as well as reduction in a- and b-wave amplitudes by day 3 and total loss by day 8 at higher concentrations [29].

N-acetylcysteine (NAC), a thiol antioxidant, has been used clinically to treat various disorders and is already approved by the FDA (the U.S. Food and Drug Administration). However, NACA, the amide derivative of NAC, has been shown to be more effective because of its neutral charge, which increases its ability to permeate cell membranes and the blood-neural barrier [48]. Independent research with NACA has demonstrated its improved penetration of cell membranes as compared to other antioxidants including NAC, vitamin E and carotenoids [49, 50]. This potent antioxidant functions by directly scavenging free radicals and indirectly by providing cysteine for GSH synthesis, substituting itself for depleted GSH, and chelating $Cu^{2+}$ that can catalyze ROS formation [51]. From the literature, NACA possesses antioxidant, anti-apoptotic, and anti-inflammatory properties [48]. As an antioxidant, NACA can scavenge radicals, chelate Pb(II), and participate in thiol-disulfide exchange between GSSG and NACA to replenish GSH *in vitro* [39, 49, 52, 53].

In our study, visual function was assessed using the flash electroretinography (ERG), a non-invasive method [54]. Using this model, we demonstrated that NACA partially maintained visual function for a short time after administration of a high dose of $NaIO_3$ (75 mg/kg), but it was unable to halt progression of retinal degeneration for the duration of the experimental time period. The subset of ERG in the scotopic view at 3000 mcd·s/m$^2$ represented a combined rod and cone response. The first negative a-wave, also called the "late receptor potential," was generated by photoreceptor hyperpolarization and reflected the general physiological health of the photoreceptors in

the outer retina [55]. In contrast, the following positive b-wave reflected the health of the inner layers of the retina, including the ON bipolar cells and the Muller cells [46, 56, 57]. Our data demonstrated that $NaIO_3$ significantly impaired photoreceptor hyperpolarization and post-phototransduction (Figure 1A-1B) and that NACA eye drops partially prevented this loss of visual function 36 hr after $NaIO_3$ injection. By the end of the study, however, NACA eye drops failed to prevent visual function loss. ROS can activate STAT3 (a transcription factor), which induces rhodopsin degradation via the ubiquitin-proteasome system. The resulting visual function impairment manifests as subnormal a-wave and b-wave measurements, which other research has shown [58-61]. $NaIO_3$ can damage the synapse between photoreceptors and depolarized bipolar cells, which results in a diminished ERG b-wave [29, 62].

ONL thickness was used as a metric for photoreceptor cell health. $NaIO_3$-induced damage to the outer segment (OS) and inner segment (IS) may explain the diminished a-wave and b-wave in our ERG results. NACA eye drops prevented the $NaIO_3$-induced thinning of the ONL, verifying its ability to partially preserve visual function as determined by ERG; however, the $NaIO_3$-induced RPE damage did not improve with NACA eye drops (Figure 2A).

GSH is the most abundant and critical antioxidant and redox buffer of the cell, and fluctuations in GSH levels following oxidative insult are largely dependent on the anti-oxidative capacity of the cell and time course of its response [63-65]. In this study GSH was found to be increased in the $NaIO_3$ group, which may have been the result of initiation of cellular defense against oxidative stress. There are many examples of GSH up-regulation under oxidative stress [25, 66, 67]. In addition to the altered GSH level, a

significant increase in the cysteine level was observed in the $NaIO_3$ group. This may have contributed to the rise in GSH levels, as cysteine availability is the rate limiting factor for GSH synthesis. The age of the of animals used in our study may also have affected GSH levels, due to their increased Nrf2 expression, as compared to older animals (noted by Sachdeva *et al*. [68]). Elevated cysteine is also known to be detrimental, as it may lead to glutamate-induced excitotoxicity [69, 70]. Although the cysteine level was significantly lower in the NACA+$NaIO_3$ group, it was still higher than in the control group.

Our results also showed that NACA decreased $NaIO_3$-induced lipid peroxidation in the ONL, which was measured by 4-hydroxynonenal (4-HNE) formation. Free radical chain reactions, initiated by oxygen or light, can damage molecules in the photoreceptor outer segments containing large concentrations of long-chain PUFAs that are particularly susceptible to lipid peroxidation and form toxic by-products such as malondialdehyde (MDA) and 4-HNE, which have been measured in the ONL in other studies [71]. Lipid peroxidation by-products can induce further production of ROS [72], which overwhelms repair mechanisms and ultimately leads to photoreceptor death and impaired visual potential. This is consistent with our ERG results and ONL thickness measurements.

To gain further insight into the mechanism of retinal degeneration induced by $NaIO_3$, we quantified the levels of phosphatase and tensin homolog deleted on chromosome 10 (PTEN) and phosphorylated PTEN (p-PTEN), using Western blot. PTEN can be inactivated by either phosphorylation or thiol oxidation [73, 74], and it has been shown that phosphorylation of PTEN at specific residues, namely Ser380, Thr382, or Thr383, decreases its association with junctional proteins [35]. Our results showed both PTEN and p-PTEN levels were increased in the $NaIO_3$ group. PTEN lipid phosphatase

activity can alter and inhibit PI3K/AKT/mTOR signalling (a known cell proliferation and survival pathway) [38, 75, 76]. However, when PTEN was inactivated, the resulting upregulation of mTORC1 through increased PI3K/Akt signaling can prolonged cone photoreceptor survival even during RPE cell malfunction or death in the $NaIO_3$ model [77]. Similar to its effect on GSH levels, $NaIO_3$-induced PTEN elevation may be the result of an active cellular defense against oxidative stress. Inactivation of PTEN leads to an epithelial-to-mesenchymal transition of RPE cells resulting in their migration out of the retina. Other independent studies, however, indicate that PTEN can be phosphorylated by ROS-activated PI3K [78]. Although ROS inactivation of PTEN is usually transient, compromised antioxidant defenses in aged RPE cells might fail to protect PTEN, leading to longer-term inactivation [77].

In summary, NACA eye drops exhibit some protective effects against $NaIO_3$-induced neuroretinal damage in a mouse model of AMD. $NaIO_3$-induced oxidative stress was evidenced by higher levels of lipid peroxidation by-product 4-HNE that was measured in the retina of animals receiving $NaIO_3$ injections. Even so, elevated cysteine and GSH in these animals may be indicative of upregulated antioxidant defense mechanisms. PTEN and its inactive form, p-PTEN, play an important role in cell adhesion and PI3K/AKT/mTOR signaling. While both forms were found to be increased in the retina after $NaIO_3$ injection, the rise in PTEN levels was proportionally greater than that of p-PTEN, likely downregulating survival signaling and resulting in photoreceptor death and ONL thinning. In NACA-treated animals, the effect on the ratio of PTEN to p-PTEN was even more pronounced. At the cellular level, NACA eye drops prevented ONL thinning but did not entirely protect RPE integrity, which may explain the

diminished a- and b-wave waveforms observed in the ERG of these animals. Overall, NACA eye drops maintained partially visual function for a short time after administration of a high dose of NaIO$_3$ (75 mg/kg), but NACA was unable to halt progression of neuroretinal damage for the duration of the experiment.

## 5. CONCLUSIONS

The primary objective of this study was to examine the effects of NACA eye drops on the preservation of neuroretina in a chemically-induced macular degeneration model. The eye drops could possibly be more conveniently administered in real-life cases. Our results showed that NACA eye drops provided short-term photoreceptor protection following NaIO$_3$-induced damage. The increased GSH and cysteine levels in the NaIO$_3$-treated groups may indicate that antioxidant defense mechanisms in the affected cells had been mobilized against the effects of the toxic lipid peroxidation by-product (4-HNE) in the ONL, and NACA eye drops were able to reduce the 4-HNE accumulation. In real life, dry AMD is a slowly progressing disease, and once it has been discovered, an effective eye drop formulation may stop the progression of dry AMD to the more severe wet AMD. Currently, there are no available experimental animal models that perfectly replicate all pathological features of dry AMD. This experimental model of acute retinal degeneration more closely approximates advanced stages of the disease but is not necessarily representative of AMD pathology in the majority of patients. However, these results can provide valuable support for further investigation of NACA eye drops as a potential therapeutic agent in age-related eye disease.

## ACKNOWLEDGEMENTS

## REFERENCES

1.    Global data on visual impairments 2010. 2012: World Health Organization (WHO), Prevention of Blindness and Deafness Programme.

2.    Wittenborn J and Rein D, Cost of Vision Problems: The Economic Burden of Vision Loss and Eye Disorders in the United States. 2013, NORC at the University of Chicago: Chicago, IL.

3.    Arnold C, Winter L, Fröhlich K, and et al. Macular xanthophylls and ω-3 long-chain polyunsaturated fatty acids in age-related macular degeneration: A randomized trial. JAMA Ophthalmology. 2013;131:564-72.

4.    Lambert NG, ElShelmani H, Singh MK, Mansergh FC, Wride MA, Padilla M *et al*. Risk factors and biomarkers of age-related macular degeneration. Prog Retin Eye Res. 2016;54:64-102.

5.    Carneiro Â and Andrade JP. Nutritional and Lifestyle Interventions for Age-Related Macular Degeneration: A Review. Oxidative Medicine and Cellular Longevity. 2017;2017:13.

6.      Nowak JZ. Oxidative stress, polyunsaturated fatty acids-derived oxidation products and bisretinoids as potential inducers of CNS diseases: focus on age-related macular degeneration. Pharmacol Rep. 2013;65:288-304.

7.      Winkler BS, Boulton ME, Gottsch JD, and Sternberg P. Oxidative damage and age-related macular degeneration. Molecular vision. 1999;5:32-.

8.      Yu D-Y and Cringle SJ. Retinal degeneration and local oxygen metabolism. Experimental Eye Research. 2005;80:745-51.

9.      Nita M and Grzybowski A. The Role of the Reactive Oxygen Species and Oxidative Stress in the Pathomechanism of the Age-Related Ocular Diseases and Other Pathologies of the Anterior and Posterior Eye Segments in Adults. Oxid Med Cell Longev. 2016;2016:3164734.

10.     Pham-Huy LA, He H, and Pham-Huy C. Free Radicals, Antioxidants in Disease and Health. International Journal of Biomedical Science : IJBS. 2008;4:89-96.

11.     Tokarz P, Kaarniranta K, and Blasiak J. Role of antioxidant enzymes and small molecular weight antioxidants in the pathogenesis of age-related macular degeneration (AMD). Biogerontology. 2013;14:461-82.

12.     Beatty S, Koh H, Phil M, Henson D, and Boulton M. The role of oxidative stress in the pathogenesis of age-related macular degeneration. Surv Ophthalmol. 2000;45:115-34.

13.     Vives-Bauza C, Anand M, Shiraz AK, Magrane J, Gao J, Vollmer-Snarr HR *et al*. The age lipid A2E and mitochondrial dysfunction synergistically impair phagocytosis by retinal pigment epithelial cells. J Biol Chem. 2008;283:24770-80.

14.     Fine  SL, Berger  JW, Maguire  MG, and Ho  AC. Age-Related Macular Degeneration. New England Journal of Medicine. 2000;342:483-92.

15.     Hageman GS, Gehrs K, Johnson LV, and Anderson D, Age-Related Macular Degeneration (AMD), in Webvision: The Organization of the Retina and Visual System, H. Kolb, E. Fernandez, and R. Nelson, Editors. 1995: Salt Lake City (UT).

16.     Sanz MM, Johnson LE, Ahuja S, Ekström PAR, Romero J, and van Veen T. Significant photoreceptor rescue by treatment with a combination of antioxidants in an animal model for retinal degeneration. Neuroscience. 2007;145:1120-9.

17.     Payne AJ, Kaja S, Naumchuk Y, Kunjukunju N, and Koulen P. Antioxidant Drug Therapy Approaches for Neuroprotection in Chronic Diseases of the Retina. International Journal of Molecular Sciences. 2014;15:1865-86.

18.    Zampatti S, Ricci F, Cusumano A, Marsella LT, Novelli G, and Giardina E. Review of nutrient actions on age-related macular degeneration. Nutrition Research. 2014;34:95-105.

19.    Buschini E, Fea AM, Lavia CA, Nassisi M, Pignata G, Zola M *et al*. Recent developments in the management of dry age-related macular degeneration. Clin Ophthalmol. 2015;9:563-74.

20.    Gorusupudi A, Nelson K, and Bernstein PS. The Age-Related Eye Disease 2 Study: Micronutrients in the Treatment of Macular Degeneration. Adv Nutr. 2017;8:40-53.

21.    Carey JW, Pinarci EY, Penugonda S, Karacal H, and Ercal N. In vivo inhibition of l-buthionine-(S,R)-sulfoximine-induced cataracts by a novel antioxidant, N-acetylcysteine amide. Free Radic Biol Med. 2011;50:722-9.

22.    Maddirala Y, Tobwala S, Karacal H, and Ercal N. Prevention and reversal of selenite-induced cataracts by N-acetylcysteine amide in Wistar rats. BMC Ophthalmology. 2017;17:54.

23.    Schimel AM, Abraham L, Cox D, Sene A, Kraus C, Dace DS *et al*. N-acetylcysteine amide (NACA) prevents retinal degeneration by up-regulating reduced glutathione production and reversing lipid peroxidation. Am J Pathol. 2011;178:2032-43.

24.    Tobwala S, Pinarci EY, Maddirala Y, and Ercal N. N-acetylcysteine amide protects against dexamethasone-induced cataract related changes in cultured rat lenses. Advances in Biological Chemistry. 2014;Vol.04No.01:9.

25.    Wnag H, Huang Y, Tobwala S, Pfaff A, Aronstam R, and Ercal N. The role of N-acetylcysteine amide in defending primary human retinal pigment epithelial cells against tert-butyl hydroperoxide-induced oxidative stress. Free Radicals and Antioxidants. 2017;7:172-7.

26.    Sorsby A. Experimental pigmentary degeneration of the retina by sodium iodate. The British Journal of Ophthalmology. 1941;25:58-62.

27.    Kannan R and Hinton DR. Sodium iodate induced retinal degeneration: new insights from an old model. Neural Regeneration Research. 2014;9:2044-5.

28.    Shen Y, Zhang WY, and Chiou GC. Effect of naringenin on NaIO(3)-induced retinal pigment epithelium degeneration and laser-induced choroidal neovascularization in rats. Int J Ophthalmol. 2010;3:5-8.

29.    Wang J, Iacovelli J, Spencer C, and Saint-Geniez M. Direct Effect of Sodium Iodate on Neurosensory Retina. Investigative Ophthalmology & Visual Science. 2014;55:1941-53.

30. Balmer J, Zulliger R, Roberti S, and Enzmann V. Retinal Cell Death Caused by Sodium Iodate Involves Multiple Caspase-Dependent and Caspase-Independent Cell-Death Pathways. Int J Mol Sci. 2015;16:15086-103.

31. Hanus J, Anderson C, and Wang S. RPE necroptosis in response to oxidative stress and in AMD. Ageing Research Reviews. 2015;24, Part B:286-98.

32. Hanus J, Anderson C, Sarraf D, Ma J, and Wang S. Retinal pigment epithelial cell necroptosis in response to sodium iodate. Cell Death Discovery. 2016;2:16054.

33. Bressler NM, Bressler SB, Congdon NG, Ferris FL, 3rd, Friedman DS, Klein R *et al*. Potential public health impact of Age-Related Eye Disease Study results: AREDS report no. 11. Arch Ophthalmol. 2003;121:1621-4.

34. Evans JR and Lawrenson JG. Antioxidant vitamin and mineral supplements for slowing the progression of age-related macular degeneration. Cochrane Database Syst Rev. 2012;11:Cd000254.

35. Kim JW, Kang KH, Burrola P, Mak TW, and Lemke G. Retinal degeneration triggered by inactivation of PTEN in the retinal pigment epithelium. Genes & Development. 2008;22:3147-57.

36. Wu Y, Zhou H, Wu K, Lee S, Li R, and Liu X. PTEN phosphorylation and nuclear export mediate free fatty acid-induced oxidative stress. Antioxid Redox Signal. 2014;20:1382-95.

37. Kitagishi Y and Matsuda S. Redox regulation of tumor suppressor PTEN in cancer and aging (Review). Int J Mol Med. 2013;31:511-5.

38. Sakagami K, Chen B, Nusinowitz S, Wu H, and Yang XJ. PTEN regulates retinal interneuron morphogenesis and synaptic layer formation. Mol Cell Neurosci. 2012;49:171-83.

39. Chen W, Ercal N, Huynh T, Volkov A, and Chusuei CC. Characterizing N-acetylcysteine (NAC) and N-acetylcysteine amide (NACA) binding for lead poisoning treatment. J Colloid Interface Sci. 2012;371:144-9.

40. Woodward WR, Choi D, Grose J, Malmin B, Hurst S, Pang J *et al*. Isoflurane is an effective alternative to ketamine/xylazine/acepromazine as an anesthetic agent for the mouse electroretinogram. Doc Ophthalmol. 2007;115:187-201.

41. Maleki S, Gopalakrishnan S, Ghanian Z, Sepehr R, Schmitt H, Eells J *et al*. Optical imaging of mitochondrial redox state in rodent model of retinitis pigmentosa. Journal of Biomedical Optics. 2013;18:016004.

42. Wu W, Goldstein G, Adams C, Matthews RH, and Ercal N. Separation and quantification of N-acetyl-l-cysteine and N-acetyl-cysteine-amide by HPLC with fluorescence detection. Biomed Chromatogr. 2006;20:415-22.

43.    Tobwala S, Wang H-J, Carey J, Banks W, and Ercal N. Effects of Lead and Cadmium on Brain Endothelial Cell Survival, Monolayer Permeability, and Crucial Oxidative Stress Markers in an in Vitro Model of the Blood-Brain Barrier. Toxics. 2014;2:258.

44.    Winters RA, Zukowski J, Ercal N, Matthews RH, and Spitz DR. Analysis of glutathione, glutathione disulfide, cysteine, homocysteine, and other biological thiols by high-performance liquid chromatography following derivatization by n-(1-pyrenyl)maleimide. Anal Biochem. 1995;227:14-21.

45.    Bradford MM. A rapid and sensitive method for the quantitation of microgram quantities of protein utilizing the principle of protein-dye binding. Anal Biochem. 1976;72:248-54.

46.    Machalinska A, Lubinski W, Klos P, Kawa M, Baumert B, Penkala K *et al*. Sodium iodate selectively injuries the posterior pole of the retina in a dose-dependent manner: morphological and electrophysiological study. Neurochem Res. 2010;35:1819-27.

47.    Tao Z, Dai J, He J, Li C, Li Y, and Yin ZQ. The influence of NaIO(3)-induced retinal degeneration on intra-retinal layer and the changes of expression profile/morphology of DA-ACs and mRGCS. Mol Neurobiol. 2013;47:241-60.

48.    Sunitha K, Hemshekhar M, Thushara RM, Santhosh MS, Yariswamy M, Kemparaju K *et al*. N-Acetylcysteine amide: a derivative to fulfill the promises of N-Acetylcysteine. Free Radic Res. 2013;47:357-67.

49.    Grinberg L, Fibach E, Amer J, and Atlas D. N-acetylcysteine amide, a novel cell-permeating thiol, restores cellular glutathione and protects human red blood cells from oxidative stress. Free Radic Biol Med. 2005;38:136-45.

50.    Offen D, Gilgun-Sherki Y, Barhum Y, Benhar M, Grinberg L, Reich R *et al*. A low molecular weight copper chelator crosses the blood-brain barrier and attenuates experimental autoimmune encephalomyelitis. J Neurochem. 2004;89:1241-51.

51.    Penugonda S, Mare S, Lutz P, Banks WA, and Ercal N. Potentiation of lead-induced cell death in PC12 cells by glutamate: protection by N-acetylcysteine amide (NACA), a novel thiol antioxidant. Toxicol Appl Pharmacol. 2006;216:197-205.

52.    Ates B, Abraham L, and Ercal N. Antioxidant and free radical scavenging properties of N-acetylcysteine amide (NACA) and comparison with N-acetylcysteine (NAC). Free Radic Res. 2008;42:372-7.

53.    Shi R, Huang CC, Aronstam RS, Ercal N, Martin A, and Huang YW. N-acetylcysteine amide decreases oxidative stress but not cell death induced by doxorubicin in H9c2 cardiomyocytes. BMC Pharmacol. 2009;9:7.

54.     Peachey NS and Ball SL. Electrophysiological analysis of visual function in mutant mice. Doc Ophthalmol. 2003;107:13-36.

55.     Pinto LH, Invergo B, Shimomura K, Takahashi JS, and Troy JB. Interpretation of the mouse electroretinogram. Documenta Ophthalmologica. 2007;115:127-36.

56.     Miller RF and Dowling JE. Intracellular responses of the Muller (glial) cells of mudpuppy retina: their relation to b-wave of the electroretinogram. J Neurophysiol. 1970;33:323-41.

57.     Berrow EJ, Bartlett HE, Eperjesi F, and Gibson JM. The electroretinogram: a useful tool for evaluating age-related macular disease? Documenta Ophthalmologica. 2010;121:51-62.

58.     Prunty MC, Aung MH, Hanif AM, Allen RS, Chrenek MA, Boatright JH *et al*. In Vivo Imaging of Retinal Oxidative Stress Using a Reactive Oxygen Species–Activated Fluorescent Probe. Investigative Ophthalmology & Visual Science. 2015;56:5862-70.

59.     Cai Z, Simons DL, Fu XY, Feng GS, Wu SM, and Zhang X. Loss of Shp2-mediated mitogen-activated protein kinase signaling in Muller glial cells results in retinal degeneration. Mol Cell Biol. 2011;31:2973-83.

60.     Ozawa Y, Kurihara T, Tsubota K, and Okano H. Regulation of posttranscriptional modification as a possible therapeutic approach for retinal neuroprotection. J Ophthalmol. 2011;2011:506137.

61.     Ozawa Y, Sasaki M, Takahashi N, Kamoshita M, Miyake S, and Tsubota K. Neuroprotective effects of lutein in the retina. Curr Pharm Des. 2012;18:51-6.

62.     Pang J-J, Abd-El-Barr MM, Gao F, Bramblett DE, Paul DL, and Wu SM. Relative contributions of rod and cone bipolar cell inputs to AII amacrine cell light responses in the mouse retina. The Journal of Physiology. 2007;580:397-410.

63.     Sternberg P, Jr., Davidson PC, Jones DP, Hagen TM, Reed RL, and Drews-Botsch C. Protection of retinal pigment epithelium from oxidative injury by glutathione and precursors. Invest Ophthalmol Vis Sci. 1993;34:3661-8.

64.     Finkel T and Holbrook NJ. Oxidants, oxidative stress and the biology of ageing. Nature. 2000;408:239-47.

65.     Ganea E and Harding JJ. Glutathione-related enzymes and the eye. Curr Eye Res. 2006;31:1-11.

66.     Schafer FQ and Buettner GR. Redox environment of the cell as viewed through the redox state of the glutathione disulfide/glutathione couple. Free Radic Biol Med. 2001;30:1191-212.

67. Tobwala S, Wang H-J, Carey WJ, Banks AW, and Ercal N. Effects of Lead and Cadmium on Brain Endothelial Cell Survival, Monolayer Permeability, and Crucial Oxidative Stress Markers in an in Vitro Model of the Blood-Brain Barrier. Toxics. 2014;2.

68. Sachdeva MM, Cano M, and Handa JT. Nrf2 signaling is Impaired in the Aging RPE given an Oxidative Insult. Experimental eye research. 2014;119:111-4.

69. Opere C, Bankhele P, Salvi A, Jamil J, Munt D, Njie-Mbye YF *et al*. Comparative pharmacological actions of N-acetylcysteine and L-cysteine on excitatory neurotransmission in bovine isolated retina (1060.4). The FASEB Journal. 2014;28.

70. Pedersen OO and Karlsen RL. The toxic effect of L-cysteine on the rat retina. A morphological and biochemical study. Invest Ophthalmol Vis Sci. 1980;19:886-92.

71. Marchette LD, Thompson DA, Kravtsova M, Ngansop TN, Mandal MN, and Kasus-Jacobi A. Retinol dehydrogenase 12 detoxifies 4-hydroxynonenal in photoreceptor cells. Free Radic Biol Med. 2010;48:16-25.

72. Ayala A, Munoz MF, and Arguelles S. Lipid peroxidation: production, metabolism, and signaling mechanisms of malondialdehyde and 4-hydroxy-2-nonenal. Oxid Med Cell Longev. 2014;2014:360438.

73. Cross JV and Templeton DJ. Regulation of signal transduction through protein cysteine oxidation. Antioxid Redox Signal. 2006;8:1819-27.

74. Wang X and Jiang X. Post-translational regulation of PTEN. Oncogene. 2008;27:5454-63.

75. Jo HS, Kang KH, Joe CO, and Kim JW. Pten coordinates retinal neurogenesis by regulating Notch signalling. Embo j. 2012;31:817-28.

76. Mao D and Sun X. Reactivation of the PI3K/Akt Signaling Pathway by the Bisperoxovanadium Compound bpV(pic) Attenuates Photoreceptor Apoptosis in Experimental Retinal Detachment. Invest Ophthalmol Vis Sci. 2015;56:5519-32.

77. Zieger M and Punzo C. Improved cell metabolism prolongs photoreceptor survival upon retinal-pigmented epithelium loss in the sodium iodate induced model of geographic atrophy. Oncotarget. 2016;7:9620-33.

78. Lee SR, Yang KS, Kwon J, Lee C, Jeong W, and Rhee SG. Reversible inactivation of the tumor suppressor PTEN by H2O2. J Biol Chem. 2002;277:20336-42.

**SECTION**

## 4. PRELIMINARY DATA FOR IN VITRO MODEL

Before investigating chemically induced retinal degeneration in *in vivo*, we supplemented our research by applying the same method *in vitro* with HRPEpiC, a primary culture of human retinal pigment epithelial cells. The purpose of this study was to evaluate redox status following $NaIO_3$-induced oxidative stress and the protective effects of NACA.

### 4.1. RESULTS

**4.1.1. Protection by NACA Against Sodium Iodate-Induced Cell Death.** The cytotoxic effects of $NaIO_3$ were evaluated in HRPEpiC after 24 hours of treatment. $NaIO_3$ induced cytotoxicity in a dose-dependent manner (Figure 4.1), and pre-incubation with 0.5 mM NACA for 4 hours prior to $NaIO_3$ treatment increased cell viability. Results are reported as percentage of the control. The cell viability was $65.5 \pm 4.1\%$ in the 5 mM $NaIO_3$ group and $104.5 \pm 7.7$ % in the NACA-pretreated $NaIO_3$ group ($n = 3$-5).

**4.1.2. The Protective Effect of NACA Against $NaIO_3$-Induced ROS Formation in HRPEpi Cells.** We further investigated the protective effect of NACA against $NaIO_3$-induced oxidative damage by determining levels of ROS formation in HRPEpiC (Figure 4.2). Fluorescence measured in the cells was indicative of intracellular ROS. The ROS levels in the 5 mM and 15 mM $NaIO_3$ groups were $3.96 \pm 0.13$ and $4.61 \pm 0.15$ times that of the control group, respectively ($P < 0.001$). The ROS level was $3.33 \pm 0.40$ times that of the control in the NACA + 5 mM $NaIO_3$ group ($P < 0.05$) and $3.61 \pm 0.61$ times the control level in the NACA + 15 mM $NaIO_3$ group ($P < 0.001$). pretreatment with NACA for 4 hours diminished $NaIO_3$-induced ROS generation.
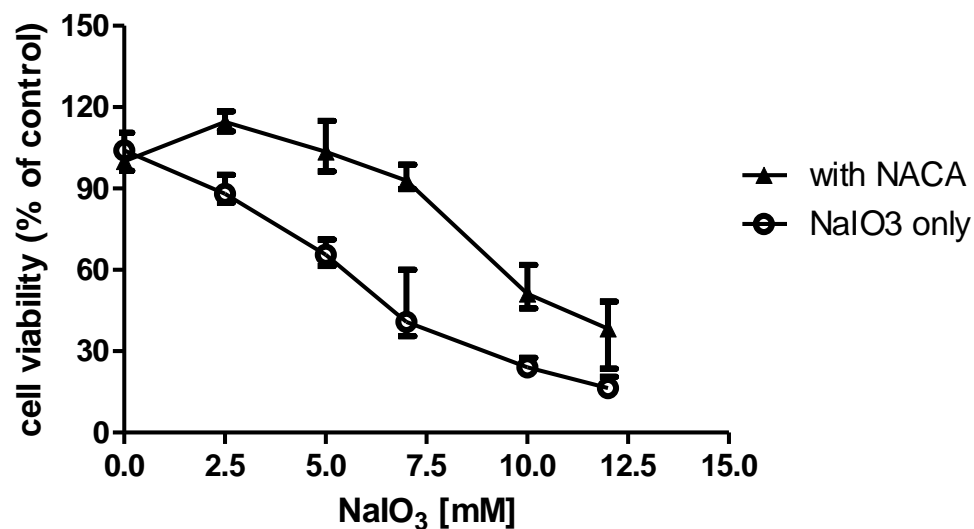
Figure 4.1 Comparison of NaIO3 cytotoxicity with and without NACA in HRPEpiC. Cells were pretreated with either 0.5 mM NACA or control media for 4 hours. This was replaced by media with various concentrations of NaIO$_3$ in which the cells were cultured for another 24 hours.
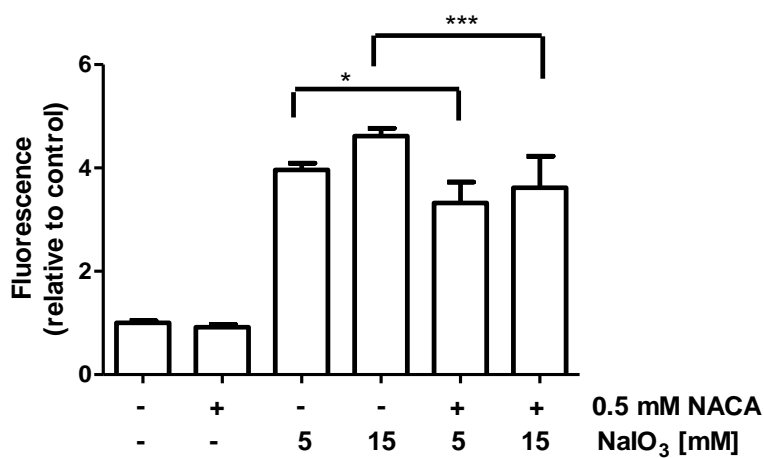


Figure 4.2 ROS levels in HRPEpiC after 4 hours of pretreatment with NACA and another 3 hours of treatment with increasing concentration of NaIO$_3$.

**4.1.3. Intracellular Glutathione Levels.** To investigate the intracellular thiol antioxidant levels as a consequence of $NaIO_3$-induced ROS generation, GSH levels were measured at two different time points during the course of the experiment. Figure 4.3A shows the GSH levels after 3 hours of $NaIO_3$ treatment, and Figure 4.3B shows the GSH levels after 24 hours of $NaIO_3$ dosing. After 24 hours, the GSH levels were significantly increased in the 5 mM $NaIO_3$ group (99.4 ± 9.1 nmol/mg protein, $P < 0.001$), but they were close to the control level in the 15 mM $NaIO_3$ group. In the 20 mM $NaIO_3$ group, the GSH levels were significantly decreased compared to the control group (14.1 ± 6.6 nmol/mg protein, $P < 0.001$). The GSH levels in NACA + 5 mM $NaIO_3$, NACA + 15 mM $NaIO_3$, and NACA + 20 mM $NaIO_3$ groups were 88.9 ± 7.1, 26.6 ± 3.3 and 4.4 ± 3.5 nmol/mg protein, respectively. The cysteine levels in the control, 0.5 mM NACA, 5 mM $NaIO_3$, and NACA+$NaIO_3$ groups were 0.53 ± 0.24, 1.85 ± 0.48, 1.11 ± 0.09 and 0.65 ± 0.25 nmol/mg protein, respectively ($n = 8$ in control and 0.5 mM $NaIO_3$ groups; $n = 4$ in other groups).
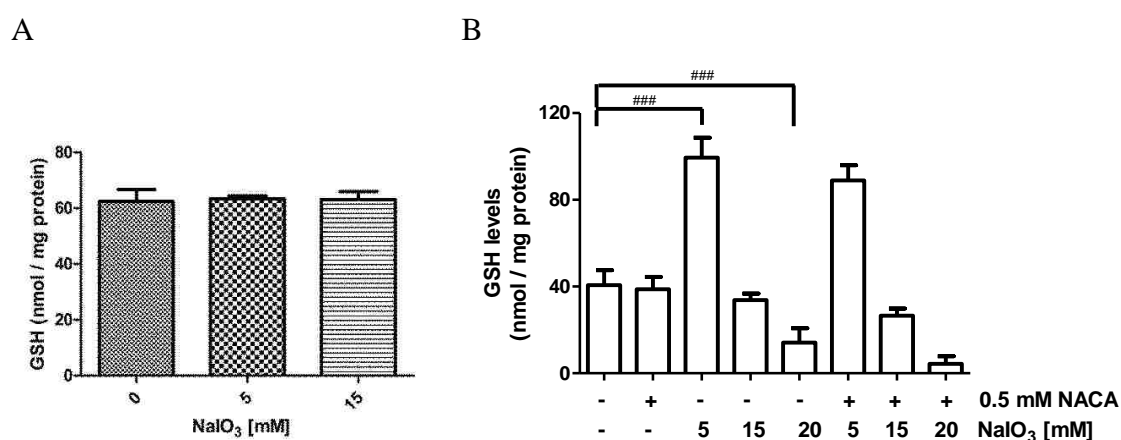


Figure 4.3 Intracellular GSH levels in HRPEpiC.
(A) GSH levels were measured after 3 hours of $NaIO_3$ treatment. (B) GSH levels were measured after 24 hours of $NaIO_3$ treatment with and without NACA pretreatment.

**4.1.4. Glutathione Reductase Activity.** Glutathione reductase (GR) reduces GSSG to generate GSH and is a very important enzyme for glutathione homeostasis. The GR levels in the control, 0.5 mM NACA, 5 mM $NaIO_3$, and NACA+$NaIO_3$ groups were $25.1 \pm 1.5$, $23.5 \pm 0.7$, $20.8 \pm 0.9$ and $21.7 \pm 0.5$ mU/mg protein, respectively (Figure 5.4).
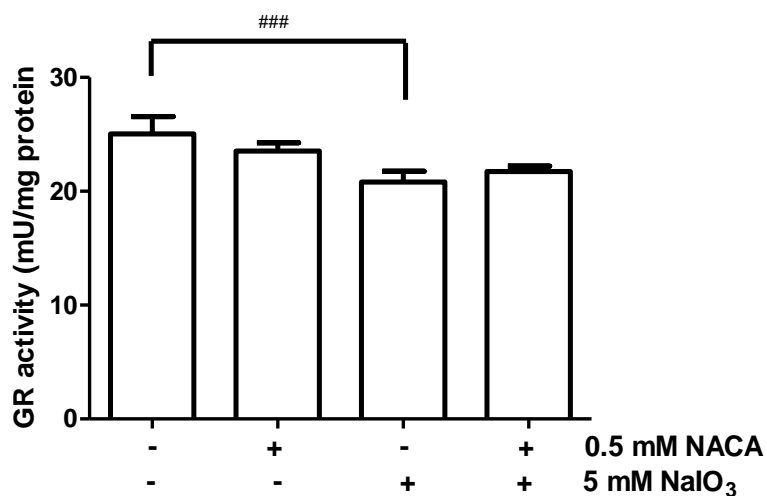


Figure 4.4 Glutathione reductase (GR) levels.
$NaIO_3$ reduced GR activity after 24-hour dosing, and pretreatment with 0.5 mM NACA did not improve GR activity.

# 5. PRELIMINARY DATA FOR *IN VIVO* MODEL

The *rd10*$^{+/+}$ strain is a spontaneous missense point mutation in *Pde6* (cGMP phosphodiesterase 6B in rod receptors) that results in increased levels of cGMP and leads to elevated ROS and oxidative stress. To further assess the effectiveness of NACA eye drops, we utilized 1-week old *rd10*$^{+/+}$ mice with C57BL/6 mice as controls. The experimental design is outlined in Figure 5.1.

Because retinal degeneration begins before the *rd10*$^{+/+}$ mice open their eyes on postnatal day (P) 17, it was necessary to change our initial research design and administer NACA via intraperitoneal (IP) injection to study its preventative effects. From P8, IP injections of either sodium phosphate buffer or 250 mg/kg NACA were administered once daily until P16. Eye drops (1% NACA/vehicle, 3 times daily, 4 drops per time) were started on P17 and continued until P25. The mice were sacrificed on P26, and the eyes were removed immediately after sacrifice. Retinal sections were evaluated by a masked observer.
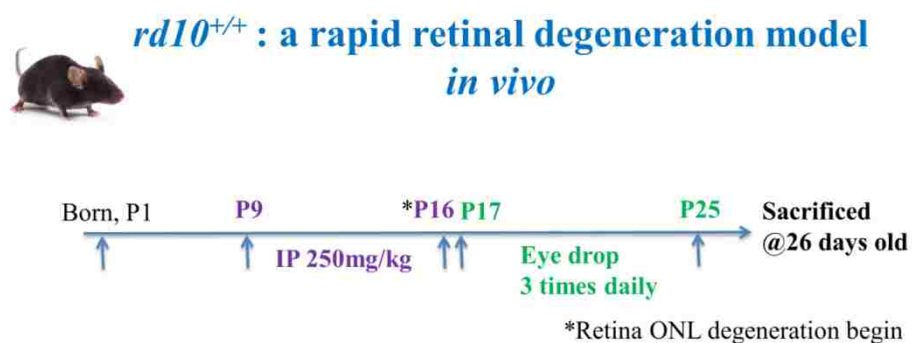


Figure 5.1 Experimental design for *rd10*$^{+/+}$ model.

Our results showed that ONL thinning in *rd10*^{+/+} mice had been significantly prevented with NACA eye drops when compared to retinal sections from mice given buffer eye drops. Figure 5.2A shows representative images of H&E staining for retinal sections and ONL thickness in the experimental groups.
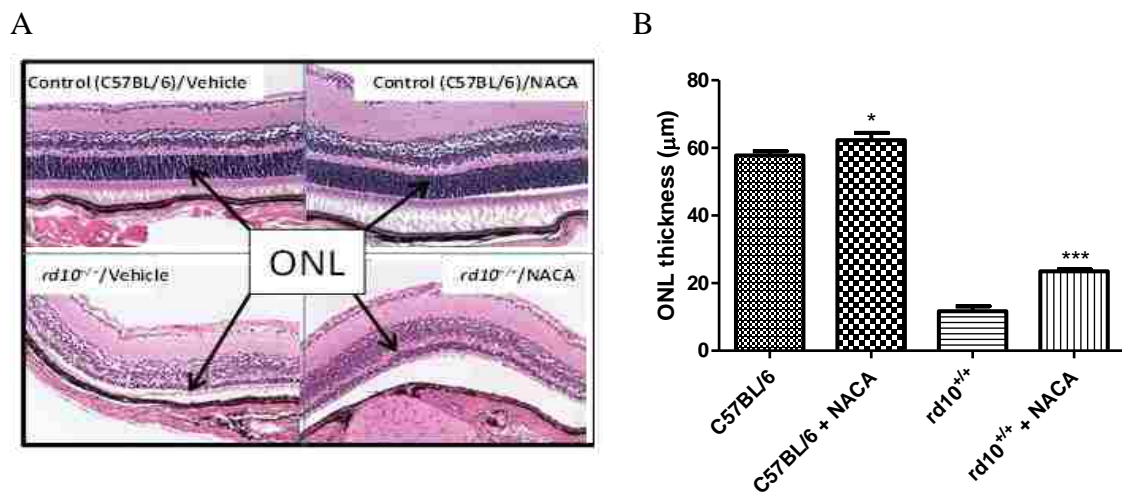
A



B



Figure 5.2 NACA eye drops prevented the reduction of ONL thickness in *rd10*^{+/+}. (A)Representative images of H&E staining for retinal sections and (B) the average ONL thickness for each treatment group ( *$P < 0.05$ & *** $P < 0.001$ compared to the control group).

## 6. CONCLUSION

AMD is a leading cause of irreversible blindness in the Western world. Oxidative stress plays a significant role in the progression of AMD, and the clinically available treatments are limited. With the prevalence of AMD and other retinal degenerative disorders expected to double in the coming decades, the development of more effective therapies to prevent their progression is imperative. Because these conditions are closely linked to oxidative stress, we designed an *in vitro* and an *in vivo* model to investigate the effectiveness of the thiol antioxidant NACA in preventing retinal pigment epithelial cell and retinal cell damage.

In the TBHP-induced HRPEpiC model, our data indicates that TBHP generated ROS, which reduced cell viability, depleted GSH levels, and inhibited GR activity. The treatment of retinal pigment epithelium with NACA protected against TBHP-induced cellular injury. NACA also inhibited oxidative stress-related breakdown of the blood-retinal barrier as measured by TEER. The proposed mechanism of action involves NACA scavenging existing reactive oxygen species and increasing levels of reduced glutathione. Our results indicate that NACA has the potential to become an effective therapeutic agent by enhancing antioxidant defenses while removing pathologically relevant ROS.

In the $NaIO_3$-induced retinal degeneration model, $NaIO_3$ increased ROS generation, leading to oxidative stress and cell death. NACA pretreatment helped protect HRPEpiC against $NaIO_3$-induced ROS formation, although it was not sufficient to restore GSH levels after depletion by $NaIO_3$. Furthermore, we investigated the beneficial effects of NACA eye drops in a chemically induced retinal degeneration model. Our results showed that NACA eye drops improved photoreceptor function following $NaIO_3$-induced

oxidative stress. NACA eye drops also reduced accumulation of the toxic lipid

peroxidation by-product 4-HNE in the retina. These results support further investigation

of NACA eye drops as a potential therapeutic agent in age-related eye disease.

**APPENDIX**

**PEER-REVIEWED JOURNAL PUBLICATIONS FROM HSIU-JEN WANG**

1.  Tang TH, Chang CT, Wang HJ, Erickson JD, Reichard RA, Martin AG et al. Oxidative stress disruption of receptor-mediated calcium signaling mechanisms. J Biomed Sci. 2013;20:48.

2.  Tobwala S, Zhang X, Zheng Y, Wang HJ, Banks WA, and Ercal N. Disruption of the integrity and function of brain microvascular endothelial cells in culture by exposure to diesel engine exhaust particles. Toxicol Lett. 2013;220:1-7.

3.  Wang HJ, Martin AG, Chao PK, Reichard RA, Martin AL, Huang YW et al. Honokiol blocks store operated calcium entry in CHO cells expressing the M3 muscarinic receptor: honokiol and muscarinic signaling. J Biomed Sci. 2013;20:11.

4.  Tobwala S, Wang H-J, Carey WJ, Banks AW, and Ercal N. Effects of Lead and Cadmium on Brain Endothelial Cell Survival, Monolayer Permeability, and Crucial Oxidative Stress Markers in an in Vitro Model of the Blood-Brain Barrier. Toxics. 2014;2.

5.  Wang H-J, Huang Y-W, Tobwala S, Pfaff A, Aronstam R, and Ercal N. The role of N-acetylcysteine amide in defending primary human retinal pigment epithelial cells against tert-butyl hydroperoxide- induced oxidative stress. Free Radicals and Antioxidants. 2017;7.

**VITA**

Hsiu-Jen (Sharen) Wang was born in Yunlin, Taiwan (R.O.C). She attended Chung Shan Medical University (CSMU), in Taichung, Taiwan, and graduated in 1994 with a Bachelor of Science in Medical Technology. Hsiu-Jen worked as a research assistant for 2 years at National Taiwan University and then returned to CSMU for her Master's Degree in Toxicology in July 1998. She worked as a research assistant for 8 years at the Division of Environmental Health & Occupational Medicine, National Health Research Institutes in Taiwan, and was promoted to Research Assistant II. In September 2010, Hsiu-Jen received her Master's Degree in Biological Sciences at Missouri University of Science and Technology (Missouri S&T) in Rolla, Missouri. From 2008 through 2010, she worked as a lab technician in the cDNA Resource Center at Missouri S&T. In January 2011, she joined Dr. Nuran Ercal's research group at Missouri S&T to pursue a PhD in Analytical Biochemistry. There, her research focused primarily on the beneficial effects of NACA on oxidative stress-related macular degeneration. Hsiu-Jen completed her PhD in Chemistry in September 2017. In December 2017 she received her PhD degree in Chemistry from Missouri University of Sciences and Technology.